



Durham E-Theses

The electrical space charge in the lower atmosphere

Bent, Rodney, B.

How to cite:

Bent, Rodney, B. (1964) *The electrical space charge in the lower atmosphere*, Durham theses, Durham University. Available at Durham E-Theses Online: <http://etheses.dur.ac.uk/8999/>

Use policy

The full-text may be used and/or reproduced, and given to third parties in any format or medium, without prior permission or charge, for personal research or study, educational, or not-for-profit purposes provided that:

- a full bibliographic reference is made to the original source
- a [link](#) is made to the metadata record in Durham E-Theses
- the full-text is not changed in any way

The full-text must not be sold in any format or medium without the formal permission of the copyright holders.

Please consult the [full Durham E-Theses policy](#) for further details.

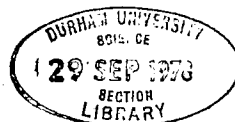
The copyright of this thesis rests with the author.
No quotation from it should be published without
his prior written consent and information derived
from it should be acknowledged.

The electrical space charge in the
lower atmosphere

by

Rodney B. Bent, B.Sc., Grad. Inst.P., F.R. Met. S.

Thesis submitted in candidature for the
degree of Doctor of Philosophy
in the University of Durham.



R. B. Bent.
November, 1964.

ABSTRACT

Two space charge collectors were designed and built incorporating a glass-asbestos medium for filtering ions from the air, the charge being measured using a vibrating reed electrometer. These collectors were rigorously tested and it was demonstrated that they collected over 99.8% of the small ions in the air at certain flow rates through the collector. An analogue-to-digital converter was built in order to digitalise the information displayed on a 16 point recorder. The unit was built incorporating semiconductors; a voltage from the recorder was converted into a frequency which was counted on decastron tubes for a certain period of time, so that the number registered was within 1% of the recorded value. This number was then punched out on paper tape and arrangements were made in order to print 'space' and 'carriage return-line feed' into the output.

Four aspirated psychrometers incorporating thermistors were built in order to measure the temperature and humidity gradients on a 21 m steel lattice mast. Wind was recorded at 1 m and 17 m and potential gradient in the surface of the earth and at the top of the mast.

Results of space charge concentrations on the mast structure show that during a period of melting snow a charge separation occurs at the ground surface under strong wind conditions. It was also shown that dry blowing snow gives rise to high positive space charge even when the snow is blowing from distant hills.

Corona space charge was observed to form at trees after a nearby lightning flash and during misty conditions there was a predominance

of negative space charge. Convection cells were apparently detected under cumulus clouds and it was observed that charge was transported by the air circulations within these cells. Perhaps the most important result observed was an electrode effect due to the mast structure towards the top. This effect could completely mask the space charge density expected at that level if the mast were not there.

CONTENTS

	<u>Page</u>
<u>CHAPTER 1 INTRODUCTION</u>	1
<u>CHAPTER 2 EARLIER SPACE CHARGE MEASUREMENTS</u>	
General	11
Electrical collection	14
Determination of space charge using earthed wire cages	15
Filtration methods of determining space charge	19
Previous results	22
<u>CHAPTER 3 THE ABSOLUTE FILTER SPACE CHARGE COLLECTOR</u>	28
<u>CHAPTER 4 DESCRIPTION AND CALIBRATION OF OTHER EQUIPMENT</u>	
General	37
The measurement of potential gradient	38
The measurement of temperature and humidity	41
The measurement of wind speed	47
Automatic recording	52
<u>CHAPTER 5 ANALOGUE-TO-DIGITAL CONVERTER</u>	
General	53
Description of converter	55
Recorder	56
Voltage-to-frequency converter	57
Monostable timing unit and gate	60
Bistable starter unit	61
The counter decatrons	62
Programmer	64
Commutator	69

	<u>Page</u>
Output amplifier and commutator gates	70
Counter deatron gates and diode matrix	72
Reset Unit	73
Binary scaler	73
Power supplies	75
 <u>CHAPTER 6 LABORATORY TESTING OF THE SPACE CHARGE COLLECTORS</u>	
General	78
Recording equipment and calibration	79
Polonium ion generator	81
The tests	82
 <u>CHAPTER 7 INSTALLATION AND OPERATION OF APPARATUS AT THE</u>	
<u>OBSERVATORY</u>	
The site	87
Installation of equipment	87
Recording procedure and analysis	93
 <u>CHAPTER 8 RESULTS</u>	
<u>Space charges over snow</u>	
Introduction	99
Results obtained	100
Discussion	104
 <u>Space charges produced by point discharge from trees</u>	
<u>during a thunderstorm</u>	
Introduction	107
Results	109
Discussion	111

	<u>Page</u>
<u>An electrode effect due to the mast and space charge collector</u>	
Introduction	114
Results	118
Discussion	120
<u>Convection cell measurements</u>	
Introduction	121
Results	123
Discussion	123
<u>Negative space charges</u>	126
<u>Space charge pulses caused by steam-engines</u>	128
<u>CHAPTER 9 CONCLUSIONS AND SUGGESTIONS FOR FURTHER WORK</u>	130
<u>ACKNOWLEDGMENTS</u>	134
<u>REFERENCES</u>	135

CHAPTER 1

INTRODUCTION

Late in the nineteenth century it became clear that air conducts electricity. Experiments performed by COULOMB in 1785 established that when an electrically charged body was exposed in air it proceeded to lose its charge. MATTEUCCI (1850) also verified that air was a conductor of electricity, but these discoveries received very little attention until observations by LINSS (1887) showed that the conductivity of air varied considerably and was greater in summer than winter. He also pointed out that the positive charge being conducted to earth would, inside 10 minutes, neutralise the negative charge on the earth. Many suggestions as to why this did not happen were made and as most of them were refuted several eminent physicists suggested modification of the basic laws of physics. However it now seems agreed that thunderstorms supply the negative charge to the earth at a rate which balances the positive charge arriving during fine weather.

Since ELSTER and GEITEL (1899) and C.T.R. WILSON (1900) independently discovered the presence of ions, the nature and origin of these charge carriers has been subject to a great number of investigations. As ions had been observed to be constantly combining with ions of opposite sign there must have been some mechanism for their production. Elster and Geitel discovered that air over land contained



radio-active matter which was derived from the earth's crust and this acted as an ioniser as well as the radio-active matter in the surface.

In the ionising process an energetic particle collides and removes an electron from a gas molecule. The resulting gas-ion is therefore positively charged and the electron soon attaches itself to a neutral molecule to form a negative ion. The energy required to produce an ion pair is about 34 eV (electron volts) and thus considering a 1 meV β particle passing through its 10 m path at ground level about 30,000 ion pairs will be produced.

In the first years of the century Elster and Geitel and C.T.R. Wilson removed radio-active matter from a quantity of air and discovered that it was still slightly conductive. HESS (1911) observed, using balloons, that the conductivity increases on rising above the earth. These results eventually led to the discovery of some extra-terrestrial ionising rays, the so-called cosmic rays. Some of these rays penetrate into the earth's crust and are excellent ionisers particularly at high levels. A source of production of ions was therefore discovered that would affect the air over both land and sea.

The average rate of ionisation over land and near the earth's surface was estimated by HESS (1928) to be about $10 \text{ ion pairs cm}^{-3} \text{ sec}^{-1}$. This value was based on an average amount of radio-active matter in the air and earth. The concentration of this matter is quite variable, depending on local conditions, but Hess suggested that the typical

percentages of the total ionisation produced at this level were as shown in Table 1.

TABLE 1

IONISER	IONISING RAY			COSMIC RAYS	TOTAL
	α	β	γ		
Radium } Thorium } in air	30 18	1 1	1 -		51
Radium } Thorium } in soil	-	1	32		33
Cosmic Rays				16	16
	48	3	33	16	100

IONISATION OF THE AIR NEAR TO THE EARTH'S SURFACE OVER LAND IN
PERCENTAGE OF TOTAL ION PAIRS PRODUCED

Later WORMELL (1953) summarised the values shown in Table 2 as typical for the number of ions produced and the number present in the lower levels of the atmosphere.

The values quoted suggest that the conductivity of the air over the sea is far less than that over land but it was discovered that this was not always the case, and in one measurement on the outskirts of Washington D.C. the value of conductivity was only one-seventh that at sea. This discrepancy was removed in 1905 when LANDEVIN discovered large ions, which have a much lower mobility, resulting in lower conductivity.

TABLE 2

NUMBER OF IONS OF EACH SIGN

	RATE OF PRODUCTION ($\text{cm}^{-3}\text{sec}^{-1}$)		NUMBER PRESENT (cm^{-3})	
	RADIO-ACTIVITY	COSMIC RAYS	SMALL IONS	LARGE IONS
OCEANIC AIR	0	ϕ 2	700	200
COUNTRY AIR	8	2	600	2,000
CITY AIR	8	2	100	20,000

NUMBER OF ION PAIRS PRODUCED AND NUMBER PRESENT IN THE LOWER LEVELS
OF THE ATMOSPHERE

When ion pairs are formed the gas molecules and free electrons will normally combine very quickly at atmospheric pressure, and free electrons would have a mobility much greater than that of the observed small ions. However the mobility of the ions was found to depend on humidity and impurities in the air; another process must therefore be present which reduces the mobility of the ions.

The small ion consists of a group of some 10 molecules grouped around a central charged molecule forming a fairly stable cluster, and because of its lower mobility compared to a single atom must be slower in recombining with ions of the opposite sign. Thus a small ion is formed and its mobility lies between 1 and 2 cm sec^{-1} per V cm^{-1} . WRIGHT (1936) suggested that the mass of the small ion to be equal to that of 10 or 12 water molecules.

As water molecules are easily polarised they will probably attach themselves to an ionised molecule in preference to a neutral molecule. CHAMBERS (1957) suggested that if a V-shape is assumed for the water molecule and the base of the V contains the negatively charged oxygen atom then these will settle more easily on positive ions giving rise to the lower mobility observed for ions of this sign.

Large ions have mobilities of about $1/500$ that of the small ions and are formed when the molecular ions combine with the nuclei on which AITKEN (1880) found moisture to condense. These condensation or Aitken nuclei are composed of a substance soluble in water as condensation will not occur on non-soluble smoke or dust particles. Approximately one-third of the condensation or Aitken nuclei present in the air are electrically neutral, the rest carrying nearly equal numbers of positive and negative charges captured from small ions.

In addition to these large ions the atmosphere may contain quantities of charged dust and smoke particles which are considerably larger. These particles also have the property of greatly reducing the conductivity above and surrounding large towns.

MUHLEISEN (1956) carried out direct observations on man-made space charges and tabulated the following results

POSITIVE	NEGATIVE
Petrol exhaust fumes	Open petrol fire
Chimney smoke	Open wood fire
Coal Fire	Pure water vapour from a
Steam Engine	metal jet

A group of intermediate ions has been observed by POLLOCK (1915) and HOGG (1939). These are comprised of ^{some} 2000 molecules and can be associated with molecules of sulphuric acid from industrial sources.

The average life of a small ion varies between 20 sec in areas of high pollution to 5 min. over the sea, whilst the average life of a large ion is approximately 20 min. over oceans and 60 min. over land.

It was found by LEMONNIER in 1752 that there is a persistent electric field in the atmosphere during fair weather. Later experiments showed this to be about 100 vm^{-1} , with the earth maintaining a surface negative charge of approximately $10^{-9} \text{ coulombs m}^{-2}$ (or $6 \times 10^5 \text{ e cm}^{-2}$) with respect to the electrosphere which is at a varying potential of about 400,000 V.

Many observers with the aid of balloons have recorded rapid decreases of the potential gradient with height and at 18 Km it is only 1/100 of its value at ground level. These results show that there must be a space charge on which the lines of force end, and presumably this is therefore on ions. This space charge constitutes the small difference between the charges carried on positive and negative ions. Concentrations of space charge have been observed to be of the order of $10\text{-}100 \text{ ecm}^{-3}$ on the average for fair-weather, but occasional values of 1000 have been recorded. Under exceptional conditions, as in thunderstorms, concentrations of $10,000 \text{ e cm}^{-3}$ can be expected.

Expressions relating space charge concentration to the potential gradient produced can be deduced using Poisson's equation provided the assumption is made of space charge being uniformly distributed in this region and assuming horizontal equipotentials. Considering two infinitely long parallel conducting planes spaced a finite distance apart in the z direction then Poisson's equation reduces to

$$-\frac{dE}{dz} = \frac{dF}{dz} = \frac{d^2V}{dz^2} = -\frac{\rho}{\epsilon_0}$$

where ϵ_0 is the permittivity of free space, ρ is the space charge density, V the potential, F the vertical gradient of potential and E the electric field.

The space charge in the atmosphere is very sensitive to the vertical distribution of conductivity. Under quasi-static conditions (where instantaneous pictures of the distribution of charge taken at different times is the same) the vertical conduction current density i would be the same at all levels and so Ohm's law can be applied. Consider a column of cross-section 1 cm^2 stretching up from the earth to the electrosphere and let its resistance be R . If V is the potential of the electrosphere then $V = iR$. Assuming that the lowest metre has a resistance r and the potential drop across this is F then

$$F = \frac{i r}{R} = \frac{i V}{R}$$

But the specific conductivity $\lambda = 1/r$

$$\therefore F = V/\lambda R$$

$$\text{and } i = F\lambda$$

Differentiating with respect to altitude as both F and λ depend on z

$$\frac{dI}{dz} = \lambda \frac{dF}{dz} + F \frac{d\lambda}{dz}$$

but

$$\frac{dI}{dz} = 0$$

and as Poisson's equation gives $\rho = -\epsilon_0 \frac{dF}{dz}$ then

$$\rho = \frac{\epsilon_0 F}{\lambda} \frac{d\lambda}{dz} = \frac{\epsilon_0 I}{\lambda^2} \frac{d\lambda}{dz}$$

This equation shows that space charge concentration is very dependent on the vertical distribution of conductivity. It is obvious that positive space charge at the ground is associated with conductivity increasing with height and negative space charge at the ground associated with conductivity decreasing with height.

The equation also shows that in order for the normal positive space charge to be present in the lower atmosphere then the conductivity must increase with height, and that in volumes of no space charge the conductivity will remain constant. The conductivity in any region thus depends on the flow of ions into and out of this region in any direction.

Measurements of potential gradients on balloons and aircraft flights have given results confirming that $F\lambda$ is constant above the 'Austausch' or mixing region but below this, and especially within 100 m of the earth's surface, results are anomalous. Most observers agree that at these levels over the sea the potential gradient decreases with height thus giving rise to a positive space charge, but over land varying

results are found. The results over the sea could be due to the "Electrode Effect" which can be explained as follows.

Consider a vertical cylinder in still air and positive potential gradient with its lower end on the ground and let F_T and F_B be the potential gradients at the top and bottom of this cylinder. The downward conduction current through the top of this cylinder is $F_T(\lambda_T^+ + \lambda_T^-)$ where λ^+ and λ^- are the polar conductivities, and where the downward-moving positive ions constitute the $F_T\lambda_T^+$ and the upward moving negative ions are responsible for the $F_T\lambda_T^-$. However at the bottom of this cylinder, assuming that no negative ions enter from the earth's surface, there can only be a flow of current to earth of positive ions, namely $F_B\lambda_B^+$, so there will be a net gain of positive charge within this volume. In other words there is a development of positive space charge at a rate given by $F_T(\lambda_T^+ + \lambda_T^-) - F_B\lambda_B^+$ in unit time. The presence of this increasing space charge will decrease the field F_T and increase the field F_B and a stable state will only be reached when the number of positive ions leaving the cylinder in this unit time is the same as the number of negative ions leaving. Thus $F_T(\lambda_T^+ + \lambda_T^-) = F_B\lambda_B^+$ where the left hand side of the equation is the conduction current at the top of the cylinder and the right hand side is the conduction current at the surface of the earth. Calculations show that the field at the surface should therefore be about 30% higher than at 1 m due to this excess space charge.

Many observers over land have reported failure to find such an effect but an explanation of this could be that the radio-activity in the earth's surface causes an increase in negative space charge in these regions. This would decrease as altitude increased and would tend to cancel out the electrode effect. Both conditions however depend a great deal on the surface wind, as disturbances could eliminate both effects.

CHAPTER 2

EARLIER SPACE CHARGE MEASUREMENTS

GENERAL

The space charge concentrations in the lower atmosphere are usually of the order of 100 e cm^{-3} , but with the aid of present day electronics the measurement of this quantity is not difficult. However a major difficulty to be overcome is the noise signal from recording instruments especially where the recording units are on aircraft or not adequately shielded from winds. Fractional electrification can be quite troublesome in the type of instrument through which air is drawn, and if local electric fields exist in the instrument erroneous results occur due to the migration of some ions away from their required path. Differences in the work functions of surfaces used and their fluctuation during differing conditions can give rise to high background signals which can be much larger than the signals due to the space charge. Space charge collectors need to be rigidly mounted on very good insulators as in humid conditions the surface insulation can easily break down. Electrical noise from piezoelectric effects can be caused when connecting cables suffer from stress changes.

Despite all these difficulties a great amount of equipment has been developed to measure space charge concentrations, and VONNEGUT and MOORE (1958) have published a review of instruments and techniques.

METHODS OF MEASURING SPACE CHARGE

One of the first methods was described and used by LORD KELVIN in 1859, 60 and 62. With the aid of a spirit lamp whose flame acted as a 'collector' by bringing the lamp to the potential of its surroundings, he was able to detect the presence of space charge which he had produced from the flame of a similar lamp connected to a Wimshurt machine some distance away. He observed this charge by noting the change in potential of the spirit lamp which was acting as the collector. Later Kelvin pointed out that if water is sprayed from an insulated metal nozzle then the nozzle is brought to the potential of the surrounding air. Using this principle he determined the potential of the air at certain points and he deduced that variations were due to the movement of space charge in the air. He further suggested that by measuring the potential gradient from a balloon as well as at the earth's surface a knowledge of the space charge between would be gained. However he assumed that the earth was a negatively charged body losing its charge to the air in contact with it.

The use of the water-dropper as a potential equilibriser and its action can be explained as follows. Consider a drop of water on the end of an insulated nozzle with the potential of the surrounding air differing from that on the drop. Lines of force must therefore end on the drop. If the potential of the air is positive with respect to the drop then these lines of force have their negative ends on the drop and their positive ends in the surrounding air or on the electrosphere. As the drop falls off therefore it carries away a

negative charge and the potential of the nozzle will rise to a value nearer to that of the surrounding air. As the process continues the nozzle will eventually reach the potential of the surrounding air which can therefore be measured. Kelvin suggested that by using an earthed wire cage enclosing a water dropper at the centre, the potential at this point would indicate the space charge concentration in the cage. This method will be discussed later in more detail; it was used by CHAUVEAU (1902), MACHE (1903) and more carefully by KÄHLER (1927), MÜHLEISEN and HOLL (1952) and KIRMAN (1954). At Bad Aibling DAUNDERER (1907) measured space charge by placing three spirit lamps whose flames were acting as collectors at 2 m, 1 m and ground level and measured the difference between the potentials of the lamps with the aid of two gold leaf electroscopes. Then using Poisson's equation as applied to two infinitely long parallel conducting planes (Chapter 1) the space charge could be calculated. NORINDER (1921), at Uppsala, measured the potential at 1 m, 2 m and 3 m above the ground by spraying water horizontally from jets fixed at the centre of insulated horizontal wires and calculated the space charge between them. SCRASE (1935) also used stretched wires with collectors at the middle points and measured the difference in potential between two wires 1 m apart at different heights.

OBOLENSKY (1925) and later BROWN (1930) used direct methods of measuring space charge in which they sucked air through a cylinder containing steel wool. The cylinder, which was connected to a Dolezalek electrometer, was carefully screened from potential gradient

changes. This method will later be examined in greater detail. Vonnegut and Moore (1958) described a method of direct collection of space charge by making the air in an insulated shielded tube highly conductive. Air containing the space charge to be measured is then sucked through the tube and by the action of its own electric field the space charge will migrate to the walls where it is collected and measured. The air in the tube can be made highly conductive by heating or irradiating with α , β , γ or X-rays.

SMIDDY and CHALMERS (1958 and 60) used double field mills to investigate the space charge concentrations. The mills were automatically brought to the potential of their surroundings and by registering the potential gradient the space charge concentrations could be calculated.

Three types of modern space charge collection will now be considered in greater detail. These are the electrical collection using ion-counters, the cage method and filtration method.

1. Electrical Collection

If air is passed through a cylindrical air condenser across which there is a sufficiently high potential difference to attract all the ions of one sign to the central electrode, then the charge collected can be measured with the help of an electrometer. In order to measure space charge however two condensers (ion counters) are needed, one to measure positive ions and the other to measure negative ions. If there are n_+ positive ions cm^{-3} and n_- negative ions cm^{-3} then $(n_+ - n_-)e$ gives the charge density. There is however

likely to be a very serious error unless the values of the air flow and ion concentration are measured to an accuracy of 0.01%. In town air we can expect that at least 10^4 ions cm^{-3} of each sign will be present with a net space charge density of 10^2 ions cm^{-3} or less. Therefore an error of only 1% in the airflow or ion concentration will completely mask the space charge density.

2. Determination of space charge using earthed wire cages

Space charge can be determined by enclosing the volume of air under examination within the walls of a conducting material, and then the potential at a point in the volume is a measure of the space charge density present. Such a cage is named after Michael Faraday who showed that inside an earthed cage there was no effect from external field changes. Three methods in this category will be described, they are by measuring, (a) the surface radial field, (b) the potential difference between the centre and edge and (c) the charge on a sphere at the centre.

The use of a wire cage requires a free flow of air through it otherwise the field set up within the cage could remove some small ions. Another requirement is that the potential equilibrates in the cage should not be affected by the potential gradient outside the cage. This could happen in two ways. Firstly, in high values of potential gradient a large mesh would not be an effective shielding whereas a small mesh would impede the air flow, and secondly the bound charge on the cage created by the earth's field could filter out charges of one sign on entering the cage. Both these effects

would give rise to high values of space charge which could account for the values observed by Kähler.

a) Space charge determination by the direct measurement of field at the surface of a spherical wire cage.

For a spherical cage of radius r containing space charge of uniform density ρ , Poisson's equation in spherical co-ordinates reduces to

$$\frac{1}{r^2} \frac{\partial}{\partial r} \left(r^2 \frac{\partial V}{\partial r} \right) = - \frac{\rho}{\epsilon_0}$$

thus
$$r^2 \frac{dV}{dr} = \int - \frac{\rho r^2}{\epsilon_0} dr$$

and as
$$\frac{dV}{dr} = 0 \text{ when } r = 0$$

then
$$r^2 \frac{dV}{dr} = - \frac{\rho r^3}{3\epsilon_0}$$

If E_r is the surface radial field then $-\frac{dV}{dr} = E_r$ and so

$$E_r = \frac{\rho r}{3\epsilon_0}$$

A suitable instrument for measuring this potential gradient is a field mill (described later), but the sensitivity of such an instrument is only about 1 Vm^{-1} . Thus in order to detect a charge density of 10 ions cm^{-3} ($1.6 \times 10^{-12} \text{ Cm}^{-3}$) a sphere of radius 15 m is needed which is inconveniently large. This method is therefore unsuitable for measuring space charge gradients close to the earth's surface unless a far more accurate instrument for measuring the potential gradient is used. MÜHLEISEN and HOLL (1952) suggested

that a cubical cage and a spherical cage of the same volume would give roughly equal results.

b) Space charge determination by measuring the potential difference between the centre and edge of the cage.

Charges inside the cage will produce a potential difference between the edge and centre of the cage. This can be measured by placing the point of an insulated probe at the centre of the cage and the potential difference can be recorded using a vibrating reed electrometer. The presence of this probe, however, introduces three difficulties. In the first case the probe will considerably alter the boundary conditions and therefore the solution of Poisson's equation for this method is no longer straightforward. Secondly, there will be a contact potential difference between the probe and the cage, and finally the probe will not be at the potential of the centre of the cage due to the low conductivity of the air.

To explain contact potentials it is first necessary to consider the work function. This is the amount of energy needed to remove an electron from inside a metal to a point outside it. The value of this work function differs from one metal to another and so there will be a difference of energy between electrons just outside two metals in contact. Considering a parallel plate condenser with one plate of, say, zinc and the other of copper, then as zinc has a lower work function than copper it is more positive. Thus when the plates are connected directly together with wire there will be a difference of

energy on either side of the condenser gap and hence a potential difference exists. If e is the electronic charge, ϕ_{cu} and ϕ_{zn} the work functions of copper and zinc respectively, then this potential difference is $(\phi_{cu} - \phi_{zn})/e$. Even if the condenser plates had been made of the same material these contact potentials would not be eliminated as dirt or other deposits on the plates affect the field between them.

In the cage and probe method therefore one conductor will be charged relative to the other and a field will exist in the cage even in the absence of space charge. This contact potential, which can be determined empirically, can be of the order of a few tenths of a volt and will therefore be of similar order to the potential due to the space charge. As it is also dependent on the nature of the surface of the material it must be re-determined from time to time.

The third difficulty mentioned was the fact that the probe will not be at the potential of the centre of the cage due to the low conductivity of the air. This can be overcome by attaching a glowing fuse or small α -source to the probe but as these could affect the potential gradient in the cage a much better method is to use a water dropper as a potential equaliser. Such an arrangement can be made which allows the probe to reach the potential of its surroundings within 30 secs.

c) Space charge determination by measuring the charge on a sphere at the centre of a cage.

It can be shown that if a small conducting sphere is placed concentric with a much larger Faraday cage then there will be a charge on the small sphere dependent on the space charge. A water-dropper insulated from the outer cage can be used as the central sphere. As the drop breaks away from the probe at the centre of the cage it carries with it a charge related to the space charge in the cage. It falls through the outer cage and is collected and measured by an external instrument. This type of space charge measuring unit has a time constant dependent only on the response time for measuring the charge on the drop and is probably the most satisfactory of the Faraday cage methods. KIDMAN (1954) compared this method with the Obolensky filter method and found good agreement.

3. Filtration methods of determining space charge

Obolensky first introduced this method when he sucked air through a tightly packed filter of steel wool which collected the ions present in the air. The filter was electrically insulated and the charge collected on it was measured directly.

Using present day techniques this charge can be measured with the aid of a vibrating reed electrometer, but doubts have been expressed as to whether such a filter will collect all the atmospheric ions. Steel wool fibres are approximately 50-100 microns in diameter

and there is a great possibility that the much smaller charged particles will completely evade detection. However when the flow of air through the filter is sufficiently slow there is a possibility that all the ions will be able to reach the filter fibres by diffusion. A difficulty arises because large ions have a mobility of approximately 30 microns sec^{-1} per V cm^{-1} and as the only electric field in the filter is probably due to that provided by the ions themselves then the time for the ions to migrate to the fibres is inconveniently large. If the air flow through the filter is consequently reduced the amount of current measured will therefore be extremely small.

Vonnegut and Moore (1958) suggest that ambiguities may also arise from charge being transferred to the nuclei by contact potential differences and by frictional effects as they pass out of the filter. These effects would give rise to an opposite polarity charge arriving on the filter.

Vonnegut and Moore have investigated a glass wool filter with fibres 0.5 to 3 microns in diameter and as the fibres are up to 100 times smaller than those in steel wool its filtration properties are far superior. The relaxation time of glass wool, which is normally considered an insulator, is less than 1 min. but immediately it captures a charge the aluminium case surrounding the filter has an identical charge induced on the outside from where it is measured.

There is a possibility that the charge on the filter will repel particles having charges of like sign and therefore record an excess of charges of opposite sign. But this equilibrium charge is normally quite small and so this disadvantage can be neglected. If necessary however this charge can be reduced by obtaining a filter with a shorter relaxation time or by putting a conductive coating on the fibres.

A filter is now available that is composed of a glass-asbestos medium which has a much shorter relaxation time than glass wool alone. This filter has a higher effectiveness in removing particulate matter from the air than the all glass medium. The high effectiveness arises from the smaller diameter of the asbestos fibres; in presence of liquid water, however, the asbestos fibre absorbs moisture and becomes pulpy and spray electrification will be produced as the bubbles break at the downstream surface.

As this direct method of measuring space charge appears to be more suitable for fine weather space charge gradient measurements than any other collector, and because of the manufacturer's claims that the glass asbestos filter medium has such a high collection efficiency in cleaning air, it was decided to investigate its properties more closely in connection with this research project at Durham.

However, as the collectors were to be installed on an earthed 21 m mast there was a possibility that as the electrostatic shield would be at earth potential and not at the potential of the surroundings, then charges of the same sign as the potential gradient may be

attracted to the cover near the inlet. This would lead to an erroneous high value of space charge, but it was assumed that by having a small orifice at the intake then the velocity of air drawn into the collector would be high enough to overcome this difficulty, even in the very much enhanced field at the top of the mast. The problems arising from this will be discussed in Chapter 8.

PREVIOUS RESULTS

The most accessible part of the atmosphere in which to study space charge magnitudes, distributions and causes is the lowest few metres, and yet very few investigations have been made in this region.

Using the flame collector method already described, Dauderer, in 1906, measured a mean annual value of space charge of $+250 \text{ e cm}^{-3}$ in the first 5 m of the atmosphere. He claimed that the winter average was approximately -1000 e cm^{-3} and the summer average approximately $+1200 \text{ e cm}^{-3}$, but SMIDDY (1958) has shown that the errors in Dauderer's calculations are considerable. Norinder's measurements in 1921 gave a mean annual space charge of -400 e cm^{-3} with once again a more negative value in winter than summer. Scrase found positive space charge in turbulent air and also in still air above 5 m but below this level in still air he found negative charge. Kähler, Obolensky and Brown all obtained positive values in winter months with lower values in summer, Obolensky's even becoming negative. Kähler's values ranged from $+400 \text{ e cm}^{-3}$ to $+1200 \text{ e cm}^{-3}$ but these could perhaps be attributed to his cage method of measurement. The filter methods of measuring

space charge gave Obolensky values between $+120 \text{ e cm}^{-3}$ in winter and -200 e cm^{-3} in summer and Brown values of between $+150 \text{ e cm}^{-3}$ in winter and $+210 \text{ e cm}^{-3}$ in summer.

Several observers have suggested that these more negative results obtained in summer are due to negatively charged dust particles raised up from the surface into the air. It seems reasonable to assume therefore that all the differences in results could be due to the different localities of the observing stations, the main factors being their position with respect to large towns and the prevailing wind directions.

With regard to the more recent space charge measurements MÜHLEISEN in 1959 at Weissenau found that space charge was related to the formation of mist and fog, and the evaporation or condensation of water. In order to explain these effects he later carried out experiments in a closed room where he had installed a filtration space charge collector. During these tests he found that the evaporation of water caused a negative space charge and by warming the air a positive space charge was produced. These effects only occurred when the relative humidity was greater than 65% and they became stronger if the air contained more condensation nuclei. From these results Mühleisen concluded that they explained the negative space charge observed during fog and the formation of positive space charge at sunrise.

CHALMERS (1952) has however found conclusive evidence that negative space charge is formed at high tension cables during periods of mist and fog. This, he explains, is due to the production of an

excess of negative ions where insulation is partially breaking down.

MÜHLEISEN (1957^b), using transportable instruments, found that clouds of space charges were produced by domestic fires, industry and traffic. These space charges could be carried more than 20 Km from their sources depending on the speed of the wind. In addition, he carried out extensive experiments in the laboratory measuring the signs of space charges produced by man made sources.

In 1959 BRASEFIELD, after measuring the atmospheric potential at 33 m, 21 m and 8 m respectively above the ground, also reported that his measurements had indicated clouds of positive or negative ions frequently passing overhead at a height of 10 m or less. He suggested that these clouds could be produced by exhaust fumes from motor vehicles. Later in the same year (1959b) he carried out tests using a wire mesh Faraday cage with exhaust fumes from motor vehicles. These were found to be generally positively charged, but diesel fumes were always very strongly positively charged. In order to explain these phenomena he measured the potential of a moving motor vehicle with respect to earth and to his surprise found it was always negative independently of whether the engine was running or not. It appeared therefore that the charge on the exhaust gases was due to contact potential differences between the exhaust pipe and particles in the exhaust such as water. In further tests he enriched the mixture so that black smoke was produced from the exhaust; this showed negative space charge suggesting that the carbon particles were negatively charged.

Sniddy and Chalmers in 1960, using double field mills, found slight negative values of space charge in the lowest 5 m of the atmosphere and associated this with radioactive effects from the earth, which CHALMERS (1946) suggested would greatly reduce any electrode effect. This suggestion by Chalmers that the electrode effect would be difficult to measure over land led MÜHLEISEN (1960) to make measurements over both Lake Constance and over a flat meadow. He found that such an effect existed to an altitude of 10 m above the surface of the lake but was non-existent over land. PLUVINAGE and STAHL (1953) found evidence of the electrode effect over the Greenland ice-cap where the 3000 m thick ice presumably cuts off all the radioactivity effects from the earth's crust.

AIKINS however in 1959 found that the electrode effect with small ions was readily observable over land at 110 cm for potential gradients exceeding 500 V m^{-1} . He also found large fluctuations of space charge in fine weather and changes of sign were not uncommon. This meant that to make an estimate of the mean fine weather space charge was difficult but it was probably about $+12 \text{ e cm}^{-3}$. In mist he recorded values up to -600 e cm^{-3} even with a positive potential gradient. In 1963 CROZIER concluded that an electrode effect existed over land during night-time low-wind periods. By measuring space charge at the surface of the earth he found a shallow layer of enhanced space charge of up to 4000 e cm^{-3} which was not registered at 65 cm above the ground. This space charge density was inversely

correlated to wind velocity especially where the latter was below 1 m sec^{-1} . Winds greater than this value, and the turbulence effects as the sun shone, largely eliminated this effect. LAW (1963) found that if he assumed that the convection current was negligible and therefore the conduction current was constant with height, then the variation of the field in the lowest metre of the atmosphere, calculated from the change in conductivity, disagreed with the space charge he observed directly. This implied the existence of a convection current comparable to the conduction current.

SAGALYN and FAUCHER (1956) investigated the nucleus concentration in the air at altitudes between 700 ft and 15,000 ft. They reported that regular variations of nucleus concentration in the exchange layer were observed from around sunrise to early afternoon, and after analysing meteorological data they discovered that this variation was due to the daily turbulent cycle.

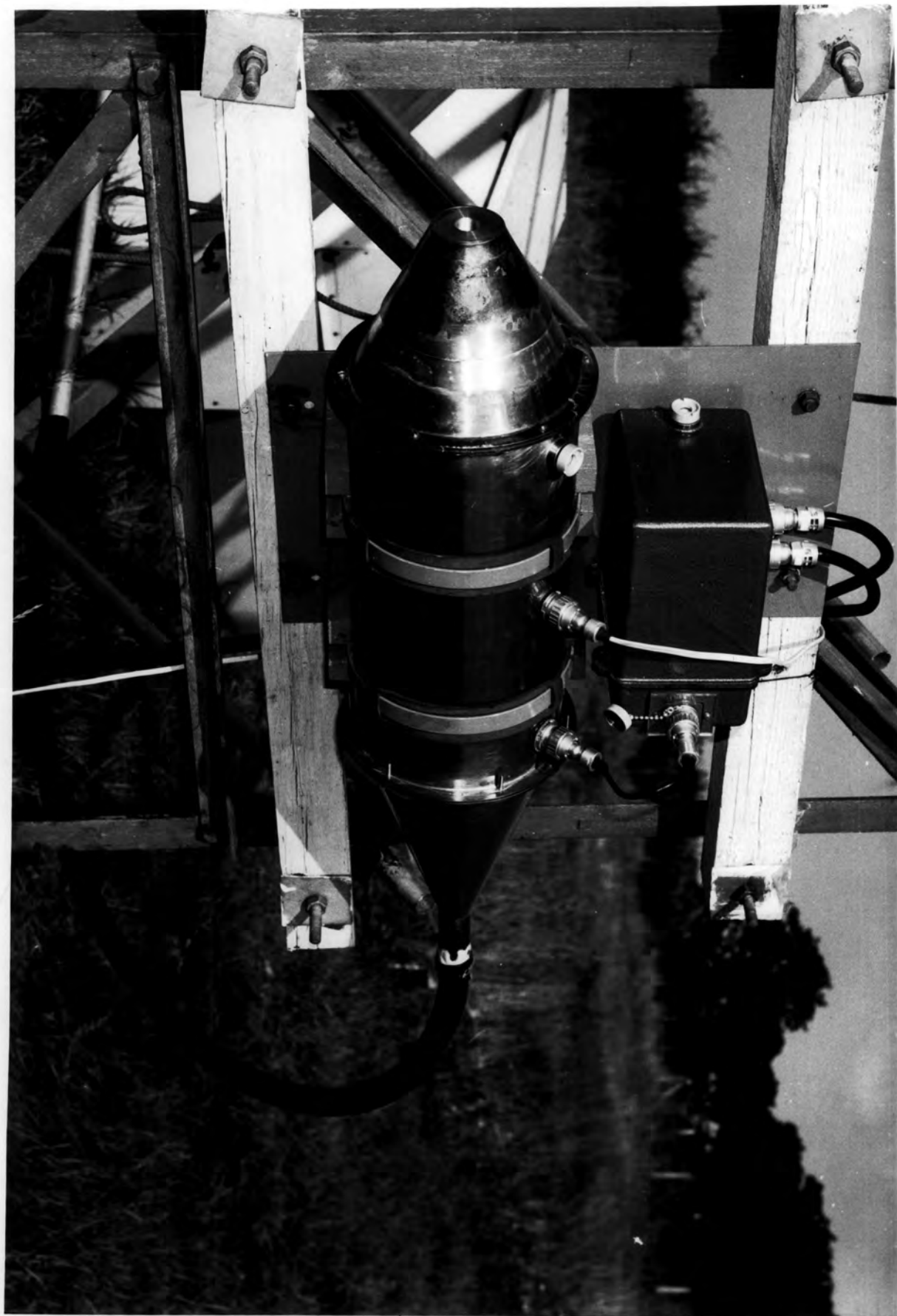
If the space charge in the lower atmosphere is responsible, during convective activity, for the initiation of electrification in cumulus clouds then the sign of the potential gradient below the cloud is dependent on the polarity of the charge entering the cloud from below. This prompted VONNEGUT, MOORE, SEMONIN, BULLOCK, STAGGS and BRADLEY (1962) to produce artificially high concentrations of space charge at the surface of the earth. By then recording the potential gradient just below the newly forming clouds they found conclusive evidence that convection currents carried this artificial charge upwards into the cloud.

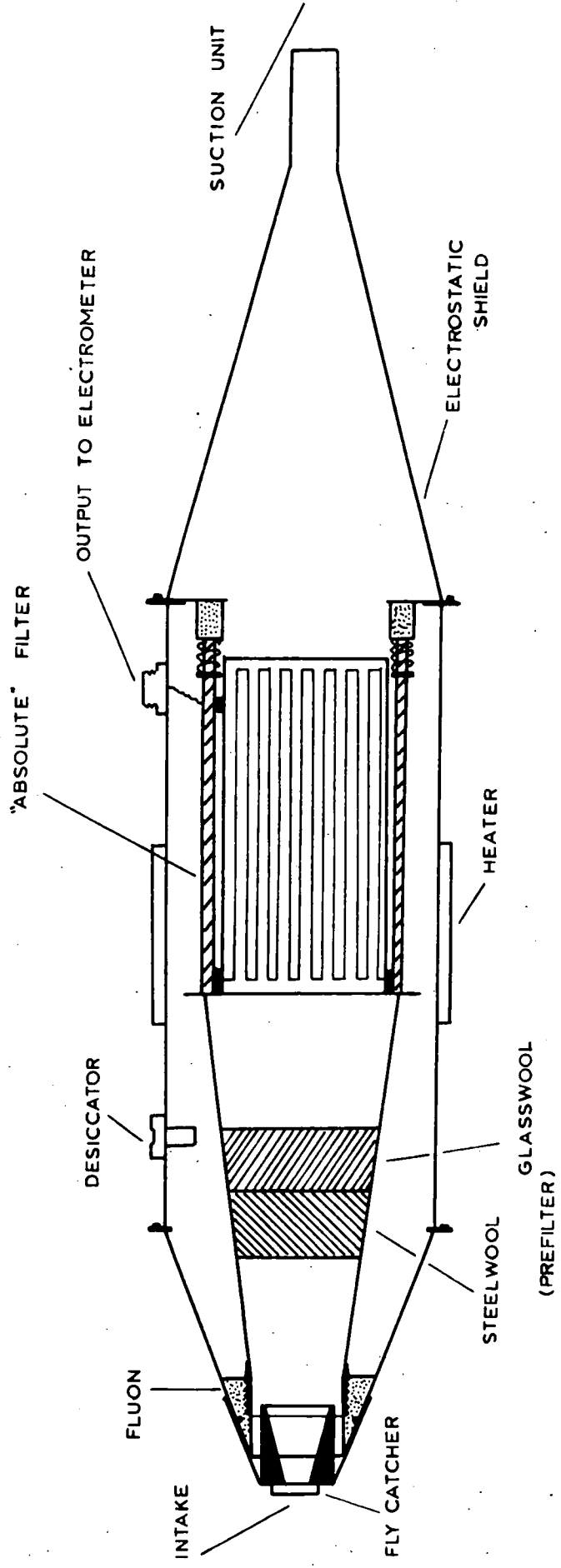
Finally KRAAKEVIK (1958) reported that in the exchange layer over the oceans a convection current existed that was probably caused by the upward diffusion of positive space charge. This, he said, decreased as altitude increased and had its maximum value at, or below, 15 m.

For the project here at Durham in which the space charge gradient was to be measured using a 21 m mast, these previous results introduced a possibility that convection currents may be detected with the space charge measurements. Hence it was decided to record the temperature, humidity and horizontal wind gradients over the height of the mast in addition to the space charge and electric field gradients.

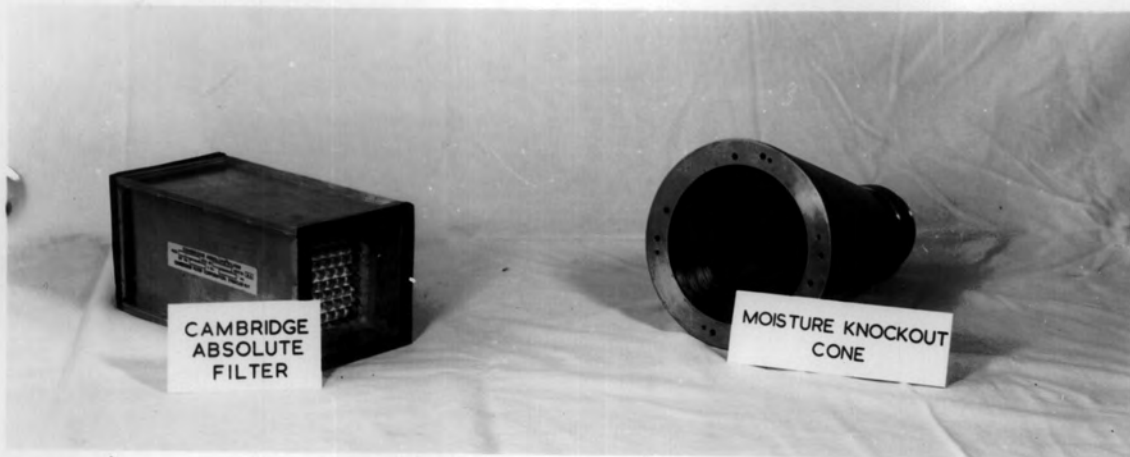
In the first phase of the project the space charge would be measured at 1 m and 2 m in order to measure the gradient close to the surface, and in the second phase at 1 m and 19 m to try and detect convection currents. Temperature and humidity would be measured at 4 different levels and potential gradient and wind at 2 levels.

FIGURE 1.

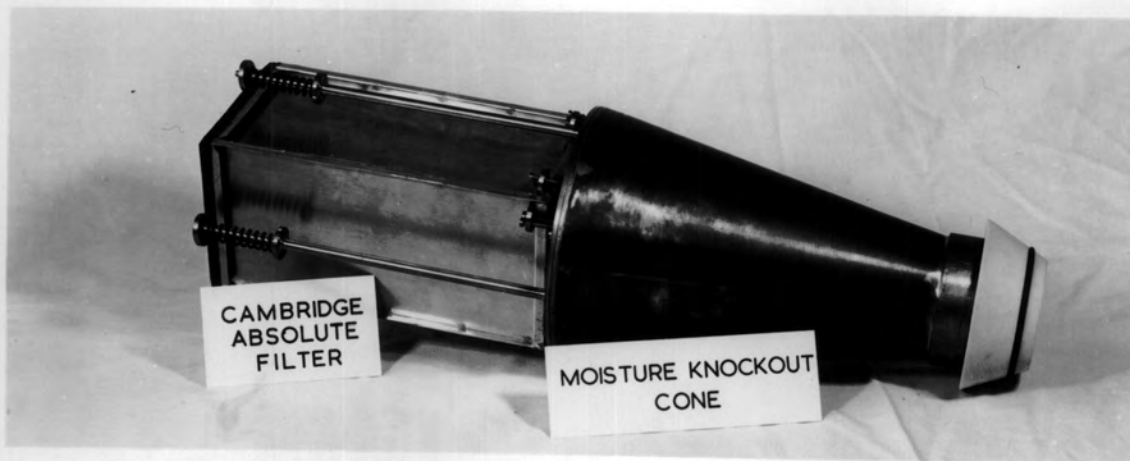




SPACE-CHARGE COLLECTOR.



(a)



(b)



(c)

FIGURE 3.

CHAPTER 3

THE ABSOLUTE FILTER SPACE CHARGE COLLECTOR

In view of the disadvantages described in the previous chapter with regard to the many different methods of measuring space charge it was decided to investigate the effectiveness of the glass-asbestos filter medium more closely.

The filter cartridges (model no's IF-20-2S) were manufactured by the Cambridge Filter Corporation, Syracuse, New York and were an improvement of the medium originally developed for the Atomic Energy Commission for removing radioactive dust from the air. The filter material was encased in an aluminium frame of dimensions 10 cm x 10 cm x 20 cm which in turn was housed in a copper tube acting as an electrostatic shield. A photograph of the collector in position on the mast at the Observatory and a schematic diagram are shown in Figs. 1 and 2, whilst photographs of the collector before assembly are shown in Fig. 3. The filters were extremely light in weight and there was no difficulty of having to build elaborate insulated supports to hold them central inside the electrostatic shield. The rest of the filter apparatus was made out of copper and brass with polytetrafluoroethylene (P.T.F.E. or fluon) insulators. The outer cylinder was constructed of half-hard 18 gauge copper, the cones of soft 18 gauge copper which makes them easily workable, and the connecting discs of 1/8th" brass plate.

Prefilters were contained in the moisture knockout cone and were wedged inside copper gauze which was in turn screwed onto brass discs soldered inside the cone. Two different materials were used in the construction of this prefilter. The first medium was stainless steel wool which helps to remove large hygroscopic particles that would damage the Absolute filter and the second medium was of glass fibre filaments held together with an organic binder. This second medium, which could easily be replaced, helped to remove the dust particles drawn into the instrument, thus increasing the life of the filter cartridge. A check must however be kept on the air flow rate through the collector as the pressure drop across the filter rises with use. The medium thereby maintains and improves its excellent filtration properties.

A rubber gasket was fitted on the edge of the aluminium frame to be screwed to the moisture knockout cone thus making a good seal and preventing space charge from bypassing the Absolute filter.

The filter unit had now to be insulated from the electrostatic shield and P.T.F.E. was selected for this purpose. The maintenance of good electrical insulation is important, not only because a film of water could possibly settle on the exposed insulator but dirt settling on it could also cause breakdown. A liquid recommended for cleaning P.T.F.E., namely trichloroethylene, was therefore obtained and a final cleaning performed using absolute alcohol. The surface of this insulator conducts far less than polystyrene under conditions of high humidity, as continuous films of water do not form on it very easily.

Another advantage of P.T.F.E. is that piezoelectric effects are negligible. The reason is that during manufacture the crystals are heated to a temperature high enough to allow the individual particles to coalesce and form a continuous amorphous structure. The material builds up a static charge quite easily however, and this has often been mistaken for piezoelectric effects. Originally the P.T.F.E. intake was exposed to frictional effects due to the air being drawn through the collector, and thus it gained quite a large static charge which removed a great proportion of the ions before they entered the instrument. To remedy this, instead of exposing the surface temporarily to a small source of γ -radiation, an earthed copper shield was placed in the intake covering the insulation but allowing a $\frac{1}{4}$ cm gap between the two materials so as not to reduce the high insulation already gained.

Four tightly sprung brass rods were fastened to the moisture knockout cone (Fig. 3b) and a rubber 'O' ring placed in a slot cut out of the P.T.F.E. nose cone. Thus, as the rear of the electrostatic shield (Fig. 3c) was screwed onto the main cylinder of the shield it caused the filter unit to be very firmly held in place, the 'O' ring preventing any air from bypassing the filter unit.

A wire was connected from the aluminium frame of the filter and led to a Plessey socket on the earthed shield. The coaxial plugs and sockets had been chosen because the P.T.F.E. insulation area was large, for leakage could interfere seriously with the results.

As the collectors would be out of doors for a considerable period of time it was decided to place heating elements and a silica-gel desiccator on the interior of the electrostatic shield. The desiccator had an indicator unit which changed from blue to pink as the moisture content in the air rose. This was a precaution against the filter medium becoming damp and causing extra electrification as bubbles form and break on the downstream surface (VONNEGUT and MOORE 1958).

The heating elements used were two electric soldering iron elements placed in series and connected to the mains supply via another Plessey socket. These elements were switched off and earthed prior to records being taken. However, during field testing of the equipment it was found that the heat supplied by these elements was insufficient and they also gave rise to slight earth currents which appeared on the records. For these reasons the elements were removed and lagged pipe heaters were wrapped around the outside of the electrostatic shields. These pipe heaters consisted of plastic covered heating wires advertised for domestic installation to prevent water pipes from freezing during winter months. The length of each wire was 20 ft and the loading 100 watts. Felt lagging was wrapped around the cylinder after the wires had been positioned and this area then covered with polythene to prevent saturation by rain.

The size of the orifice at the air intake is extremely important if readings are required during gusty conditions. With a wide intake orifice erratic values have been recorded during gusts. If air is not entering at a velocity greater than the highest wind speed, erroneous results will be observed as the air deposits its charge and returns through the intake, hence evading detection in the flow measuring equipment to the rear of the filter. This condition could be overcome by reducing the size of the orifice. Hence a brass sleeve was inserted in the earthed tube at the entrance. This sleeve was inserted in the earthed tube at the entrance. This sleeve had a conical hole cut through it as can be seen in Fig. 2; the hole having dimensions related to the speed of the air intake necessary. With this method it is possible to retain a constant volume of air flowing through the filter under all conditions. Excellent results have been obtained during wind gusts of up to 20 m sec^{-1} .

Indication of disturbances in the measuring apparatus caused by large insects have been found and precautions taken to stop them from occurring. If a large fly is drawn into the equipment and then attempts to escape it could well land on the earthed intake cone and then be sucked back into the filter which is not quite at earth potential. In a period of excitement this process could occur quite often as the insect bounced from one conductor to another. On occasions where erratic readings have occurred a large fly has been found in the equipment. The smaller insects do not affect the result as they do not have the strength to return to the earthed outer cone.

In order to stop this activity a $\frac{1}{2}$ cm wire mesh was placed across the entrance with the diameter of the wire less than 1% of the mesh spacing. This would cause a negligible migration of ions to the mesh in passing into the air intake and would practically eliminate displacement currents. The mesh was removed when the collector was not in use and the hole blocked with a rubber bung to prevent rain from entering. It was found unnecessary to have a 'fly catcher' on the collector at the top of the mast. To enable the collector input hole at this 18 m height to be blocked without climbing the mast a spherical brass bung was loosely fixed on one end of a pivoted arm. This could be swung into position by pulling a long length of wire attached to the other end.

The space charge collectors and their respective vibrating reed electrometer head units were fixed side by side on a $\frac{1}{8}$ " steel plate for easy erection on the mast. Air was drawn through the filter using a powerful extractor fan with provision for altering the speed of the motor by voltage regulation. The flow rate was measured using standard gas meters with an accuracy of 1% which were modified to give a continuous record electronically some distance away.

The glass asbestos filter medium being almost non-conducting gives the impression that there will be a delay in the recording of the trapped charge. This is not so, for as soon as a charged particle is caught in the filter it attracts an equal and opposite charge on the inside of the filter housing. In turn, this liberates a charge equivalent in every respect to that on the trapped ion on the outside

of the housing whence it is immediately measured. The charge on a particle caught in the steel wool filter is measured directly and connected to the same output terminal.

This out of balance current flows to earth through a 10^{12} ohm resistor and the voltage across this is measured using a vibrating reed electrometer. Negative feedback in the amplifier reduces the effective input resistance to about 10^{10} ohm. Thus insulation requirements of 10^{13} ohm between the filter housing and the electrostatic shield are not excessive. With such an instrument giving a full scale deflection of 3 mV it is possible to record a space charge of 6 ions cm^{-3} full scale for a flow of only 3 litres sec^{-1} .

A time constant of 10 sec was placed on the input to the recording equipment in order to smooth out the erratic fluctuations in the space charge concentration (ADKINS 1959).

The manufacturers of the vibrating reed electrometers recommend that the cable length between head unit and space charge collector be less than 2 ft to reduce the noise level. Anti-microphonic cable was used but in high winds this gave rise to piezoelectric effects. To overcome this difficulty the cable was passed through a $\frac{3}{8}$ " diameter copper pipe which was soldered to the plugs on each instrument. Another disadvantage in high winds was that the steel plate, although apparently rigidly fixed, bent slightly which again gave rise to piezoelectric effects in the connecting cable. The plate had therefore to be strengthened using 1" x $\frac{1}{2}$ " steel angle to prevent bending.

An aluminium cover was placed over the head unit to protect it from precipitation as moisture caused insulation breakdown in the cable connections to it.

During initial testing it was observed that both collectors gave similar slight fluctuations in output whilst no air was being sucked through the units. The possibility of earth currents being the cause was ruled out as the collectors were insulated from the mast, but it was later noticed that these effects coincided with the sun being covered and uncovered by clouds. On placing a heating element close to the copper pipe surrounding the head unit input cable the same effect was noticed and it appeared that the very slight expansion in this pipe caused movement in the cable and therefore piezoelectric effects. The copper pipe and cable were normally under considerable tension and the actual expansion of the pipe was audible as 'clicks'. The aluminium cover for the head unit was therefore extended to provide an umbrella for the copper pipe and the fluctuations in the output disappeared.

A possible cause of error whilst recording lay in the geometry of the instrument. The distance between the P.T.F.E. shield and the inner copper cone was only of the order of $\frac{1}{4}$ cm and during periods of very high space charge the potential difference between the two could be of the order of 1 v. A potential gradient of 4 V cm^{-1} would therefore exist and there would be a possibility that some ions would be attracted to earth without being registered in the recorder. The small ions would have a velocity of approximately 8 cm sec^{-1} in this

potential gradient and thus the airflow near the edge of the filter must be large enough to prevent very much migration. The diameter of the orifice at this point was 5 cm and with an airflow as small as 1 litre/sec the velocity of the ions due to the airflow through the filter is very much larger than the velocity due to the potential gradient, and hence this source of error can be neglected.

In order to calculate the space charge collected by the filter, assume the concentration to be n elementary charges cm^{-3} ($e \text{ cm}^{-3}$). Let the airflow through the filter be $Q \text{ cm}^3 \text{ sec}^{-1}$ and I the current in amperes recorded with the vibrating reed electrometer.

Then

$$n = \frac{I}{1.6 \times 10^{-19} Q} e. \text{cm}^{-3}$$

where 1.6×10^{-19} is the charge on an electron in coulombs.

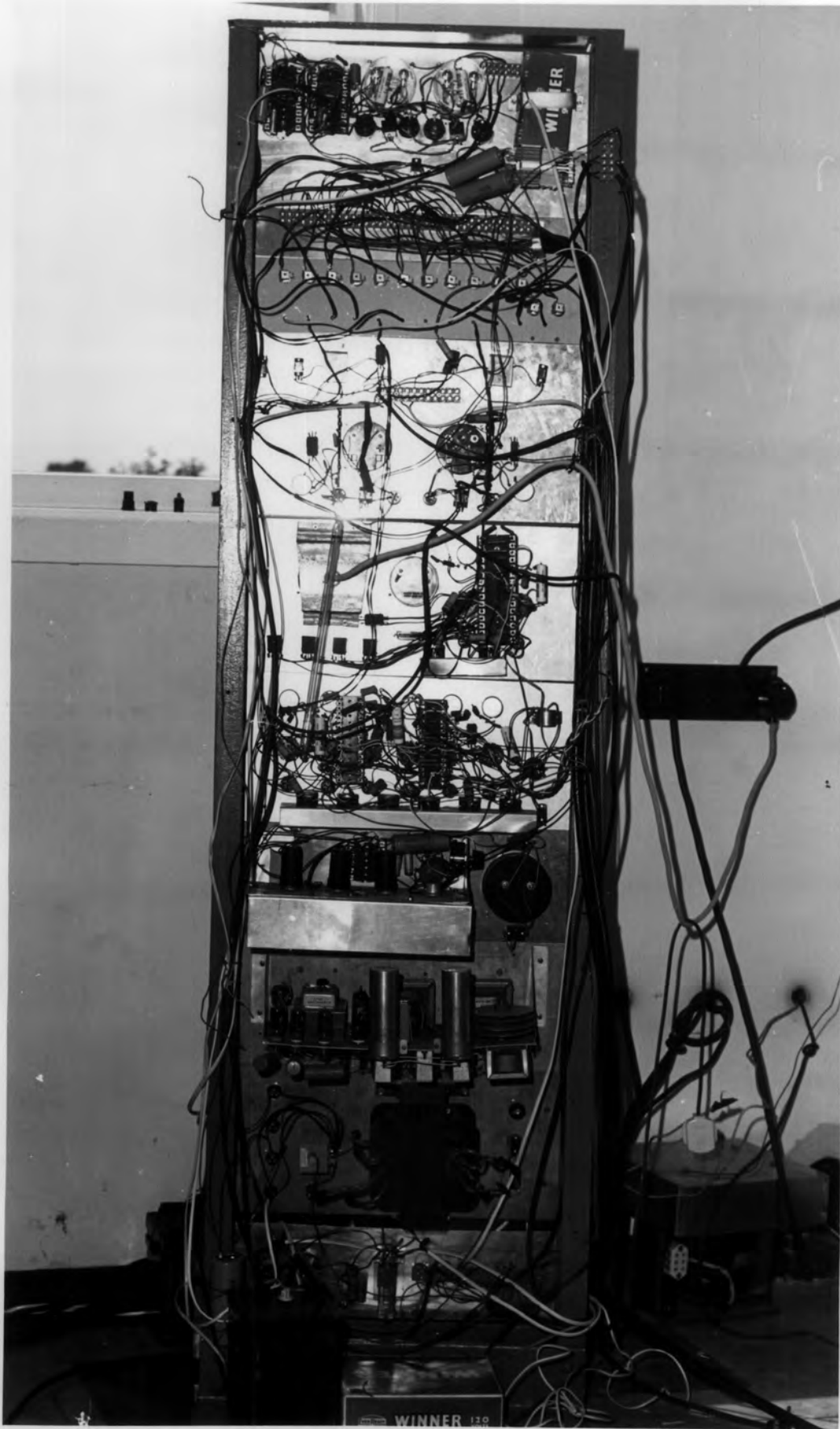


FIGURE 4.

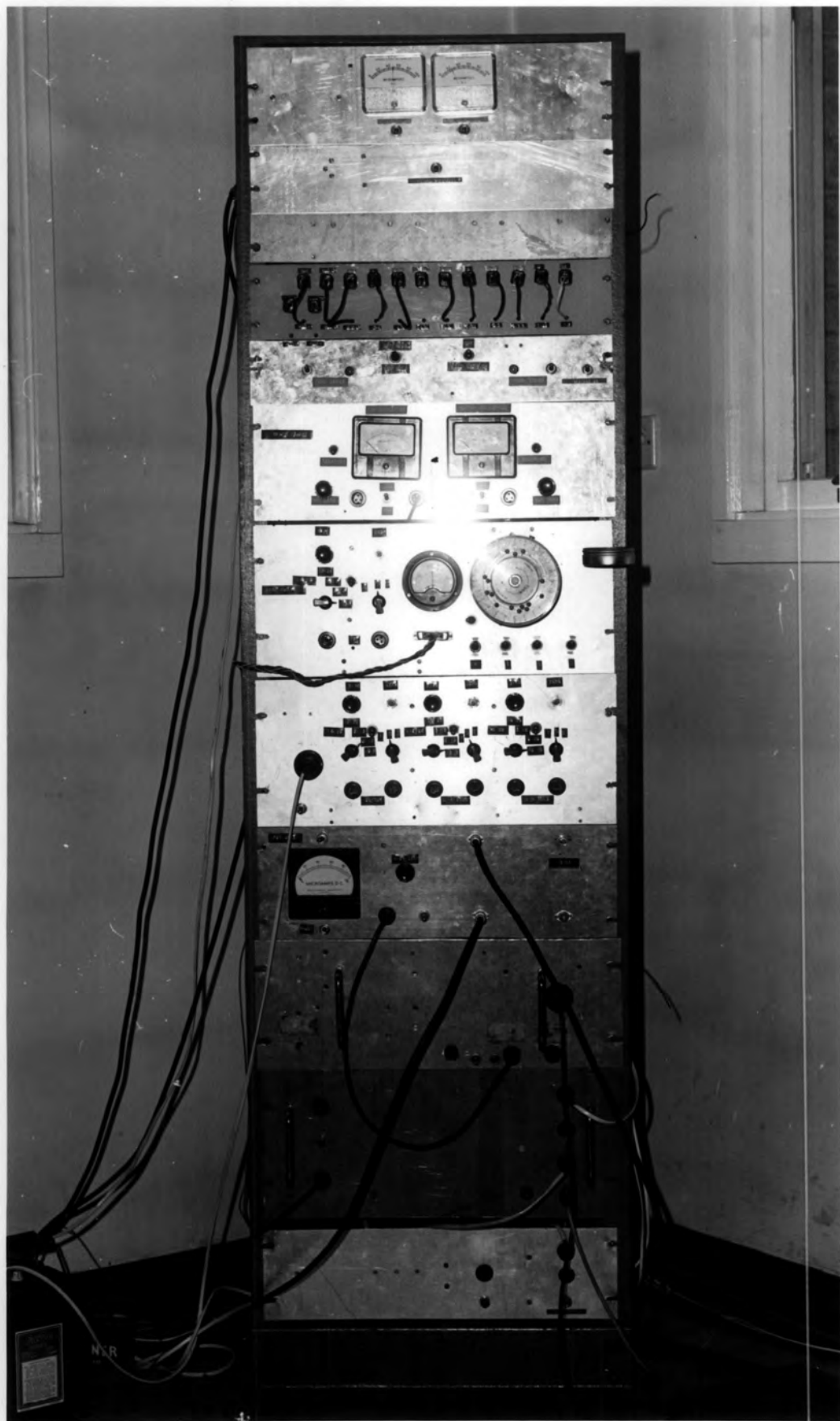


FIGURE 5.

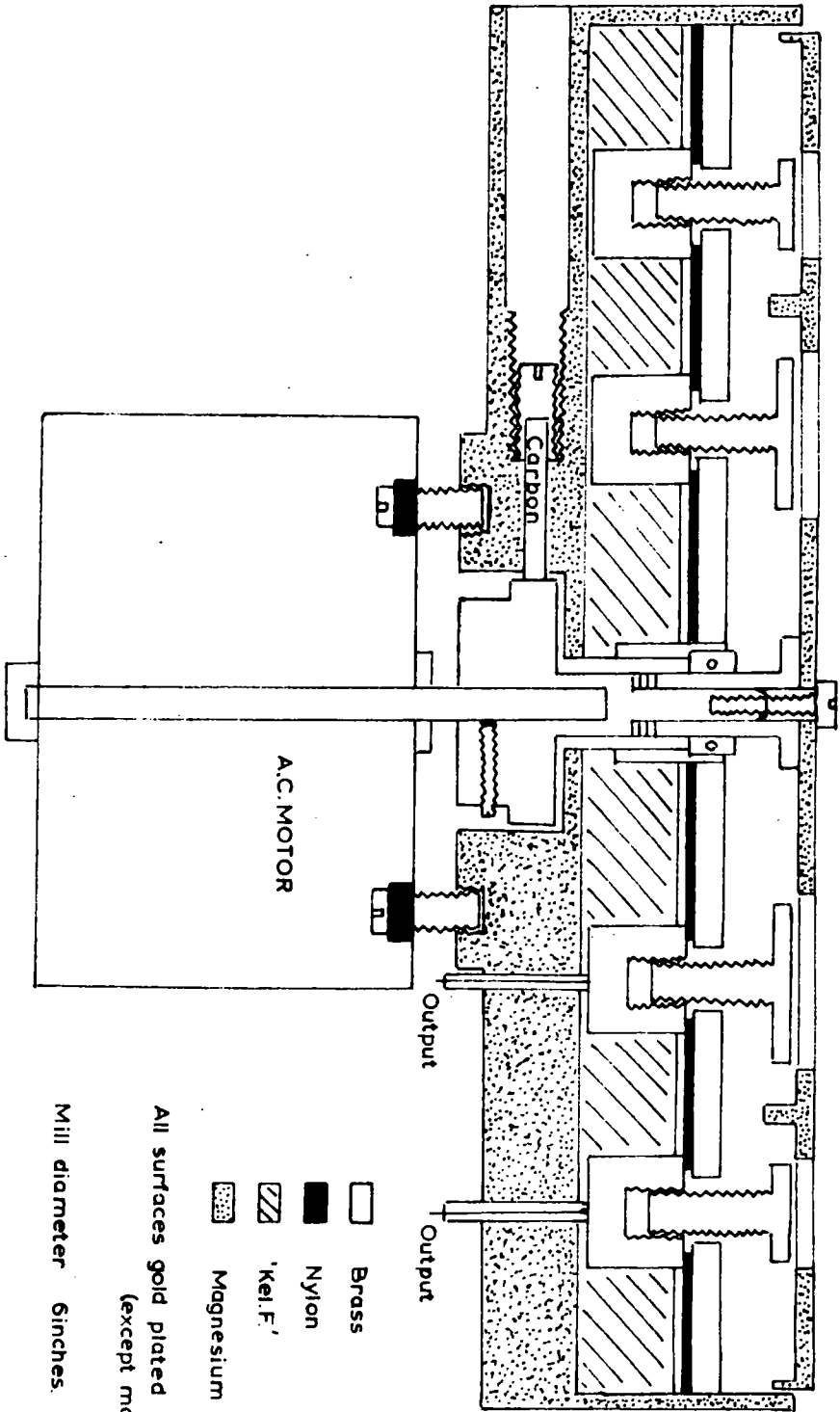
CHAPTER 4

DESCRIPTION AND CALIBRATION OF OTHER EQUIPMENT

The recorder to be used was a $\pm 2\frac{1}{2}$ mV 16 channel multipoint Honeywell Brown instrument with an amplifier matched to an input impedance of 16 K. The inputs to the recorder could be fed into different channels using a jack plug arrangement which can be seen close to the top of the monitoring rack in Fig. 5; a rear view of this rack can also be seen in Fig. 4.

The 100 mV and 1 mA outputs from the vibrating reed electrometer used in recording space charge were fed to a monitoring panel and the current outputs were displayed on two ammeters fitted with reversing switches, whereas the 100 mV outputs were passed through potential dividers including sensitivity controls before being fed into the recorder. The vibrating reed electrometers were calibrated by connecting accurate low-voltage inputs to their indicator units and the sensitivity control on the monitoring panel was adjusted to give a correct reading on the recorder.

A three stage 240 V A.C. centrifugal fan, which had been used for extracting air from air-raid shelters was obtained and encased in an earthed tube of diameter 15.5 cm. The flow of air extracted through the space charge collectors was registered on gas meters obtained from the Northern Gas Board and in order for this flow to be observed at a distance microswitches were fitted close to cams within



□ Brass
 ■ Nylon
 ▨ 'Kel.F.'
 ▩ Magnesium

All surfaces gold plated
 (except motor).

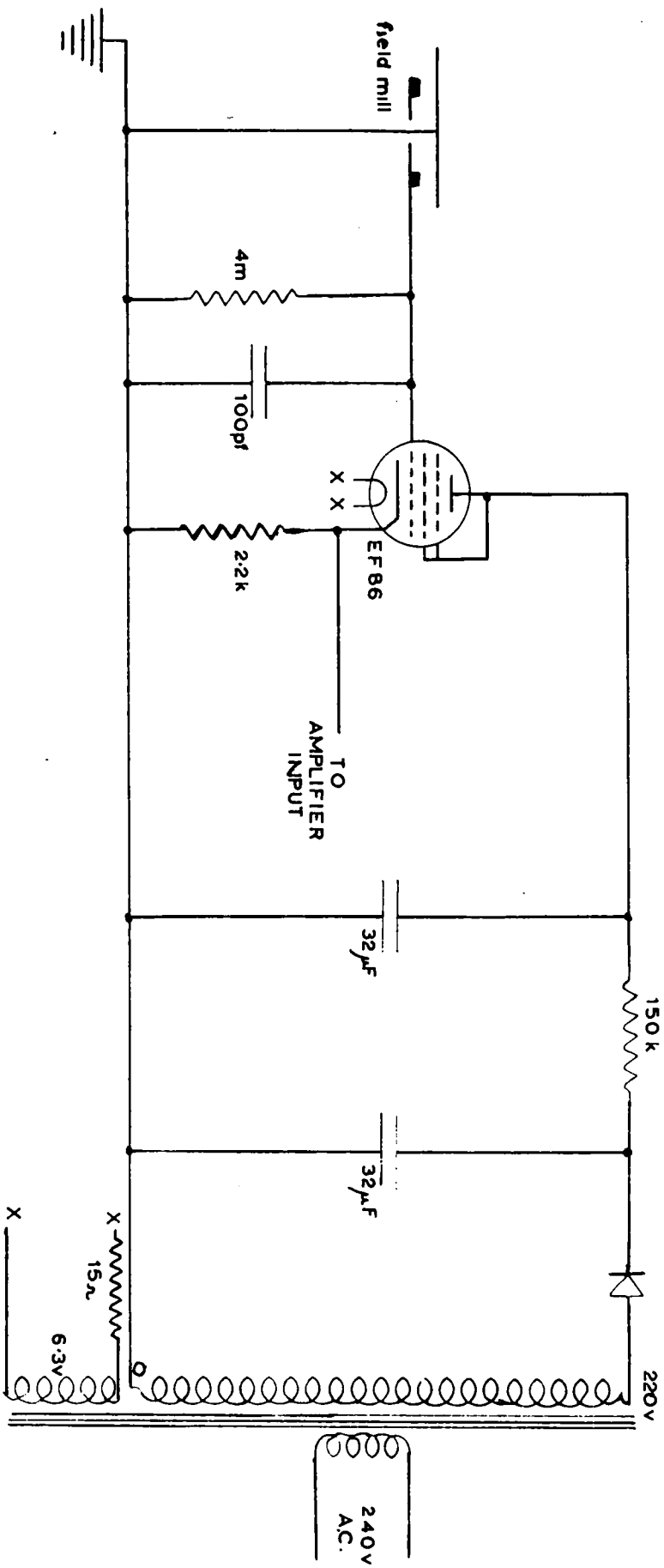
Mill diameter 6inches.

A SECTION THROUGH THE SURFACE FIELD MILL

the gas meters, and 24 V bulbs were thereby caused to glow whenever the switches closed. The frequency of these flashing lights was therefore an indication of the flow through each space charge collector. The gas meters were calibrated with the kind assistance of the Northern Gas Board to an accuracy of 0.5%.

The measurement of potential gradient

The potential gradient was to be measured at both the top and bottom of the mast. Another research student, Mr. Collin, kindly offered the use of his field mill situated at 21 m on the mast; this had been calibrated allowing for the exposure factor due to the mast. Another field mill was set up in the surface of the earth some 30 m from the mast to save having to estimate an exposure factor. A suitable mill was already available, though some modification was necessary. This field mill used was designed by WILMAN (1962) as a research project in this Department and built by Cornstock and Westock Inc. of the U.S.A. for installation on a rocket. A section through this mill is shown in Fig. 6. The stator was made up of 12 small brass studs and 4 large brass studs mounted in two concentric brass rings but as only one output was required the outer ring containing the 12 studs was connected to the recording unit and the inner ring was earthed. This mill has been described in greater detail by WILMAN(1962). However it was discovered during initial testing that the 24 V D.C. motor installed to drive the rotor gave rise to considerable spurious noise in the mill output and had therefore to be



FIELD MILL HEAD UNIT, CATHODE FOLLOWER AND POWER SUPPLY

FIGURE 7

FIGURE 8.

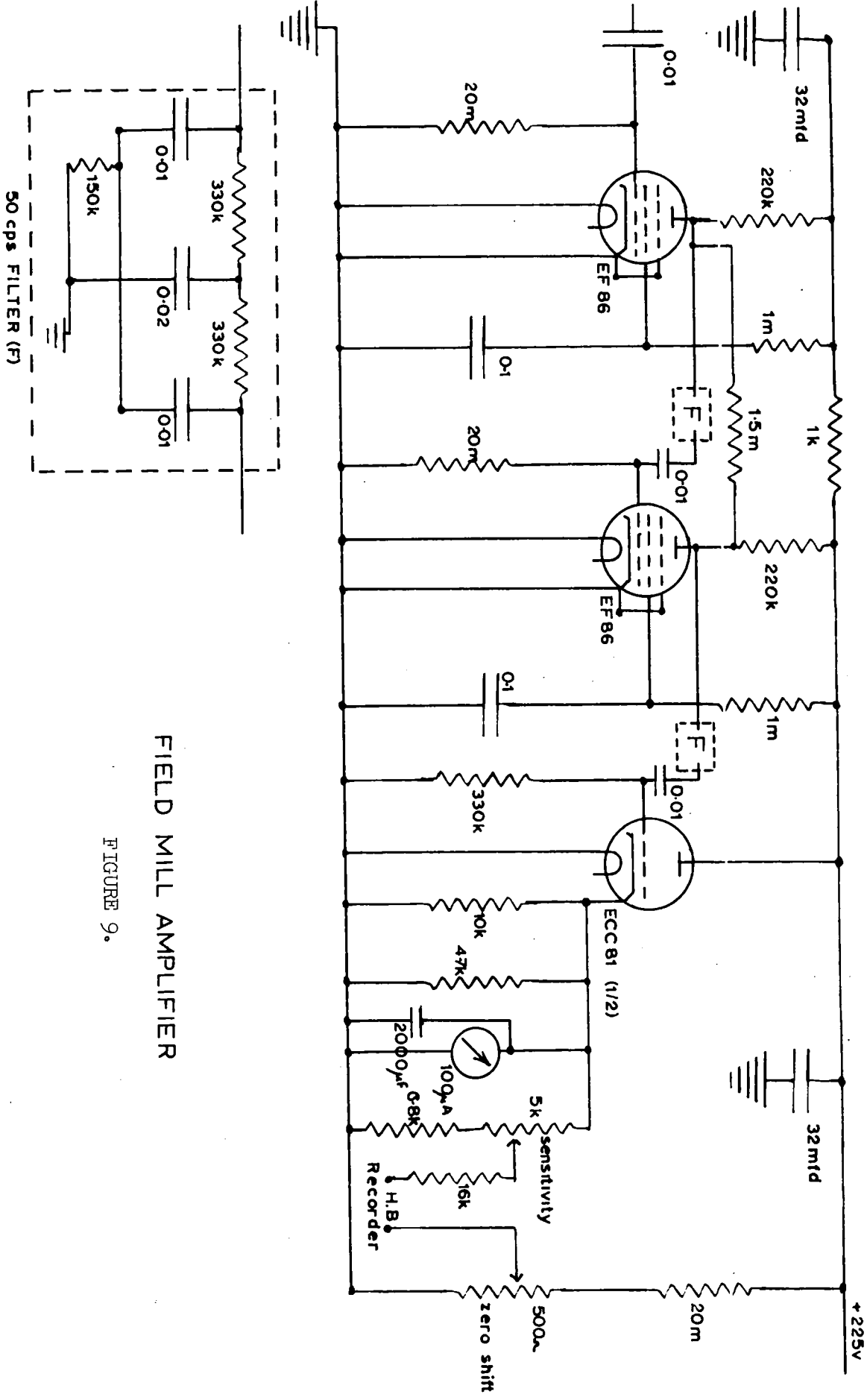


changed. In its place a 240 V A.C. synchronous motor was installed thus giving a mill output frequency of 0.6 Kc/s. As this motor had a shaft of smaller diameter than the previous motor a new brass sleeve was constructed in the lathe for connecting the shaft to the earthed rotor.

The alternating voltage appearing across the head-unit resistor was fed into an 6F86 low noise-level valve wired as a cathode follower. This was necessary because the cathode follower matches the high output impedance of the mill to the low impedance presented by the 100 m of coaxial cable carrying the signal to the amplifier unit. The field mill head unit, cathode follower and power supply can be seen in Fig. 7 and the whole of this unit was encased in a small aluminium box. To reduce vibrations of the valve whilst the motor is in operation the valve base was mounted on a foam-rubber pad; the motor was also screened to prevent pick-up in the output leads.

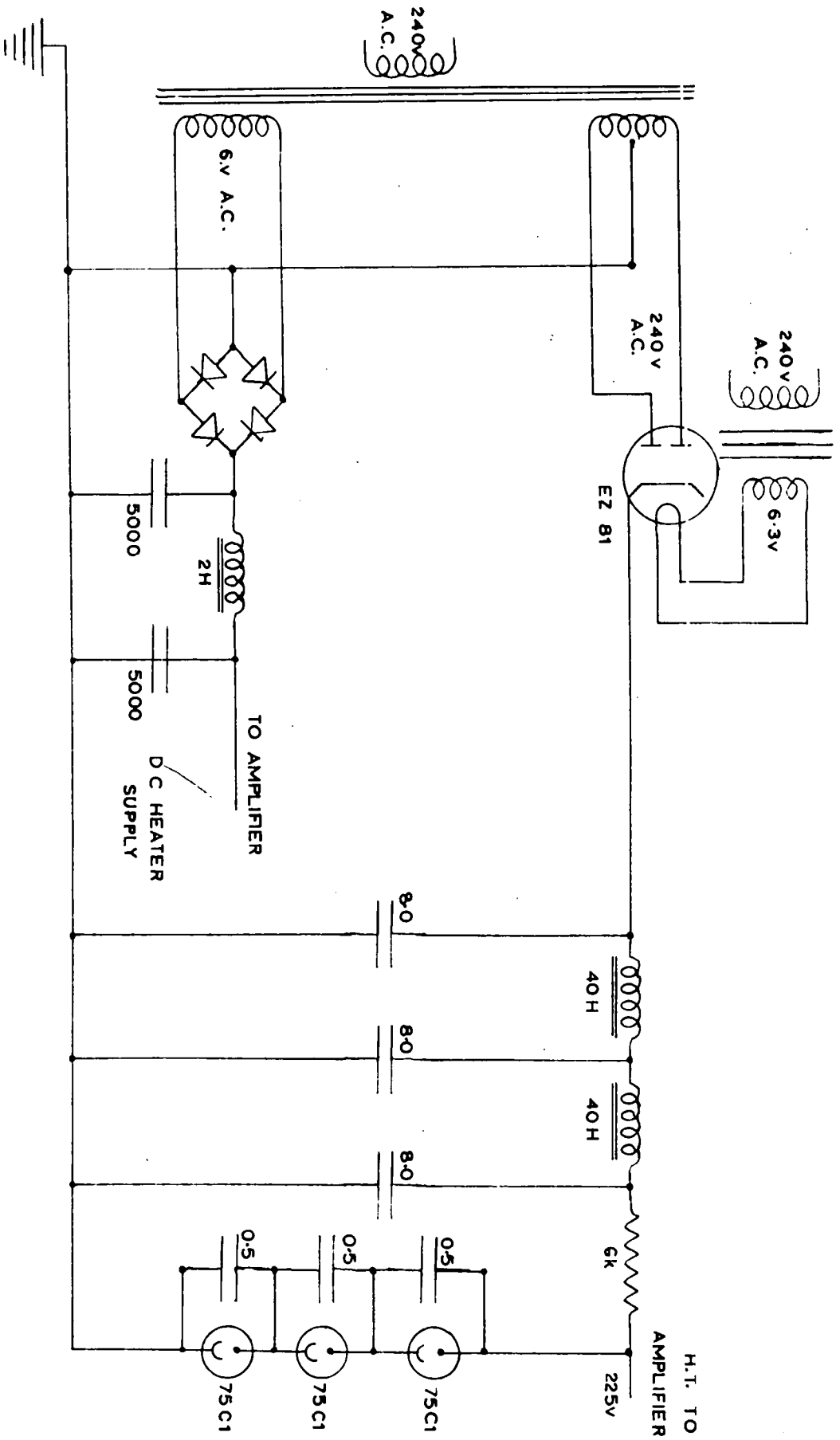
As the near-sinusoidal output from the mill does not discriminate between positive and negative potential gradients a constant field was artificially imposed on this output thereby allowing values of either polarity to be recorded.

This artificial field, which was chosen to be approximately $+1000 \text{ Vm}^{-1}$, was originally obtained by applying a potential difference between earth and a semi-circular plate fixed 2 cm above the stator as seen in Fig. 8. This plate was gold plated to match the surface properties of the field mill but it was later found that varying contact potential differences due to the changing surfaces could



FIELD MILL AMPLIFIER

FIGURE 9.

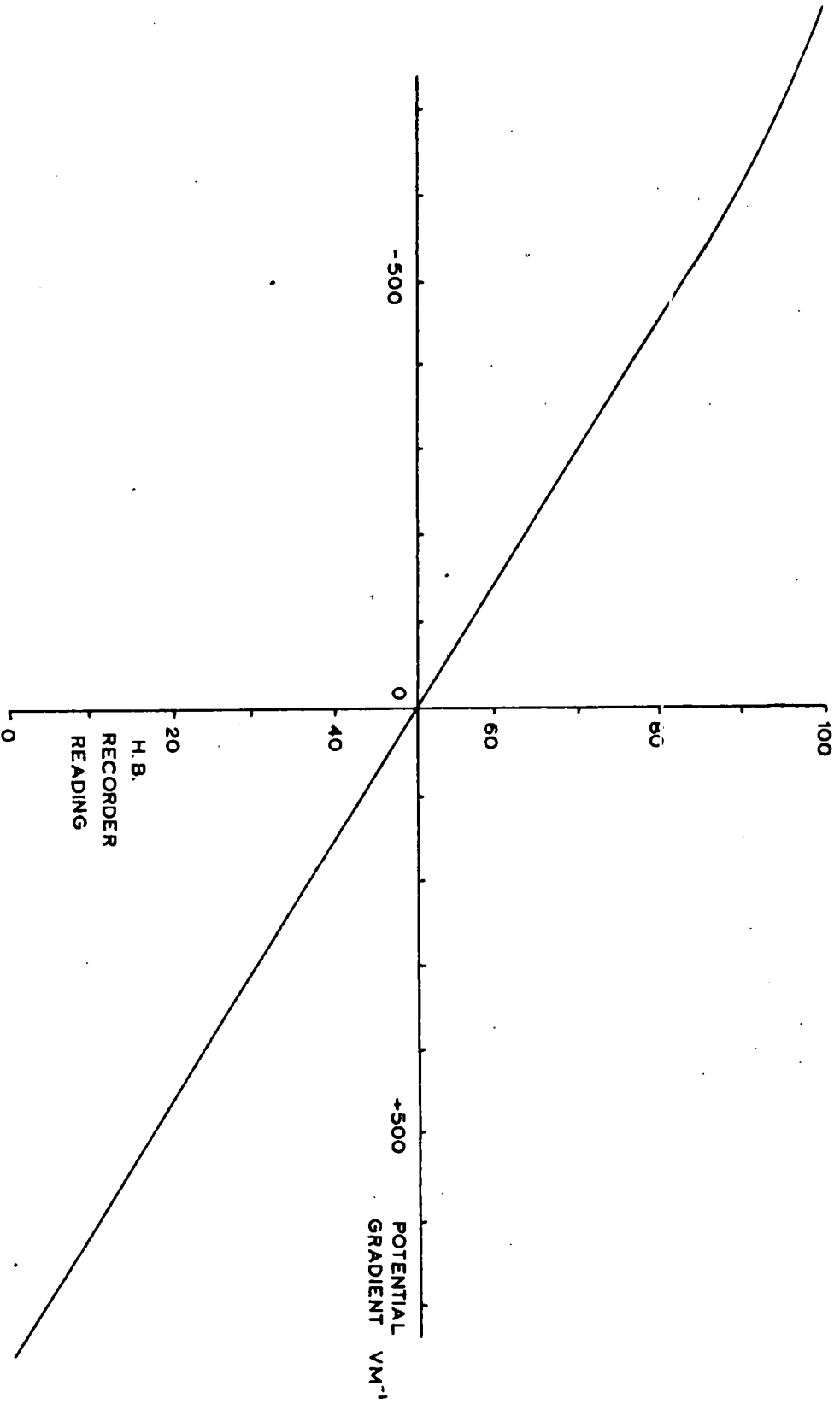


FIELD MILL AMPLIFIER POWER SUPPLY

FIGURE 10.

affect the 5 V potential difference between the plate and stator by at least 5%. For this reason the plate was reduced in size to cover only one stud and its potential increased accordingly thereby reducing the varying contact potential effect to the order of 1%. This plate voltage however was applied via a potentiometer which could be adjusted to correct for these changes in the contact potential differences during calibration.

The mill output is fed via the cathode follower into a 2 stage R-C coupled amplifier (Fig. 9) which was designed especially for this project and incorporated low noise pentode valves. The feedback between the two anodes of the amplifier valves was increased until the gain of the amplifier was reduced to a value of 500; the output, via a cathode follower, could therefore be monitored on a micro-ammeter. The voltage output was also biased before being fed into the centre-zero recorder. It was necessary to insert two 'parallel T' networks in the amplifier tuned to reduce the 50 c/sec signals picked up between the head unit and the C.R.O. used for observations. This signal was thereby reduced from about 5 V to about 3 mV peak-to-peak in the output and therefore could be neglected. The valve heaters were also supplied with D.C. power in an effort to avoid any mains ripple being fed into the amplifiers this way. The L.T. supply along with the 225 V D.C. supply was obtained from a power pack built as shown in Fig. 10. The H.T. supply, after being appreciably smoothed, was stabilised at +225 V with three 75CI neon discharge stabiliser tubes.



A TYPICAL FIELD MILL CALIBRATION

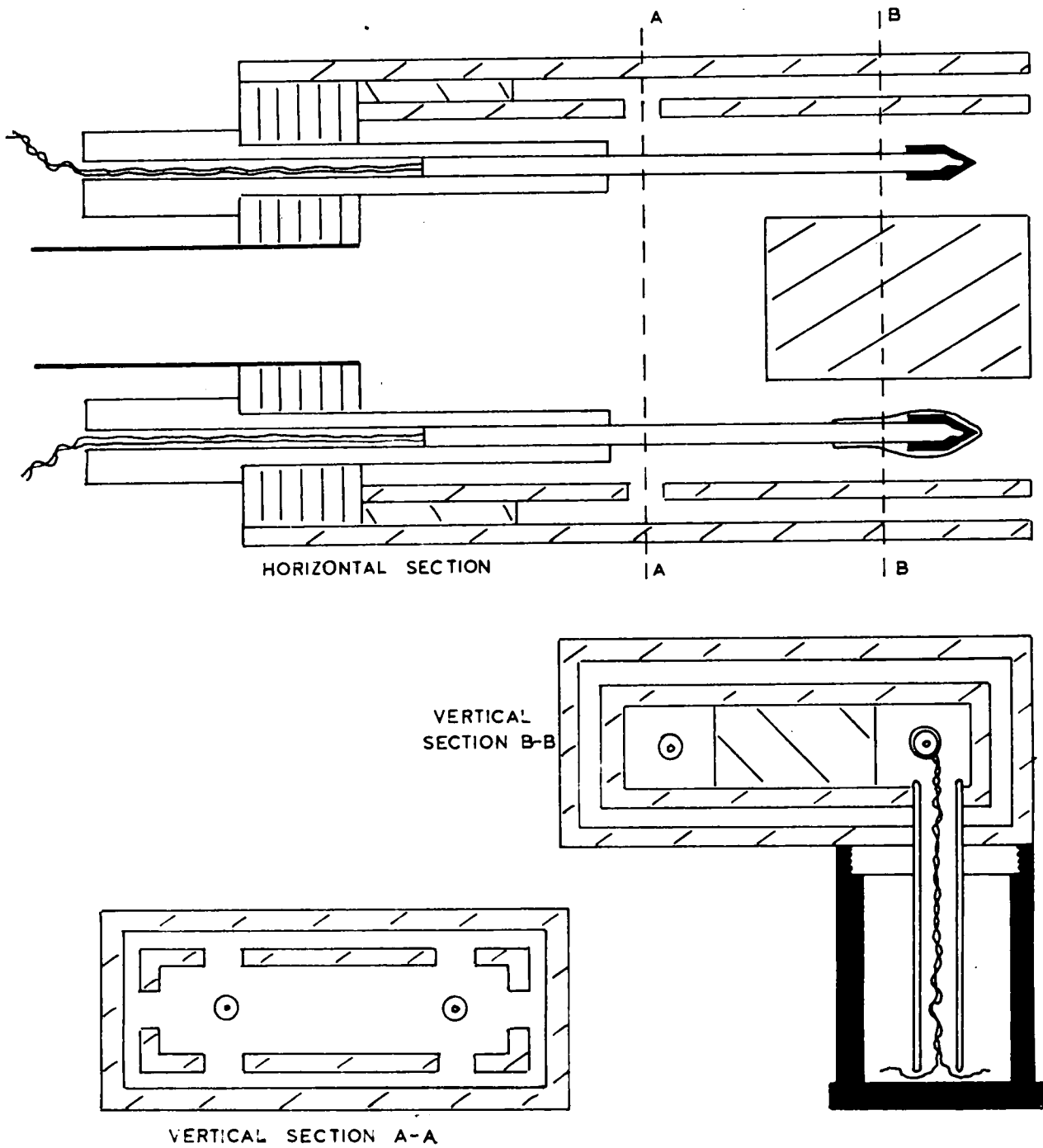
FIGURE 11.

A calibration was performed on this field mill by applying a potential difference between two large parallel aluminium plates, one of which had the mill stator level with its surface and was connected to earth. From the results obtained the curve shown in Fig. 11 was drawn. The non-linearity at the high negative potential gradients was caused by the non-linearity of the diode rectification. Fluctuations from the calibration will however be caused by varying contact potential differences, mains frequency fluctuations and power pack voltage fluctuations but these are unlikely to total more than 5%.

The measurement of temperature and humidity

In order to measure the temperature and humidity gradients within the height of the mast it is necessary to install more recording instruments within the first few centimetres above the earth as it is in this region that the greatest changes occur. The instruments therefore would be placed at $\frac{1}{2}$ m, 1 m, 2 m and 19 m on the mast and their values would be recorded on an instrument some 100 m distant. Thermistors were chosen for the temperature sensitive elements as the working conditions were unsuitable for glass thermometers and as thermocouples would require some form of amplification before the temperature could be printed on the recorder available.

A thermistor is a temperature sensitive resistor having a large negative temperature coefficient of resistance which is usually in the range 1-5% deg. C⁻¹. The type chosen for this project is the Standard Telephones and Cables thermistor no. F23 which has a

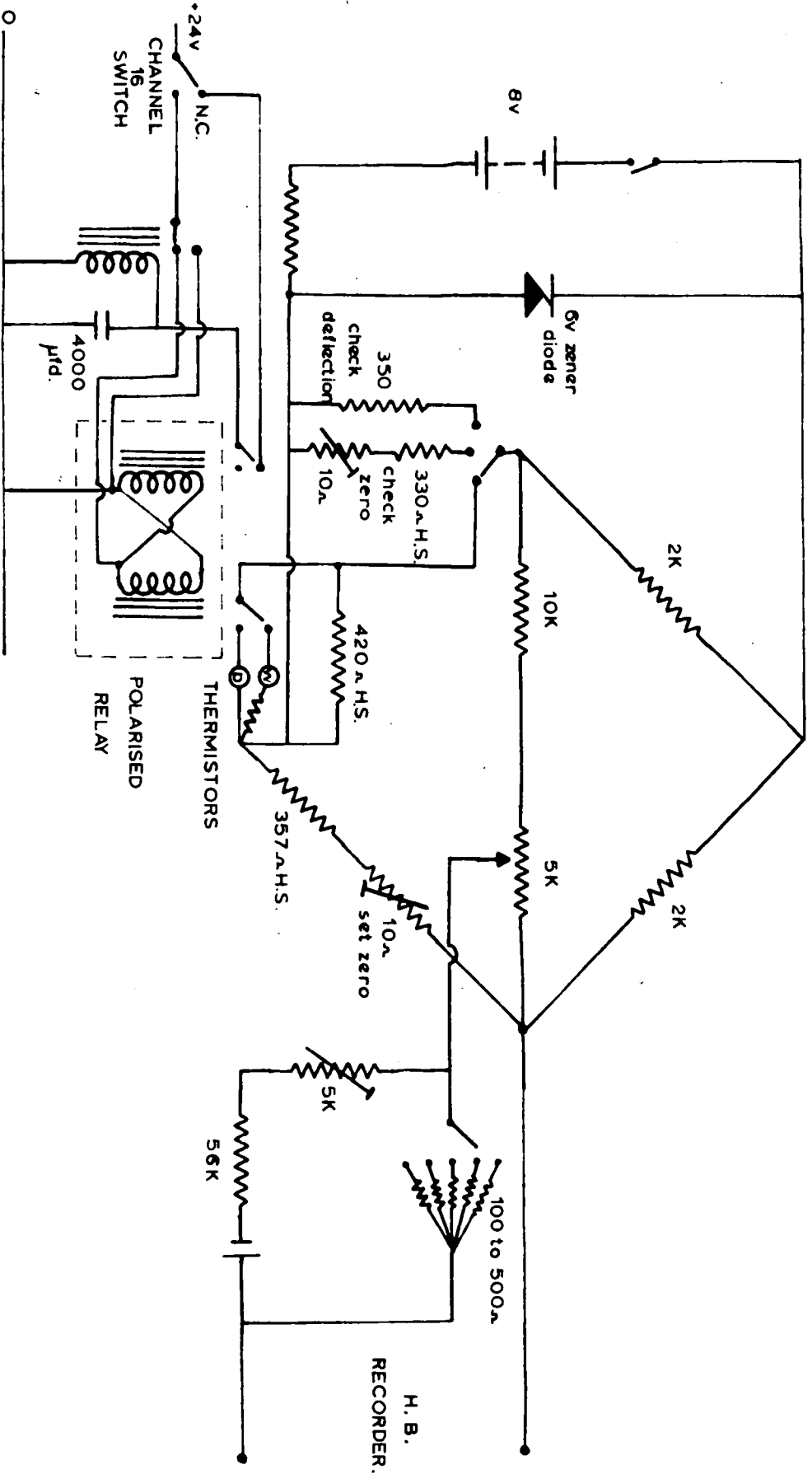


HORIZONTAL AND VERTICAL SECTIONS OF
THE THERMISTOR PSYCHROMETER
(drawn to scale) 1:1

FIGURE 13.

temperature coefficient of over 3% deg. C^{-1} and has a resistance of 2 K at 20°C . It is a directly heated bead-type thermistor and the actual resistance element has a diameter of only 0.5 mm . The bead of this rapidly acting thermometer is sealed in glass thus protecting the element against liquid or gaseous action from the air. One of these thermistors could also be covered in wet muslin and therefore act as a wet bulb thermometer.

A typical instrument in which to incorporate a wet and dry bulb thermistor would be the aspirated psychrometer described by PASQUILL (1949) which could be built with ease. This type was therefore chosen and four units were constructed. A photograph of a completed psychrometer is shown in Fig. 12 and a sectional view drawn with identical measurements is shown in Fig. 13. The psychrometer housing was constructed from 3 mm thick perspex sheet and precautions are provided by forced aspiration of the air past the bulbs, a double wall in the housing which is also aspirated and by painting the outer surface with white enamel with a high gloss finish. The perspex sheets, after being cut to size, were fixed together with perspex cement. Holes had been drilled in the inner housing, as can be seen in the vertical section A-A, to provide aspiration of the interwall space. The thermistors were cemented in holes drilled through tufnol bars which were then pushed into locating holes in the perspex block at the rear of the psychrometer.



A TYPICAL THERMISTOR BRIDGE NETWORK SHOWING RECORDER BIASING AND AUTOMATIC WET TO DRY BULB SWITCHING UNIT.

FIGURE 14.

The thin-walled aspiration tube is made of brass as is the water chamber provided for sustained operation of the wet bulb. This water chamber, which can be seen in the vertical section B-B, is screwed on locating threads directly underneath the bead of the wet bulb thermistor. A tufnol tube passes through the walls in the housing to allow the wick from the muslin to be constantly immersed in water. In order to separate the two thermistor elements and thus allow for independent aspiration a perspex block was fitted in the entrance of the psychrometer.

During initial testing of the units it was discovered that the thermistors were far too sensitive to sudden small changes in temperature and therefore small brass 'bulbs' were made ^{and} / fixed over the bead of the thermistors thereby adding a time constant of about 10 sec on the variable element resistance. Because these brass bulbs should not be glued to the thermistor beads with a material of low conductivity solder was used which had a melting point of only 60°C. Wires from the thermistors were led away to the recording unit.

To measure temperature with a thermistor it is good practice to connect it as one arm of a Wheatstone bridge and 4 such circuits were built for this purpose, one of which is shown in Fig. 14. The power supply to the bridge network was stabilised using a 6 V zener diode, located in a heat sink, because slight fluctuations in voltage will be recorded on the temperature output due to the high sensitivity of the circuitry. For this reason also high stability resistors were chosen and provision was made for checking both the zero setting and a pre-determined reading by switching in pre-set resistors to the arm

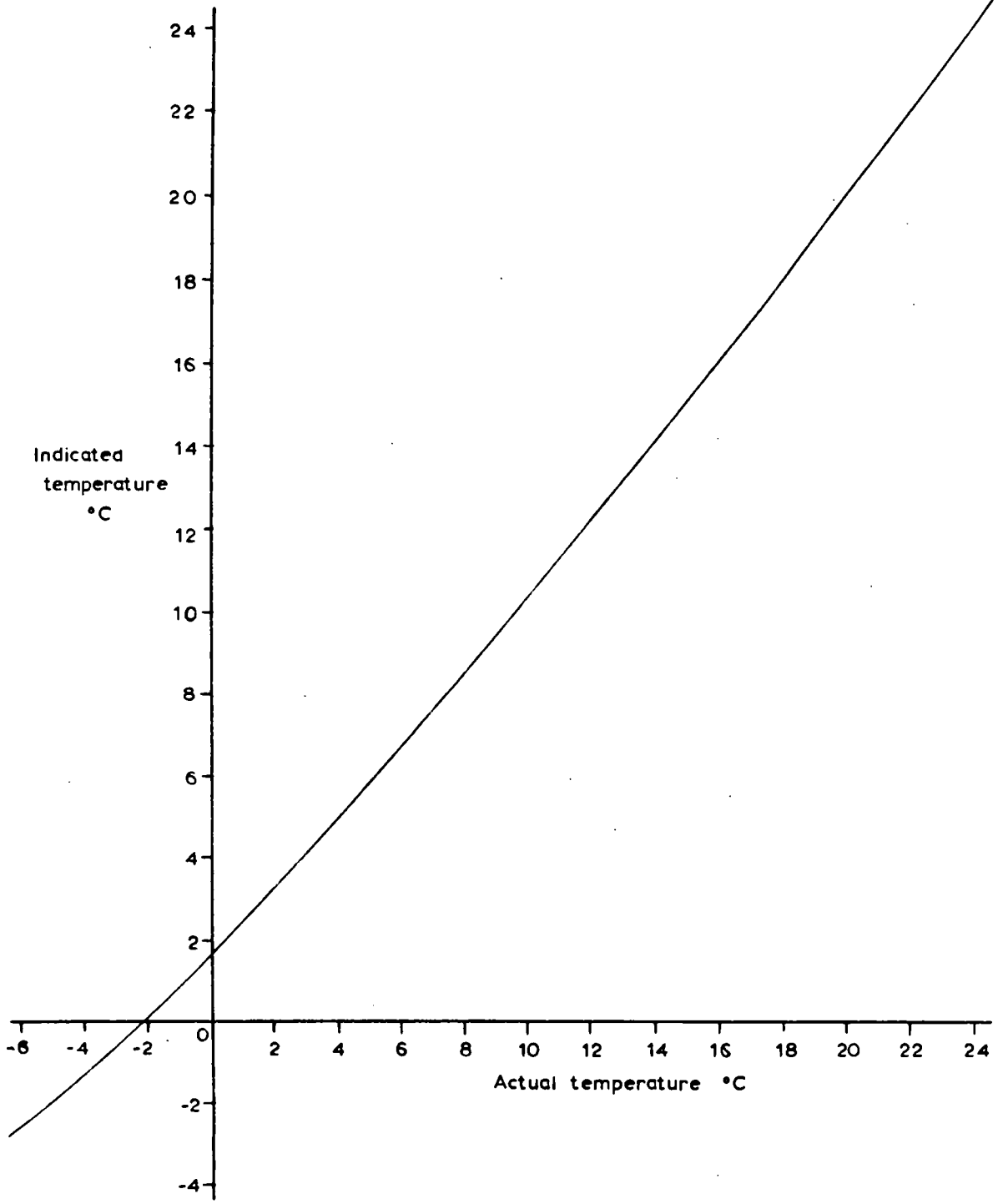
normally occupied by a thermistor. In event of any component giving rise to an output error a 10 ohm potentiometer was connected in the arm adjacent to the pre-set resistors and the variation of this component would return the bridge network to its calibrated position.

The resistance-temperature graph of a thermistor is exponential but it is possible to obtain a more linear characteristic by connecting resistors in shunt or series with the thermistor. The resultant network will not have a temperature coefficient that is less than that of the thermistor alone and, in general, the larger the reduction in temperature coefficient the better the linearity. A 420 ohm resistor was therefore shunted across the thermistor. The output was taken from a 5 K potentiometer which acted as a sensitivity control and was fed into a biasing unit before entering the centre zero recorder. Before this biasing system can be explained in more detail it is necessary to consider the temperature range needed on the recorder.

During winter months with a dry bulb temperature of -4°C the wet bulb depression must be measured to an accuracy of 0.1°C in order for the relative humidity to be calculated to within 3% of its value. A 0.2°C limitation in recording would cause this error to rise to 6% relative humidity. In summer months however this type of error is not as great, as with a dry bulb temperature of 16°C and the wet bulb depression measured to within 0.1°C of its value the relative humidity is accurate to 1%. It was therefore decided to have an output which the recorder would print accurate to 0.1°C . This would mean that the full scale reading of the recorder would cover

only 10°C . Considering the biasing system therefore it was necessary to have several high stability resistors which could be switched in the circuit one at a time and each resistor adding an extra $2\frac{1}{2}$ mV negative bias, or half scale (5°C), to the recorder. As the temperature range over the year would probably be within -5°C and 25°C there had to be 5 temperature ranges or 5 biasing resistors. A note of the range used was made during each recording period.

Only one bridge network was used for the wet and dry bulb thermometer inputs from one psychrometer. These were switched into the circuit in turn using a polarised relay and during one printing cycle (16 channels) of the recorder the four dry bulb temperatures were taken, whereas during the next printing cycle the four wet bulb temperatures were taken. The pulse from the recorder was obtained by fitting a microswitch which was closed whenever Channel 16 printed, but as this pulse length was insufficient to hold a relay closed for a whole cycle of operations a circuit containing the polarised relay was built. The polarised relay contains two coils and as a pulse is fed into one coil the relay switches are thrown one way, but the next pulse must be fed into the second coil for the relay switches to be 'thrown' back again. The relay therefore could not be used by itself by cross-coupling the pulse input wires as it would chatter during an input pulse so the circuit shown at the bottom of Fig. 14 was built. Considering the circuit diagram

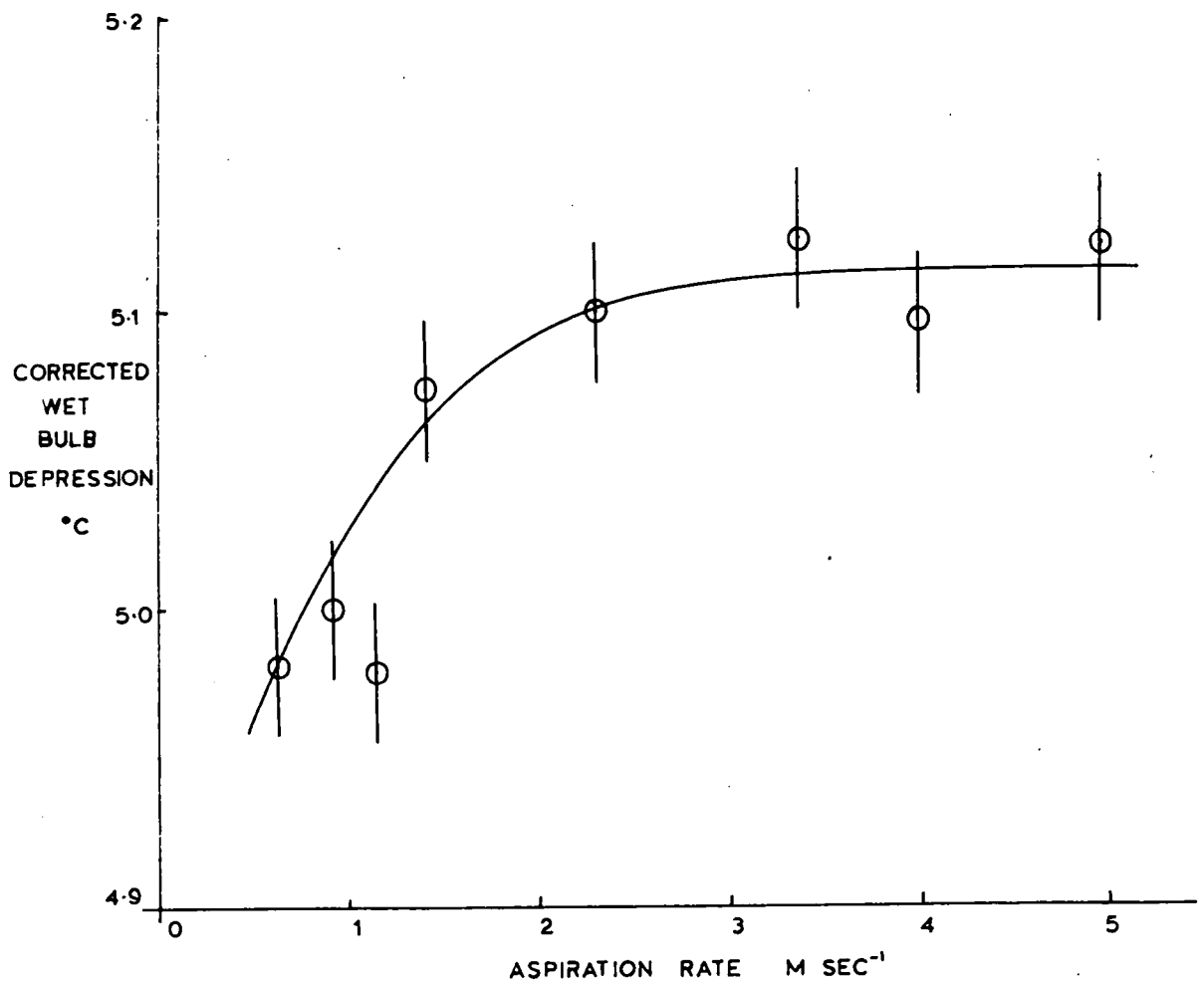


A TYPICAL THERMISTOR CALIBRATION (Greatly reduced)

FIGURE 15.

with the switches as they are shown, that is with the Channel 16 micro-switch in its normally closed position, the 4000 μF condenser is charged and its adjacent relay is held closed. The time constant of this unit will hold the relay closed for a period longer than the pulse from the microswitch. As this pulse flows it passes via a switch in the single coil relay into one coil of the polarised relay, switching in one thermistor for the next 16 channels and also diverting the supply away from the 4000 μF condenser. A few seconds after the pulse has ended the single coil relay opens thereby feeding the next pulse into the second coil of the polarised relay, which switches in the second thermistor and returns the unit to the original condition.

The calibration of the thermistors was carried out using an H.P.L. calibrated mercury thermometer and vacuum flasks containing salt solution. The solution was constantly agitated during calibration. As the resistance of the 100 m cables connecting the thermistors to the bridge network would be equivalent to some 1 deg. C on the output the units were calibrated with the cables connected. The sensitivity potentiometer was adjusted to give approximately 10°C full scale deflection on the dry bulb thermistor. The wet bulb thermistor was then shunted or had resistors connected in series to bring its effective resistance at a particular temperature to that of the dry bulb thermistor. Calibration curves were drawn on large scale graph paper thereby allowing temperatures to be read to 0.1°C over the 30°C range. A typical calibration is shown in Fig. 15 where the indicated temperature is that recorded on the Honeywell Brown recorder.



VARIATION OF WET BULB DEPRESSION WITH
 AVERAGE ASPIRATION RATE IN THE SPACE
 IMMEDIATELY SURROUNDING BULB

FIGURE 16.

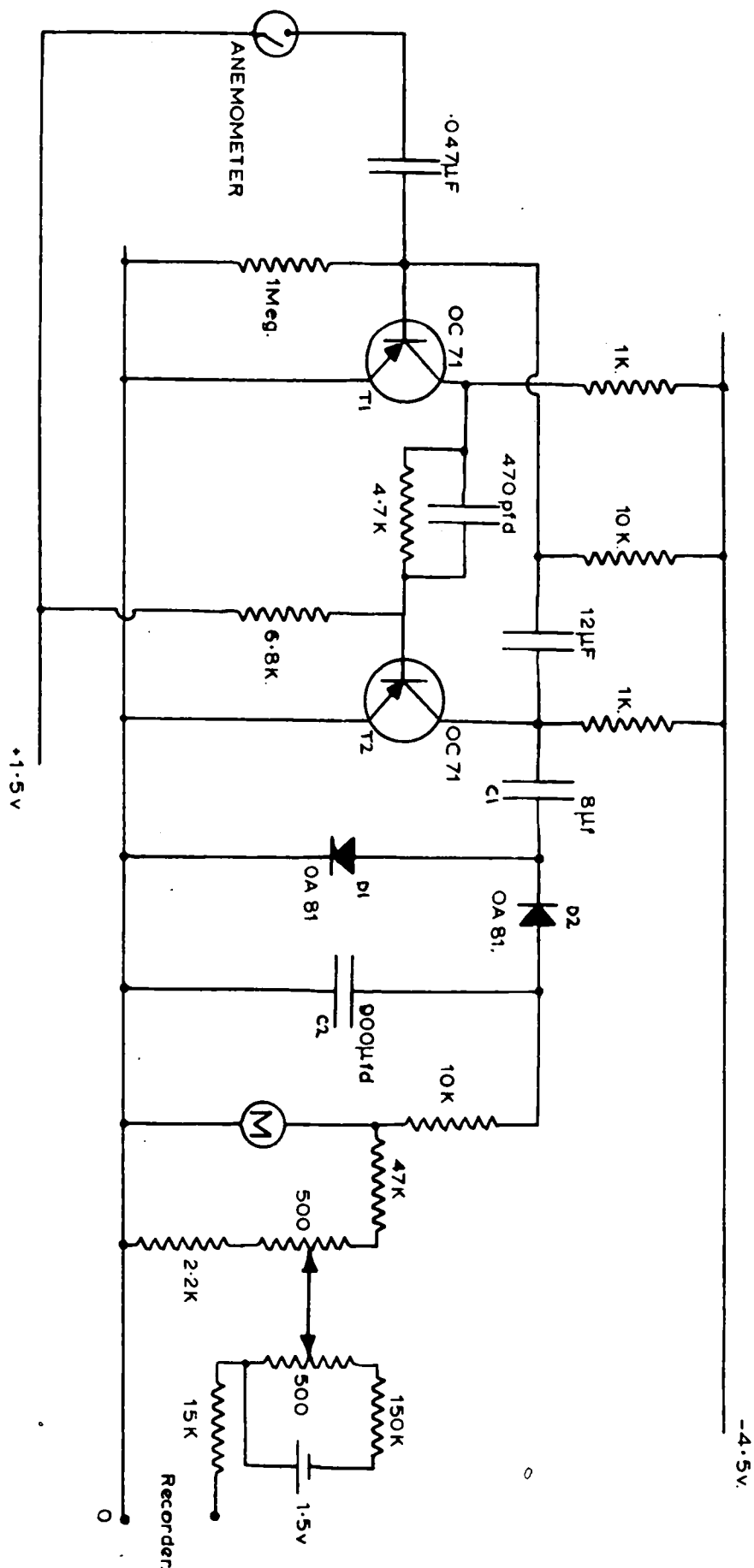
The question now arose as to what aspiration rate should be used in order to obtain the maximum wet bulb depression under constant humidity and dry bulb temperature conditions. Tests were therefore carried out using two psychrometers each with its own suction unit. One psychrometer was constantly aspirated at a speed greater than 6 m sec^{-1} and the flow through the other could be varied and measured using a gas meter. These two psychrometers were fixed at the same height above the ground on a dry day with fairly constant relative humidity. The outputs from the respective psychrometers were recorded as the flow through one was varied between 0.5 m sec^{-1} and 5 m sec^{-1} . The record of the constant flow psychrometer showed almost constant wet bulb depression, and the graph drawn in Fig. 16 was drawn making corrections for any fluctuations in the depression of the constant flow instrument. The large errors on the readings are equivalent to the recorder error of $\pm \frac{1}{10}\%$, but even so it was obvious that if the aspiration rate was greater than 3.5 m sec^{-1} the wet bulb depression for a particular relative humidity and dry bulb temperature was at its maximum. Aspiration through all the psychrometers was therefore adjusted, using the gas metres, to be greater than 3 m sec^{-1} .

The measurement of wind speed

It would be advantageous if measurements of wind speeds at the two levels on the mast could be performed at the lowest values possible as well as at speeds of around 12 m sec^{-1} . The possibility of using hot wire anemometers was discarded after a period of

experimentation owing to their poor response to the higher wind speeds. However the Meteorological Office offered to loan the Department two sensitive contact-pattern cup anemometers and their offer was accepted. This type of anemometer gives readings down to air velocities lower than had been thought possible before with a rotating system but a limitation is that it must not be exposed to winds greater than 15 m sec^{-1} . The anemometer cups are made of pressed aluminium and the steel spindle runs in a cup-shaped jewel bearing. Low frictional torque results and the stopping speed is only 0.1 m sec^{-1} whilst the starting speed is only slightly higher. For every other revolution of the cups a very light contact is held closed for the complete revolution and hence remote reading can be obtained. A 1.5 V battery was connected across the contacts and this gave a pulse which could be registered some distance away.

It was necessary to convert the pulse from the anemometer into a directly observable reading which could be constantly recorded. Depending on the anemometer rotation rate the pulse could have a width of between 0.080 sec and 6 sec and the time between the start of one pulse to the start of the next could vary between 0.16 sec and 12 sec. Some form of counting rate circuit had therefore to be built which would accept pulses occurring at varying times and having varying width and indicate on a meter the average rate of occurrence of these pulses. This can be achieved if each pulse causes a charge to flow through a meter, the magnitude being independent of the size or shape



CONTACT ANEMOMETER INTEGRATOR.

FIGURE 17.

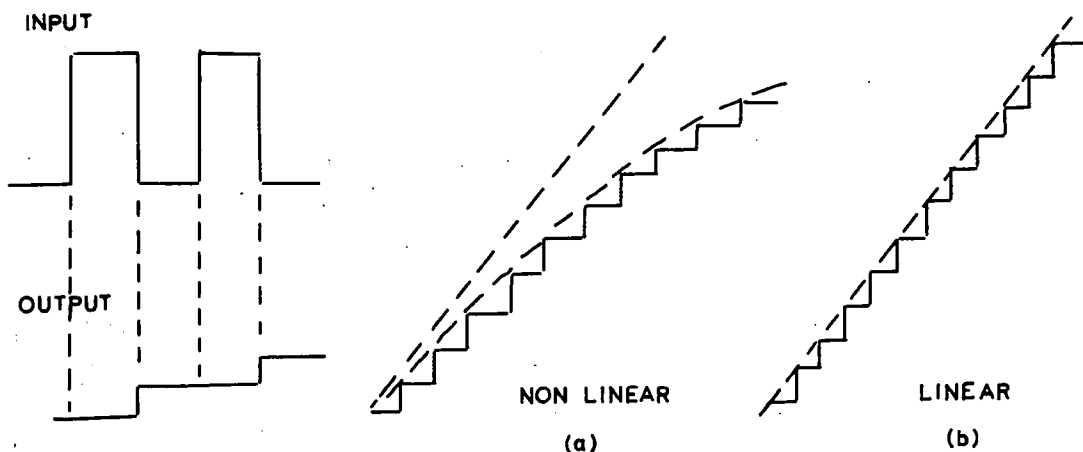
of the pulse itself. In the first case it is wise to cause the anemometer pulses to trigger a flip-flop monostable circuit which will deliver pulses of uniform amplitude and width. The circuit employed for this purpose is shown in Fig. 17 and is that part of the circuit to the 'left' of the $8 \mu\text{F}$ condenser. A stipulation is that the output pulses must be shorter than the time between two input pulses so that the monostable circuit will not accept another input pulse before it has had time to return to its stable state.

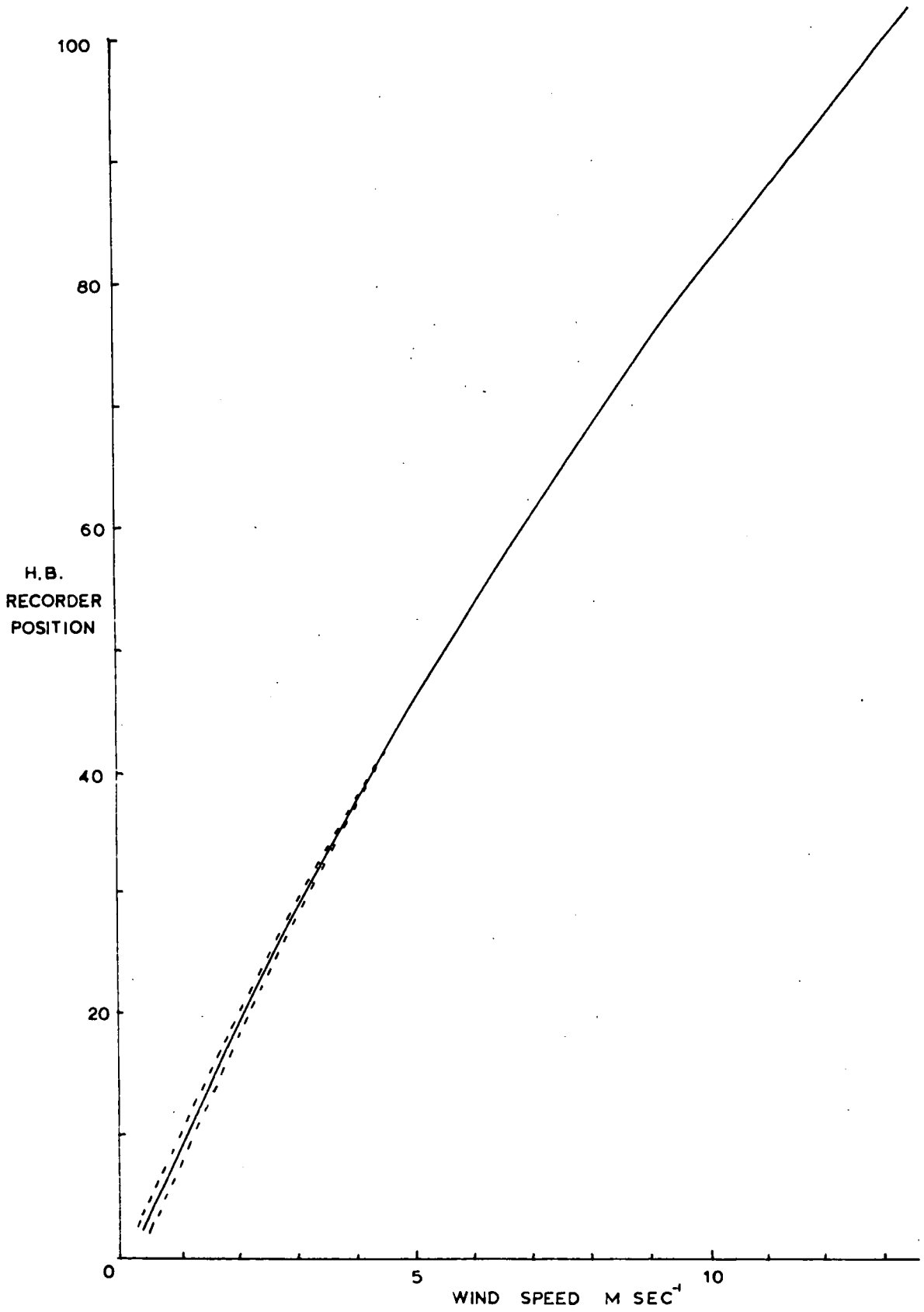
EARNHEAW (1956) stated that if a pulse was of constant amplitude and width it would be suitable for feeding into a diode pump integration circuit. As this circuit was to be used a recommendation that the input pulse should be as wide as possible was accepted and the width chosen to be 120 m sec.

The action of the flip-flop can be explained by first considering it in its stable state. Transistor T1 has its base connected via a 10 K resistor to the negative supply and this transistor is therefore conducting hard between collector and emitter. Its collector is hence at zero potential and with the potential dividing action of the 4.7 K and 6.8 K resistors the base of T2 is positive and so this transistor is cut off. The $12 \mu\text{F}$ condenser is now charged to almost the whole supply potential. The input pulse from the anemometer causes the base of T1 to go positive thereby cutting off this transistor and switching on T2. The time taken by the $12 \mu\text{F}$ condenser to discharge through the 10 K resistor, namely the required 120 m sec, is therefore the time for the base of T1 to go sufficiently negative for it to conduct once

more which causes the circuit to return to its stand-by state. The output taken from the collector of T2 is a pulse of constant width of 120 m sec occurring at unequally spaced intervals of time. This is now fed into the diode pump integrator comprising the rest of Fig. 17 whose action can be explained as follows.

The first input pulse to the diode pump must be long enough to allow C_1 to charge completely through D1. During this pulse D2 has been cut off. In the interval between pulses the time must be long enough to allow C_1 to discharge through D2 as D1 will now be cut off; C_2 is therefore charged. C_1 must be small compared with C_2 so that the voltage change across C_2 is small compared with the amplitude of the input pulse. The next input pulse again charges up C_1 through D1 and at the end of the pulse a small incremental charging again occurs in C_2 . Thus there is a series of steps on the output meter which give an output voltage staircase waveform.





A TYPICAL ANEMOMETER CALIBRATION
FIGURE 18.

Ideally the staircase voltage should show equal increments as in (b) above, but each successive pulse will cause a progressively smaller voltage rise across C_2 and a drooping non-linear output results as seen in (a). It can be shown that C_1 must be as small as possible compared with C_2 in order to obtain a near linear output but unfortunately the smaller C_1 then the smaller the output voltage steps. For this reason, after experimenting with various condenser values, C_1 was chosen to be $8 \mu\text{F}$ and C_2 to be $900 \mu\text{F}$ as these gave the most linear output. The addition of the leakage resistor across the $900 \mu\text{F}$ condenser provided a continuous discharging path with a time constant of 10 sec. As the recorder had a centre zero position a biasing arrangement was necessary on the output from the diode pump in order to achieve a full scale calibration. A sensitivity potentiometer was also connected in circuit.

In order to calibrate the system, pulses were applied to the monostable circuit from a pulse generator for the higher frequency ranges and with a manual switch for the lower frequencies. A steady succession of pulses was fed into the circuit and as these were counted on a scaling unit the number per sec was obtained using a stop watch whilst the recorder reading was noted. For the lower frequencies however the $900 \mu\text{F}$ condenser has time to discharge more before the next pulse arrives thus giving a varying output and the spread of this error is shown by the dotted lines in Fig. 18. Calibrations were also carried out of wind speed registered on the two meters which can be seen at the top of the monitoring panel in Fig. 5.

When the anemometers were finally connected to the circuit from a distance of about 100 m the whole system appeared to perform excellently.

Automatic recording

A 24 hour electric clock was purchased which could switch power to a socket at any predetermined time. This was achieved by pressing pins into holes on the clock face placed at $\frac{1}{6}$ hour intervals. This clock can be seen at the centre of the monitoring rack in Fig. 5. The supply from this socket, after being passed through a transformer and rectified, was able to operate a relay which was connected in circuit so as to switch on all the recording instruments. The instruments could therefore be made to record automatically, switching on and off at any predetermined times. However, during periods of precipitation, damage could occur in the space charge collectors and use was therefore made of a rain detector built by Mr. Collin. With the first drop of rain a relay was made to operate, cutting off the supply to the recording instruments. In order to supply power to this relay and also to others that are in the circuits a 24 V power pack was built which could pass a current of 15 amp. Remote switching of all the instruments was now arranged using an assortment of relays.

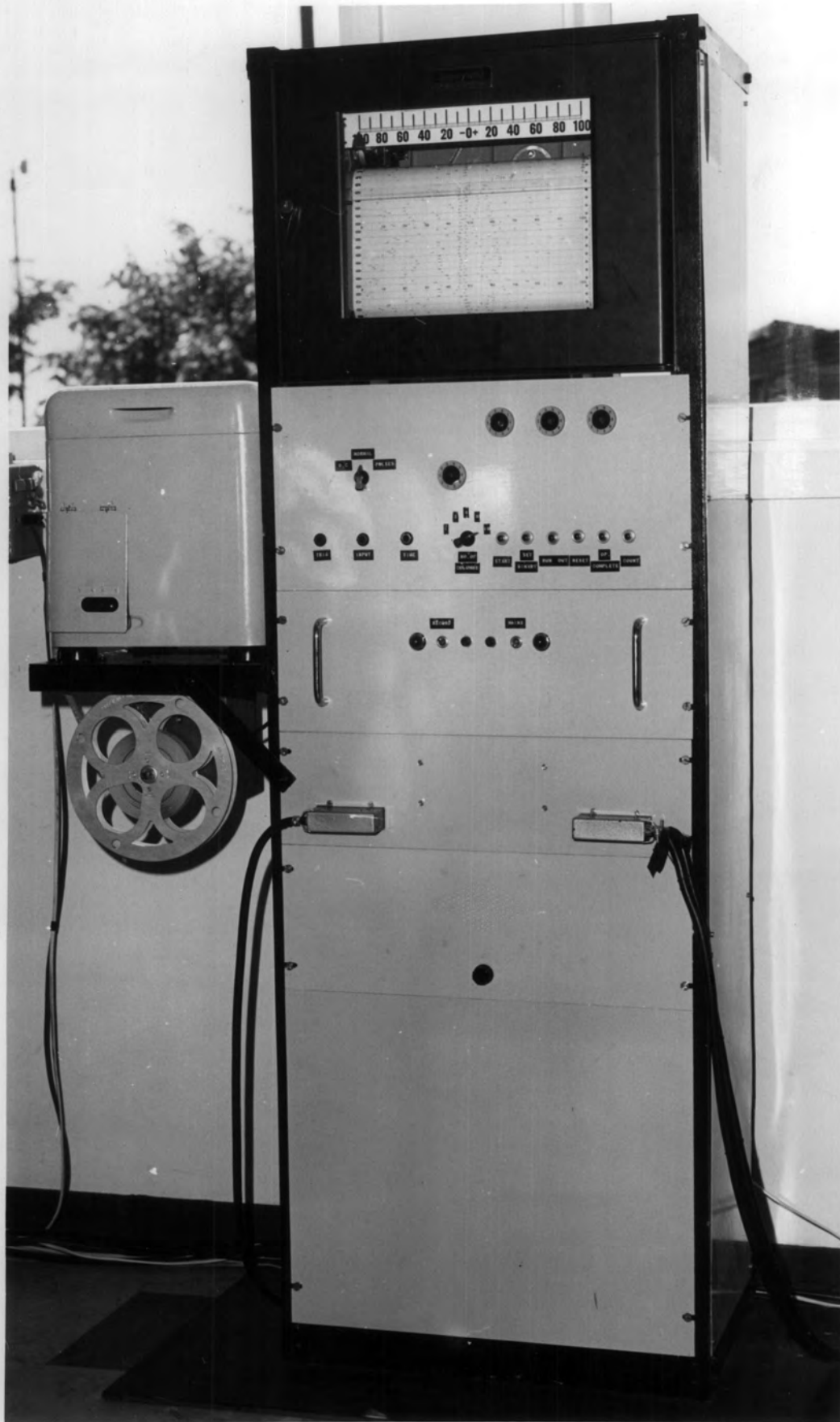


FIGURE 19.

CHAPTER 5

ANALOGUE-TO-DIGITAL CONVERTER

GENERAL

With the type of records obtained in atmospheric electricity the analysis of results is a very laborious task, particularly if there are 14 variables as in the case of this work. In earlier parts of this course a photographic recording system was used but it soon became evident that to read the results from the photographic paper would be a major task in itself. For this reason, and also with an eye on future needs in the Department, it was decided to look into the possibility of purchasing equipment which would give punched tape output available for feeding straight into a computer.

With the help of another research student (Mr. Collin) who was interested in recording during precipitation periods, information was obtained on different types of digital recording systems. In the meantime a 16 point Honeywell recorder had been obtained, but it was found that digital gear for such a recorder would cost over £600. The system employed in this case used a shaft encoder fixed on the pen drive mechanism of the recorder, which gave 999 counts for the recorder pen movement. This output then needed a translator, power unit, programmer and tape punch.

Unfortunately the expense was far too high, even for the shaft encoder alone.

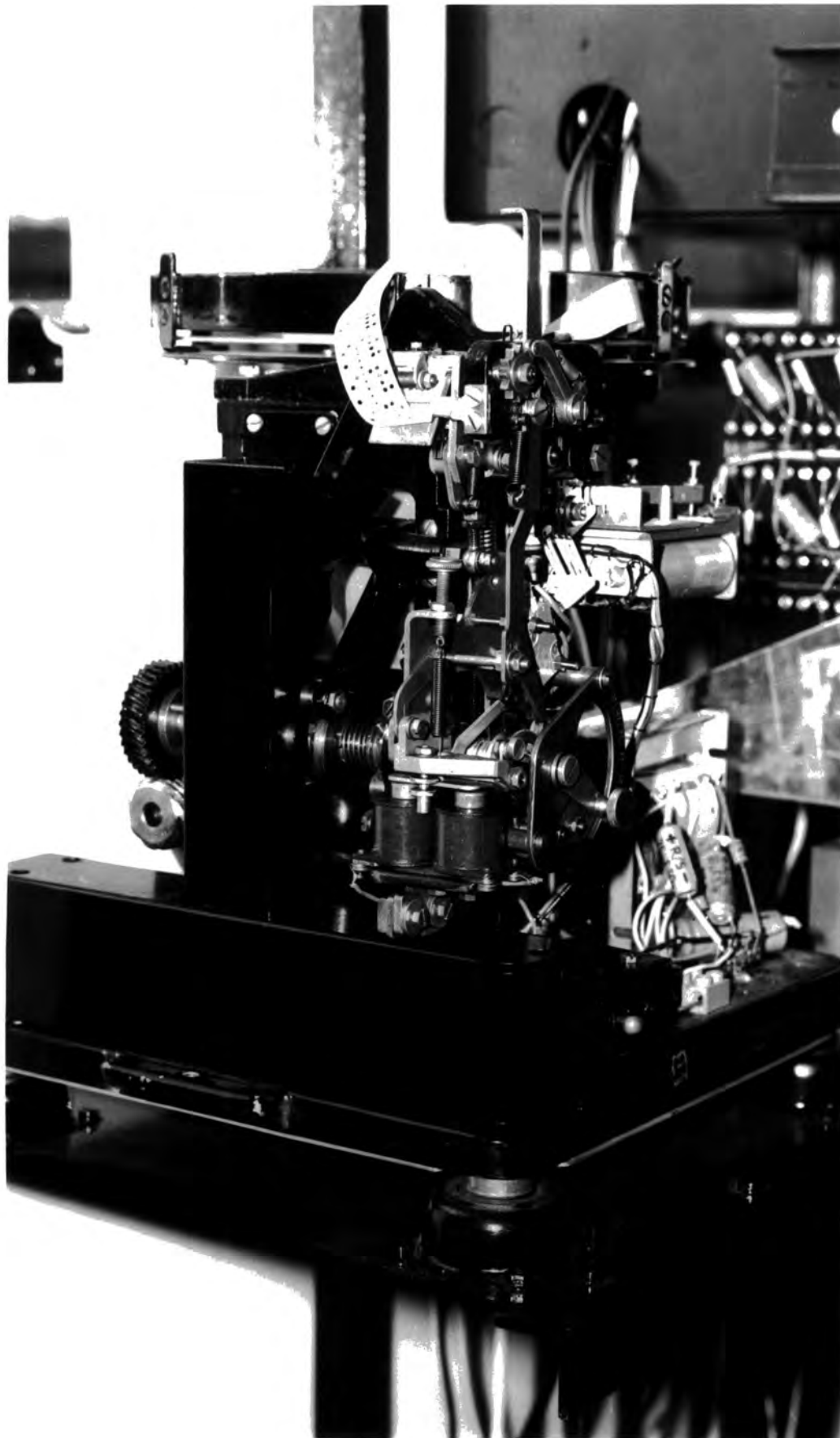


FIGURE 20.

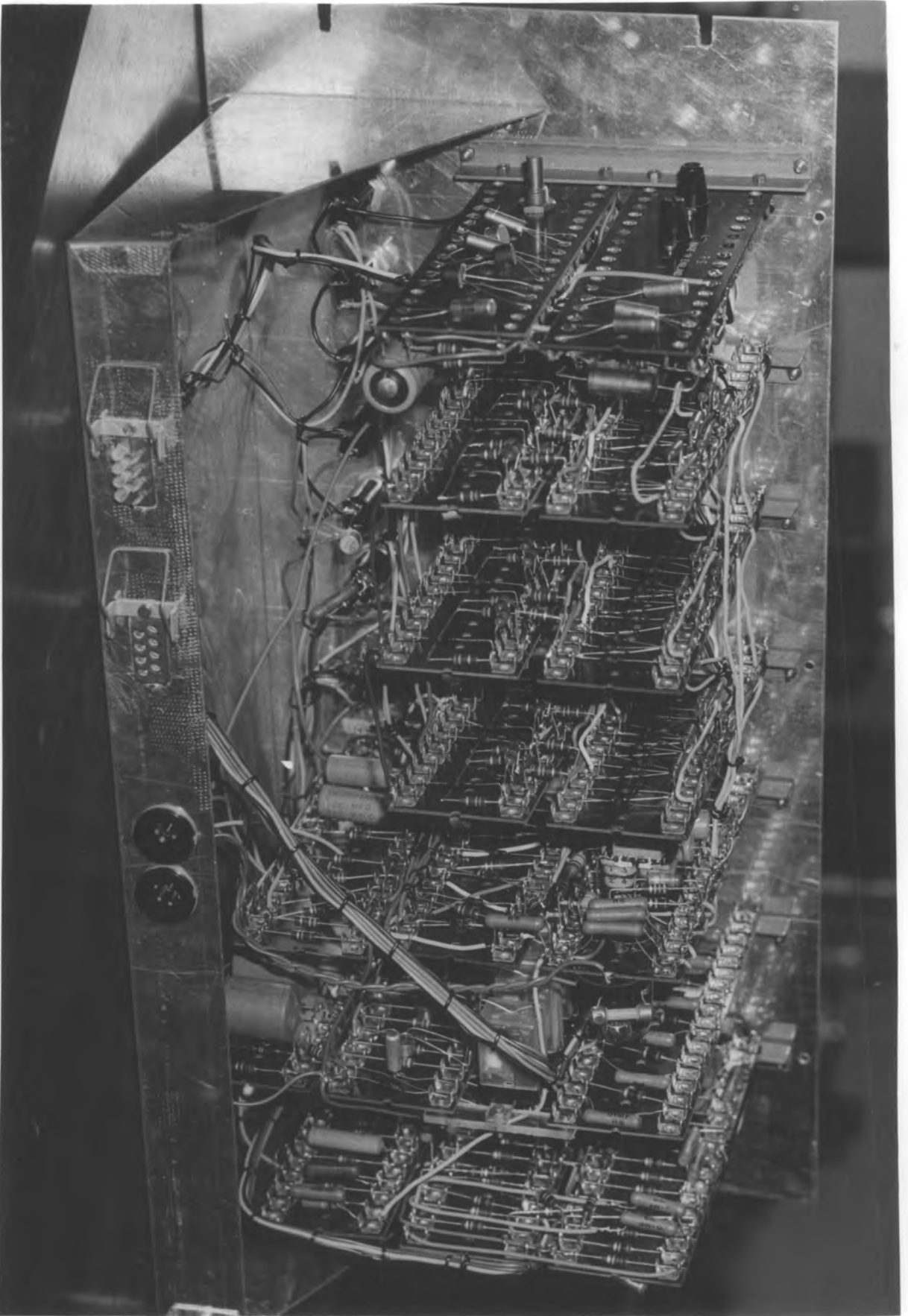


FIGURE 21.

However with the very kind assistance of Dr. Molyneux from Newcastle University we realised that an analogue-to-digital converter with an accuracy of 1% could be built for under £180 (including punch). This required a potentiometer to be fixed to the recorder slidewire. A voltage tapped off this is converted into a frequency corresponding to the recorder signal. In turn this was counted on decatron tubes and the result punched on paper tape which was finally wound onto a spool.

A second hand 5-hole tape punch was obtained and modified. A small power supply was then built in the punch housing, and a micro-switch fitted to a cam in order that an "operation complete" signal could be obtained after a hole had been punched. Fig. 20 shows a photograph of this punch.

The circuit to be built was of a design that electronic companies would be reluctant to manufacture owing to its limited accuracy in an age where more precision is required. However the 1% accuracy was well within the requirements of the field instruments to be considered.

Over 70 transistors and 100 diodes were used in the building of the equipment. In order to simplify fault finding the components were mounted perpendicular to the front of the panel and were easily removeable (Fig. 21). The transistors most commonly used were the p-n-p silicon OC200 and the n-p-n silicon 2S701. These are general purpose transistors with low leakage current.

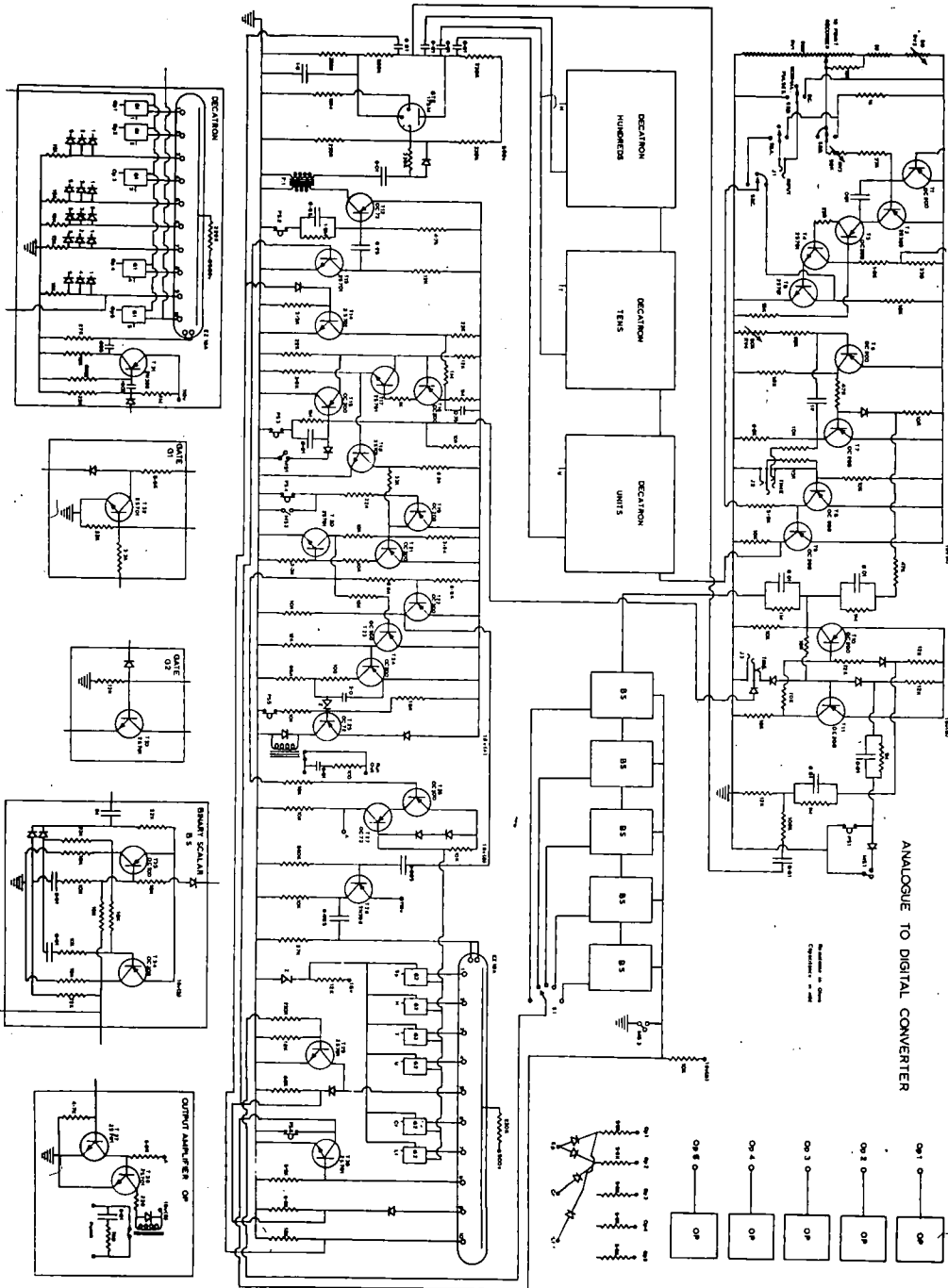
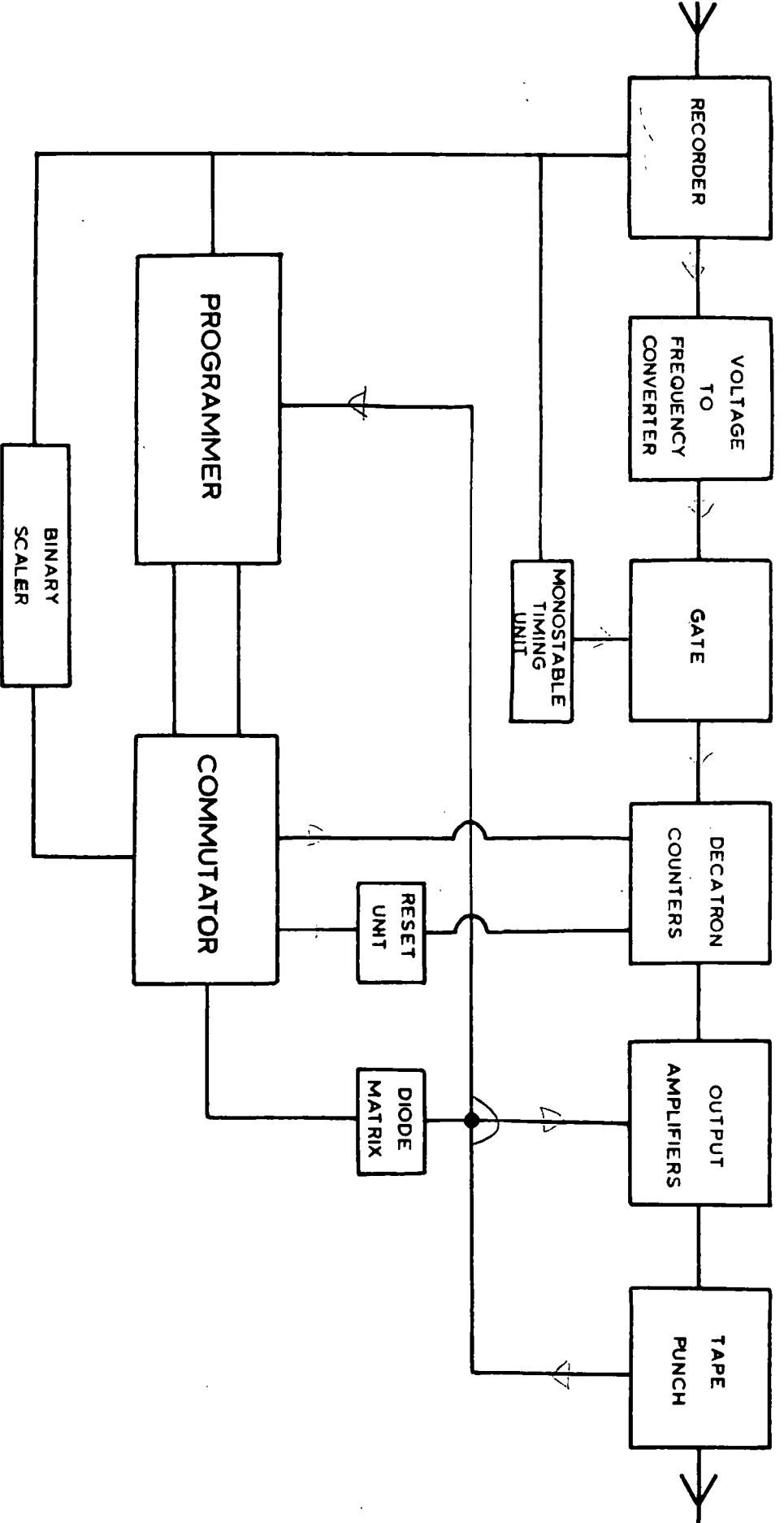


FIGURE 22.



BLOCK DIAGRAM OF ANALOGUE TO DIGITAL CONVERTER

FIGURE 25.

The whole unit was assembled by Mr. Collin and myself and mounted on a rack built especially for the purpose (Fig. 19), with the decatron tubes visible and the manual controls easily available. These controls allow the performance of the instrument to be checked as all the operations can be performed slowly.

The chart drive and tape punch are controlled by a switch on the power supply. This can also be controlled remotely by switching a relay in the power unit. By these means the units may be switched on by a control clock at any predetermined times.

DESCRIPTION OF CONVERTER

A simplified block diagram of the converter is shown in Fig. 23. The recorder accepts signals from the field instruments and prints them on a chart. A precision potentiometer is fixed to the output slider of the recorder and a voltage is tapped off corresponding to the position of the pen. This voltage from the potentiometer is constantly being converted linearly into a frequency. The whole cycle of operations is started by the closing of a microswitch as the recorder is about to print. Firstly a timing unit opens a gate for a definite short period of time. This allows a number of pulses corresponding to the input signal into a decatron counter unit where they are stored. Secondly a start pulse is given to the programmer and a count pulse is given to the binary scaler. The programmer, with the aid of another decatron acting as a commutator, selects in turn what is to be punched. It provides power to various diodes in

the diode matrix which selects the punching characters, and also to the decatron counter gates which correspond to the numbers to be punched. These in turn are fed through the output amplifiers which are energised just at the moment of printing, and finally into the tape punch. When a character has been punched, a signal from the tape punch tells the programmer to go ahead with the next character until while the required characters and numbers corresponding to the channel just recorded are punched. The reset unit is now activated to set the decatrons back to their stable state; thus the cycle of operations is completed before the recorder selects the next input. The binary scalar counts the input channels recorded and will arrange for 'carriage return line feed' to be punched in particular places on the tape, permitting tabulation of the results on a teleprinter.

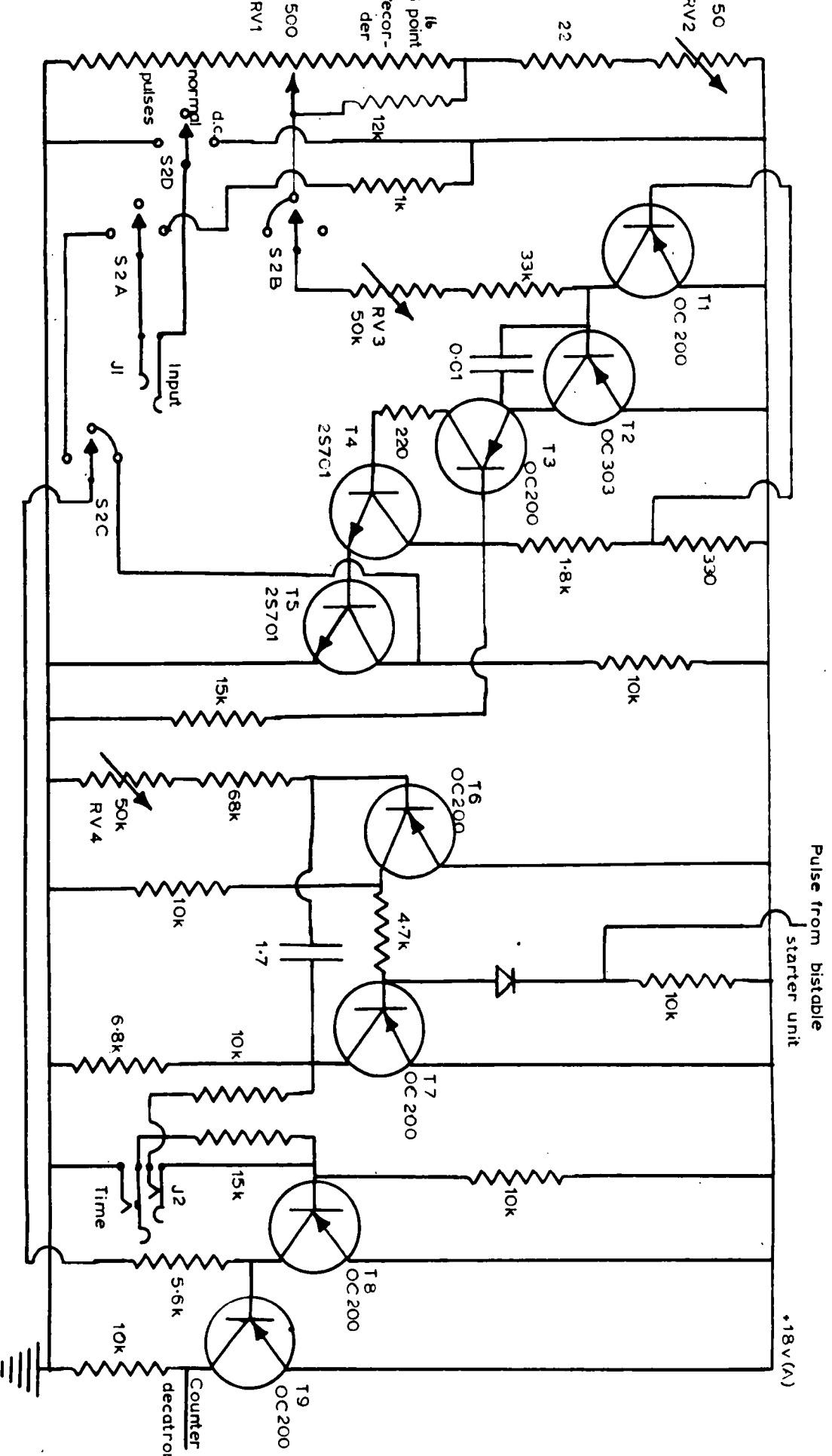
The circuit employs negative logic, and current is arranged to flow into the output amplifiers where no hole is to be punched.

Messrs. Honeywell Controls Ltd. quote an accuracy of $\pm 1\%$ for the recorder and the only other cause of error in the analogue to digital converter is the voltage change to frequency. This, determined experimentally, is about $\pm 2\%$; the overall error of 1% for this equipment is well below the field instruments' zero fluctuations.

CIRCUIT DESCRIPTION

RECORDER

The recorder used is a 16 point instrument with a range of ± 2.5 mV. Its input channels are printed in the form of points on a chart at the



VOLTAGE TO FREQUENCY CONVERTER, MONOSTABLE TIMING UNIT AND GATE

FIGURE 24.

rate of one every 2.4 sec, and alongside is printed the corresponding channel number. This Honeywell recorder employs a 16 way commutator switch which connects the external inputs in turn into its potentiometer circuit. The incoming voltage is measured against the slidewire voltage and any difference between the two is amplified by a unit which energises a balancing motor. This motor moves the contactor on the slidewire until the difference in voltage is zero. A zener diode regulator provides a constant voltage to the measuring circuit. A microswitch was fitted to the printing arm, and one was also fitted to a cam which closes the switch after channel 16 has printed in order to reset the scalars. The precision potentiometer which supplies the voltage-to-frequency converter is shunted by a 12 K resistor, in order to help to restore the linearity of the frequency output which is slightly non-linear for low input voltages.

VOLTAGE-TO-FREQUENCY CONVERTER (FIG. 24)

This is a unit which receives the voltage from the recorder's external potentiometer (RV1) and converts it into the repetition rate of a short pulse.

The voltage input to the converter is fed into T2 between its base and emitter, and from now on for this unit is referred to as negative with respect to the +18 V line.

If the emitter of T3 is more negative than the base of T3 no current will flow from its collector and therefore T4 and T5 will not conduct. The potential of the base of T3 is therefore fixed by the resistors 15 K, 1.8 K and 330 Ω at about -2 V with respect to this

+18 V line. Suppose that for a start the emitter of T3 is at about -17 V and the potential at the slidewire contact RV1 is more negative than 0.4 V (the potential required for base current to flow in T2); then the potential at the emitter of T3 will go positive at the rate determined by the 0.01 μ F condenser and the resistors 33 K + RV3.

When the emitter of T3 reaches a potential of about 0.4 V positive with respect to its base the transistor conducts and the collector current which passes into the base of T4 is fed back into the base of T3. The consequence of this is for the conduction to increase further and so both the emitter and base of T3 are taken rapidly negative.

This conduction will come to an end when the current through the emitter of T3 is insufficient to hold T3 and T4 in the 'bottomed' condition. [A P.N.P. transistor is "bottomed" when the input voltage is sufficiently negative to cause maximum collector current to flow. The collector potential is then only slightly more negative than the emitter potential, usually about half a volt]. When this happens the emitter of T3 is now at about -17 V and conduction stops abruptly leaving the base of T3 to return to the potential determined by its resistors.

During the period where the emitter of T3 is going positive the base of T1 is held at about -0.3 V by the resistors 15 K, 1.8 K and 330 Ω . This voltage is smaller than that required for base current flow and so T1 will not conduct during this period. The base of T3

is held at almost earth potential during the flyback period and so the base of T1 has now gone sufficiently negative for base current to flow. This means that the charging and input currents are diverted from the base of T2 to the +18 V line. If T1 were not in circuit the oscillations would only occur over a limited range of input voltages, due to the fact that the collector current of T2 at high input voltages will maintain T3 and T4 in the bottomed condition. The potential drop across the capacitor changes in a rapid linear manner in the first phase of the flyback period and in the second phase the potential on the capacitor is almost constant at a value close to that of earth.

The output frequency is not a linear function of the input voltage, but for values up to 2000 c/s the error is only ± 0.7 c/s. However as the oscillator will not start for input potentials lower than 0.4 V and as the linearity is poorer for low voltages it is desirable to lift the input voltage by a constant amount and reset the counter decatron to a negative number. This enforces a zero count to be made and thereby gives an almost linear output. The resistors RV2 + 22, which are connected in series with RV1 ensure that there is a large enough voltage applied to T2 and this can be changed by RV2 to a predetermined value.

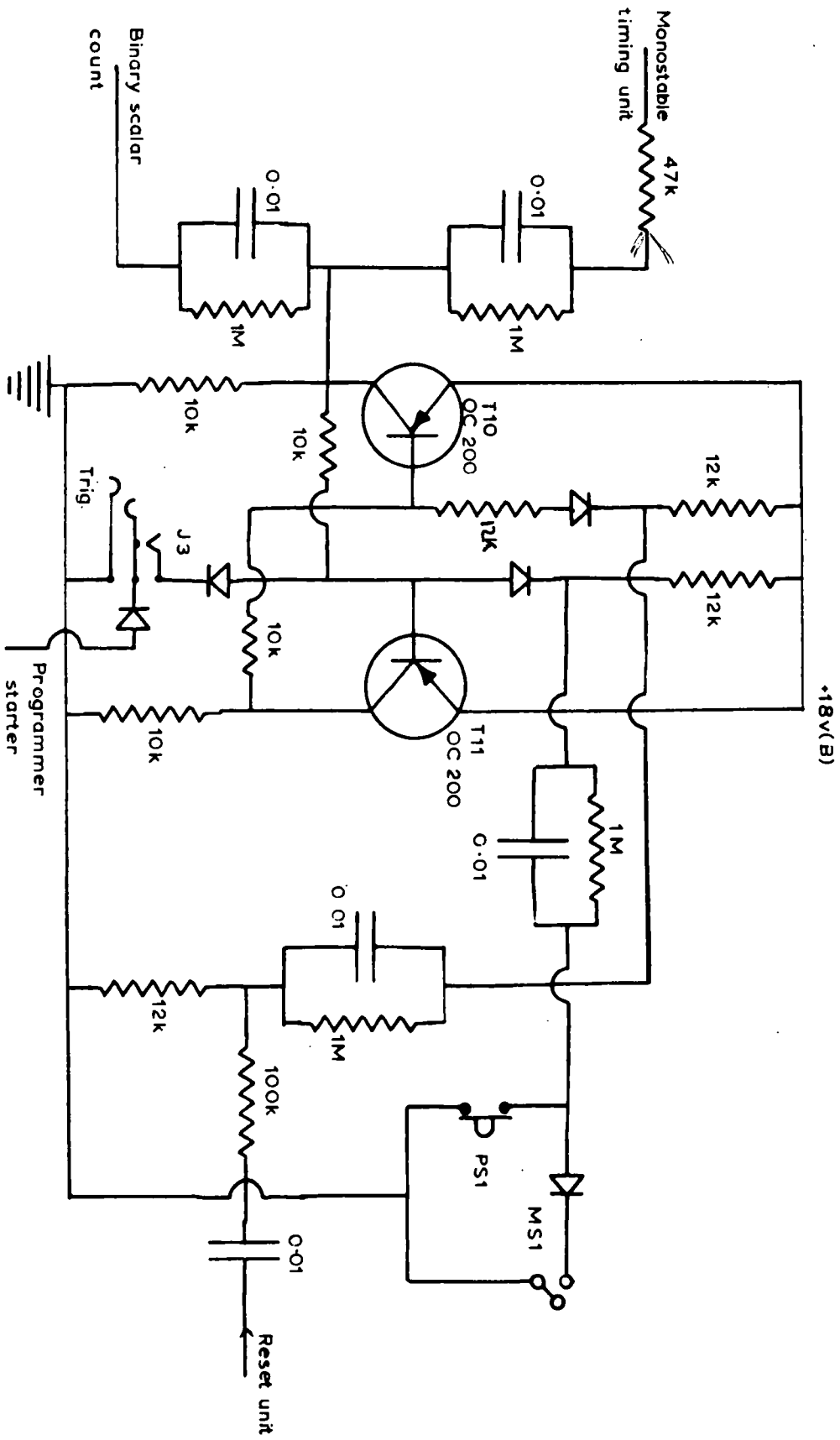
The use of silicon transistors renders the circuit relatively insensitive to changes in ambient temperature although any change in the input resistors and the 0.01 μ F condenser will directly affect

the frequency output. These components were therefore obtained with low and complementary temperature coefficients. T5 is purely for amplification purposes.

The 4 pole 3-way switch S2 and its adjacent jack J1 are to allow inputs not recorded on the 16 point recorder to be fed directly into the analogue-to-digital converter either in pulse form thereby bypassing the voltage-to-frequency converter, or in voltage form similar to that supplied by RV1.

MONOSTABLE TIMING UNIT AND GATE (FIG. 24)

From now on potentials are referred to as positive with respect to the earth line. The voltage-to-frequency converter is operating continuously and its input is allowed into the counters for about 1/10th sec. This time interval is determined by a monostable multi-vibrator comprising T6 and T7. The monostable circuit has one quasi-stable and one stable state. A negative trigger pulse from the starter unit flips the circuit into the unstable state, and the circuit subsequently flops back into the stable state. The stable state is with T6 conducting and T7 cut off. The trigger pulse switches on T7 thereby switching T6 off. The collector of T7 goes positive and takes the base of T6 positive with it thus cutting off T6. The 1.7 μ F condenser now discharges through RV4 and the 68 K and the circuit automatically switches back when the base-emitter voltage applied to T6 is approximately zero. The duration of the quasi-stable state is governed by the 1.7 μ F condenser and RV4 + 68 K resistors. This



BISTABLE STARTER UNIT

FIGURE 25.

monostable flip-flop therefore delivers one output pulse of a pre-determined length for each input pulse from the starter unit.

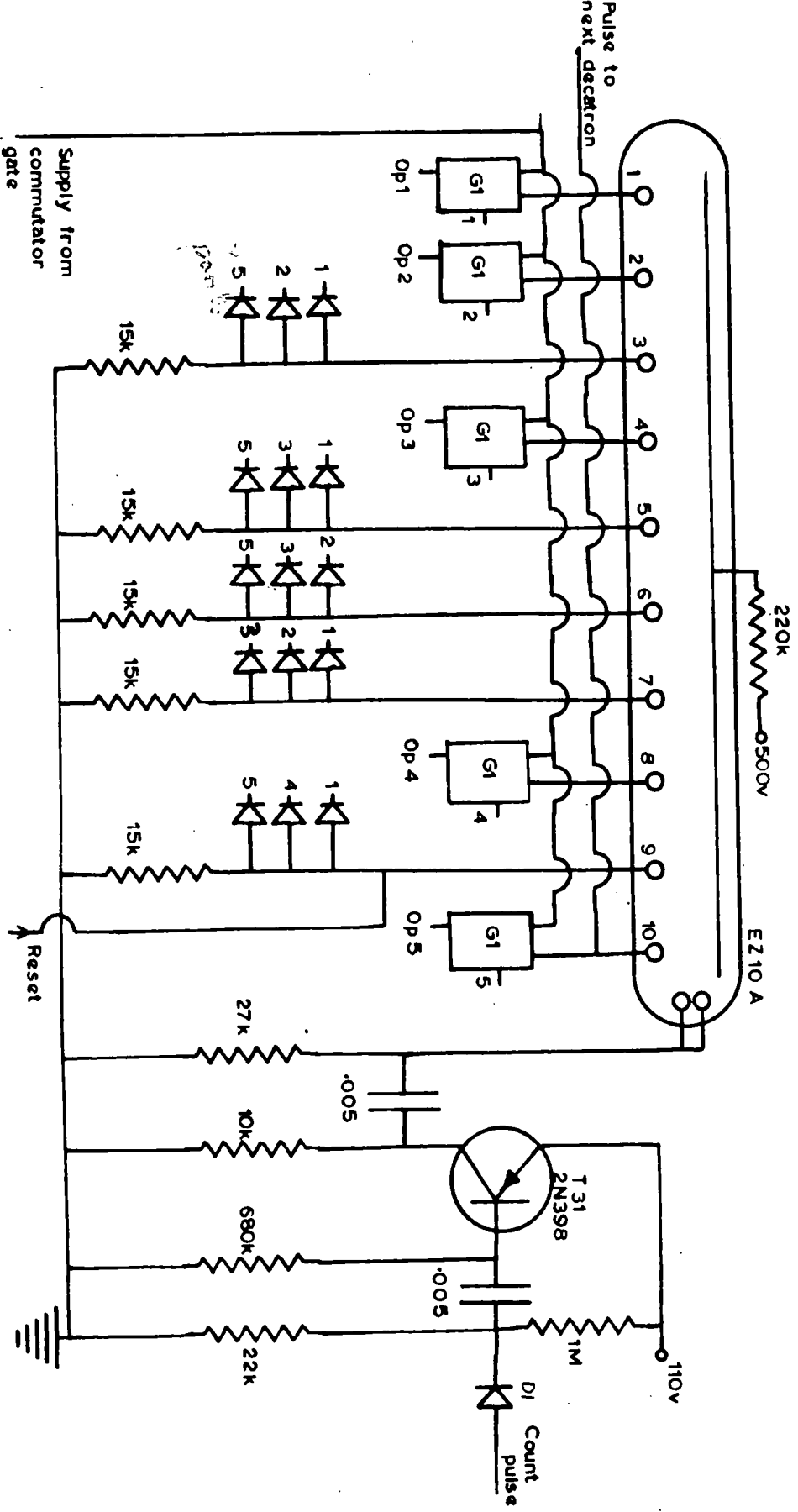
The positive timing pulse obtained from the collector of T7 is inverted by T8 and together with the frequency output from T5 is fed into the base of T9. In the steady state the collector of T8 and hence the base of T9 is held at about +18 V and therefore T9 will not conduct. However for the duration of the timing pulse the voltage from T8 is zero and so the frequency output from T5 causes T9 to conduct at the pulse rate. This is inverted at the collector of T9 and allowed into the counter decatrons.

The jack J2 allows any other timing pulse to be fed in as required.

BISTABLE STARTER UNIT (FIG. 25)

The recorder microswitch M81 or manual switch P81, either of which sets off the whole cycle of operations in the analogue-to-digital converter, were both found to chatter during initial testing of the equipment. This gave double and treble counts on the decatrons depending on the number of pulses passing into the timing unit. Because of this mechanical chatter a bistable multivibrator was built in order to give a single triggering pulse.

It consists of two transistors T10 and T11 connected one to the other in such a manner that there is positive feedback round the loop. Each transistor has two stable conditions, bottomed or cut off. The application of a trigger pulse will cause the transistors to



A TYPICAL DEATRION IN THE COUNTER UNIT

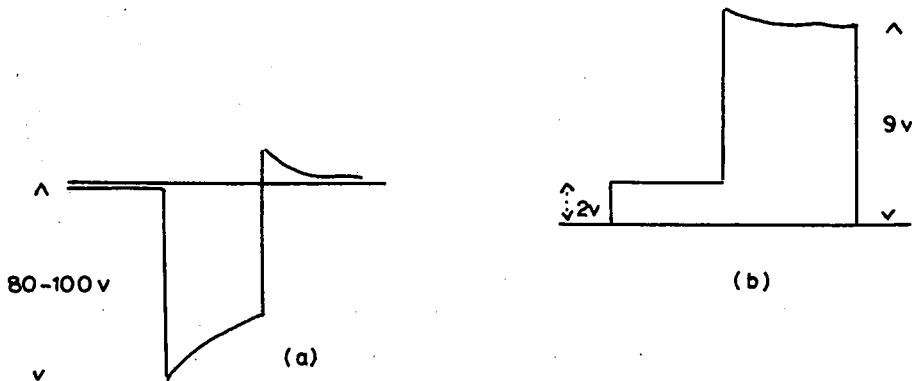
FIGURE 26.

change their states from T10 bottomed T11 cut off to T10 cut off T11 bottomed or vice versa. In the normal state T10 is bottomed and T11 cut off, but one (or more) negative pulses from MS1 to the base of T11 will tend to switch it on. This will cause the collector of T11 to go positive which in turn makes the base of T10 positive, and this causes T10 to cut off thereby causing its collector and the base of T11 to go negative causing T11 to conduct. The unit is then insensitive to any more input pulses and therefore a single negative pulse can be taken from the collector of T10. To reset, or return the unit to its original state, a negative pulse is applied to the base of T10 but this will be dealt with later.

Jack J3 allows for the insertion of a separate negative pulse to bring about the cycle of operations described.

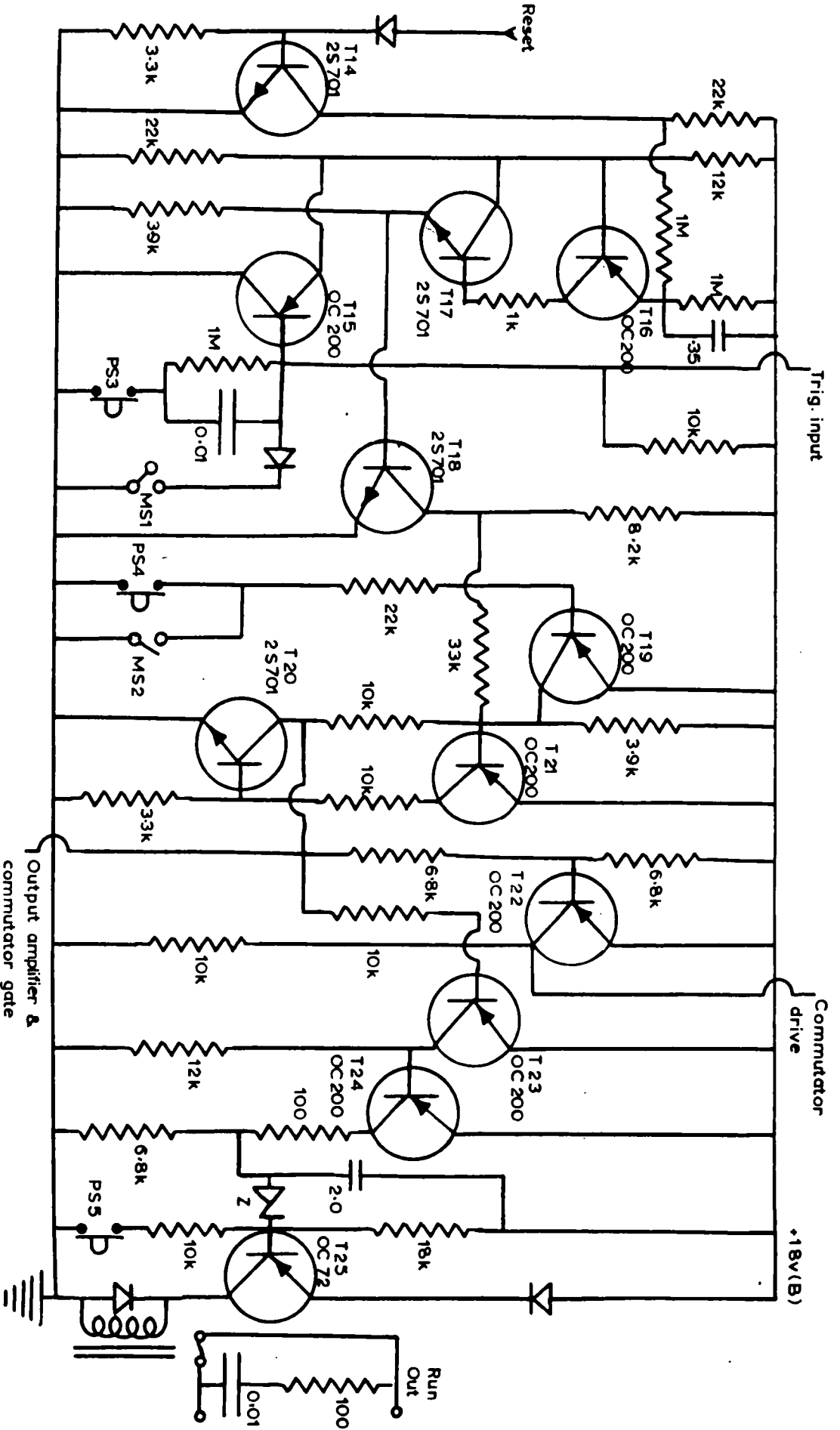
THE COUNTER DECATRONS (FIG. 26)

By using cold cathode decade counter tubes for single pulse operation for this unit, the count could be displayed visually as well as being read out electrically. A negative input pulse steps up the glow in succession through each of the ten main cathodes. The type used (EZ10A) permits counting rates up to 300,000 pulses per second which was well above the rate required in this equipment. The action of the EZ10A is independent of the shape of the input pulse but the manufacturers recommend that a differentiated square pulse with 80-100 V peak amplitudes be used (Fig. a). The amplitude of the output pulse is about 7 V (Fig. b).



It will be noted that the main output pulse is preceded by a 'pre-pulse' of lower amplitude of about 2V. The pre-pulse has a duration comparable with that of the auxiliary cathode pulse and it occurs because the main cathode is pre-ionized by the discharge of its adjacent cathode. This pre-pulse was found to affect the action of the following decade and hence it was necessary to use a diode gate circuit in the tens and hundreds counters.

The diode D1 is therefore biased to 2 V by a potential divider and this allows only the top part of the cathode pulse from the previous counter to pass into the base of T31. It was also necessary when assembling the apparatus to connect the anode resistor directly to the tube socket to avoid self-capacitance which led to parasitic oscillations causing false counts.



PROGRAMMER

FIGURE 27.

The positive pulse of amplitude 7 V is passed into the base of T31 which is a high voltage germanium switching transistor. The collector of T31 goes sharply negative and the differentiated pulse is the decatron driving pulse.

The output from each decatron is taken from gates G1, one gate corresponding to each hole in the tape. As the code used is binary coded decimal it means the gates will occupy positions 1, 2, 4, 8, 0 on each decatron. The cathodes from the other positions on the decatrons are connected to their appropriate gates through diodes which prevent feedback.

To reset the counters to any number a short negative pulse of about 120 V is applied to the corresponding position.

As mentioned earlier it was necessary to reset the counters to 989 and so a zero count of 11 will overcome the non-linearity of the voltage-to-frequency converter.

PROGRAMMER (FIG. 27)

This complex logic circuit has the power to activate, in order, any section of the analogue to digital converter when it receives signals to do so, and also waits for one action to be completed before starting with another. By these means no part of the converter can be overlooked and every character will be punched. The programmer works in close contact with the commutator decatron (Fig. 28), the workings of which are described later.

a) Clock pulse generator

Consider firstly that the glow is resting on the zero cathode of the commutator as this will be the rest position. Due to this, therefore, some current passes into the base of T14 switching it on and putting its collector at earth potential. It is held in that state because there is an effective short circuit between the emitter and collector. This maintains the emitter of T16 at about 9 V due to the potential dividing action of the two 1M resistors. T16 will not conduct unless its emitter is more positive than its base and without any current flowing the base potential ^{is} fixed by the 12 K and 22 K resistors to be about 12 V.

If somehow the glow can be made to move from the zero cathode then T14 no longer conducts and the oscillator will run. The glow is removed by the recorder momentarily closing the switch MS1 or by manual control PS3. This passes a sharp negative pulse into the base of T15 which then conducts for a short period of time. This causes the emitter of T15 and hence the base of T16 to go sharply negative and thus T16 conducts. As it does so T17 conducts, and so does T18 which produces a clock pulse from its collector. The effect of this clock pulse is to produce one driving pulse to the commutator deatron and thus the glow moves from the zero position to position 1. Because there is no longer any current flowing from the zero position T14 no longer has any base current and therefore cannot conduct; hence T16 cannot conduct. The complex of T16, T17 and T18 therefore proceeds to oscillate, and the rate at which it

oscillates is governed by the IM resistor and 0.35 μ F condenser.

The operation of the oscillator is as follows. Assuming that a clock pulse has just been formed the emitter of T16 will be somewhere near earth potential. The capacity is charged to about 18 V but it doesn't stay like that. It proceeds to discharge, or charge positively through the IM resistor going more and more positive. Sooner or later it will get positive with respect to the base of T16 and when it does T16 conducts slightly. The potential on the base of T17 now causes this transistor to conduct slightly between collector and emitter which has the effect of lowering the potential on the base of T16. This action now allows T16 to pass more current and the process continues very quickly causing T16 and T17 to go hard into conduction. The emitter of T16 is driven in the negative direction thus recharging the 0.35 μ F condenser to the condition started with. The conduction of course stops when this point is reached due to the emitter being negative with respect to the base, so that the condenser discharges via the IM resistor again. The oscilloscope picture of the voltage across the condenser will therefore be a saw-tooth waveform which shows the voltage going slowly positive and rapidly negative. Each time conduction takes place the emitter current of T17 goes into the base of T18 which merely serves as an amplifier and thus a clock pulse is produced at its collector. So naturally when switch MS1 or PS3 is closed, the programmer starts with an artificial clock pulse and thereafter runs itself until the glow once more rests on the zero cathode.

The duration of the clock pulse is adjusted by varying the capacitance so that it is just a little longer than the time the punch takes to complete a punching cycle. The object of this will be seen later but it ensures that the punch is working fast and there is no possibility of missing parts of the code.

b) Memory unit (Bistable)

Silicon transistors have negligible leakage current, that is to say no current flows in the collector circuit unless there is base current of the order of $100 \mu\text{A}$. This unit is made up of a combination of a p-n-p (T_{20}) and an n-p-n (T_{21}) transistor. In the stable state neither T_{20} nor T_{21} are taking current and therefore there is no collector current. This means the base of T_{20} is naturally at earth potential. Similarly the base of T_{21} is at +18 V and it will stay like this forever unless the base potentials are altered. The negative clock pulse is fed into the base of T_{21} and this transistor will now momentarily conduct. Current will flow from its emitter to collector and hence a small amount of current flows into the base of T_{20} . This transistor therefore conducts and supplies further base current to T_{21} . The circuit therefore rapidly goes into a conducting state in which the current is limited only by the resistances in the emitter collector lines and the load.

The transistors T_{20} and T_{21} are now very heavily bottomed and so the clock pulse has succeeded in causing the complex of T_{20} and T_{21} to maintain itself in the 'on' position. The unit therefore has two stable states, either both conducting or both cut off.

When the unit is in the 'on' condition it causes power to be supplied to the output amplifiers, commutator gates and run out relay and also drives the commutator on one position. The run out relay starts the punching action and when this is complete a cam in the punch closes switch MS2 (the 'operation complete' switch). This switch makes the base of T19 negative with respect to its emitter and thus switches it on, thereby diverting the current from the collector of T20 away from the base of T21. This therefore breaks the memory unit loop and T20 and T21 turn themselves off.

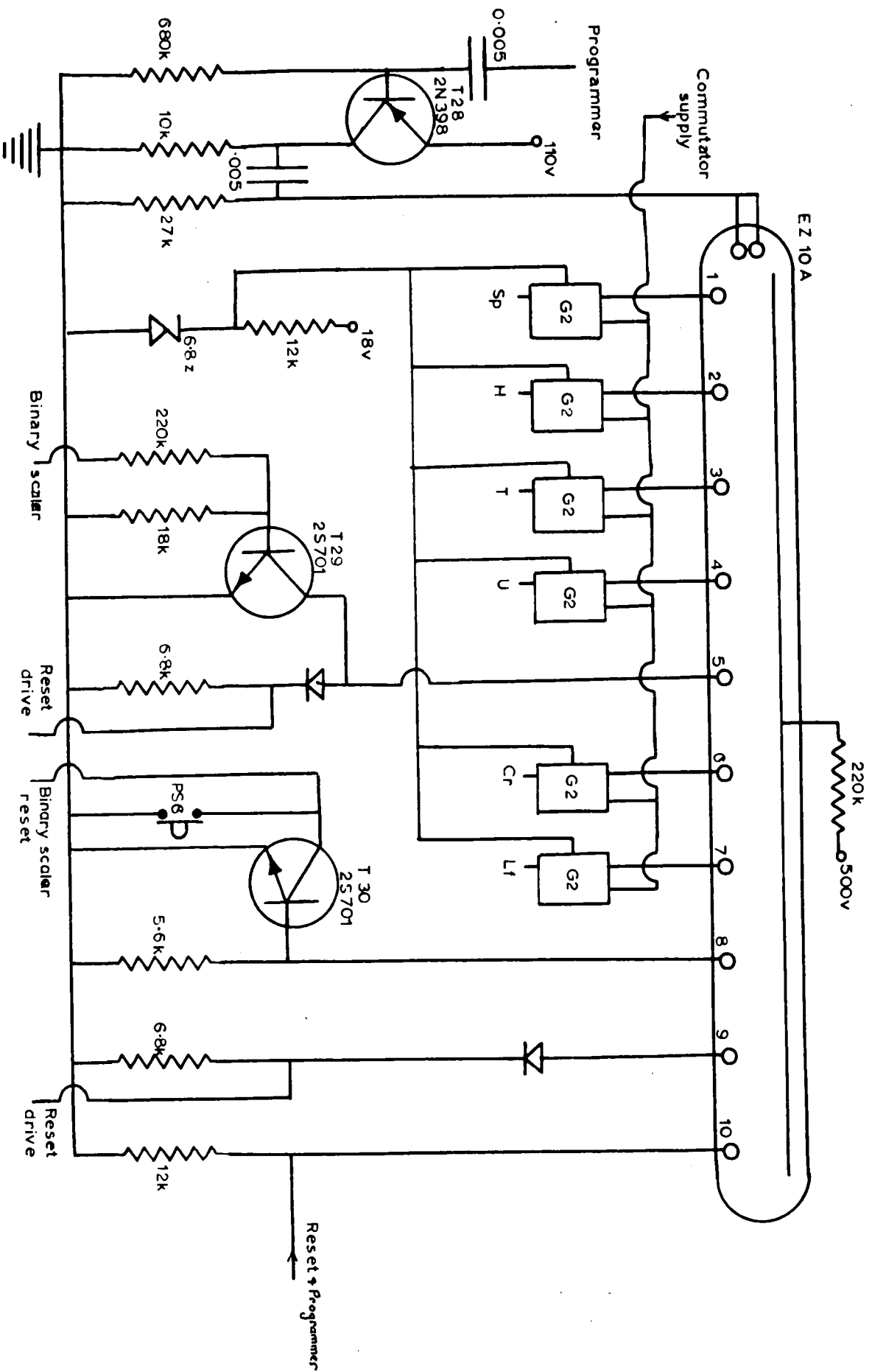
c) Run out Amplifier

This unit comprises T23, T24, and T25.

The relays in the output amplifiers operate electromagnets in the punch which bring plungers into position in order for holes to be punched. They are driven through the tape by a cam connected to the punch motor through an electromagnetically operated clutch. This is controlled by the run out amplifier relay operated by T25. The closing of P35 manually will have the same effect on the run out relay as the "bottoming" of the transistors in the memory unit.

The negative step voltage from the collector of T20 passes into the base of T23, is inverted and passed into T24 which, whilst normally conducting, is now switched off.

In consequence of this the 2.0 μF condenser begins to charge; this introduces a slight time delay which allows the output relays to bring the plungers into position before the punching action commences. The base of T25 begins to go negative until, when the transistor



COMMUTATOR UNIT

FIGURE 28.

switches, the run out relay is operated. The zener diode Z is in circuit to increase the time delays as the potential has to rise to a particular level before the zener diode allows the transistor to conduct. The diodes in the emitter and collector lines protect the transistor from emf's induced in the relay coil when it is switched on or off.

d) Commutator drive

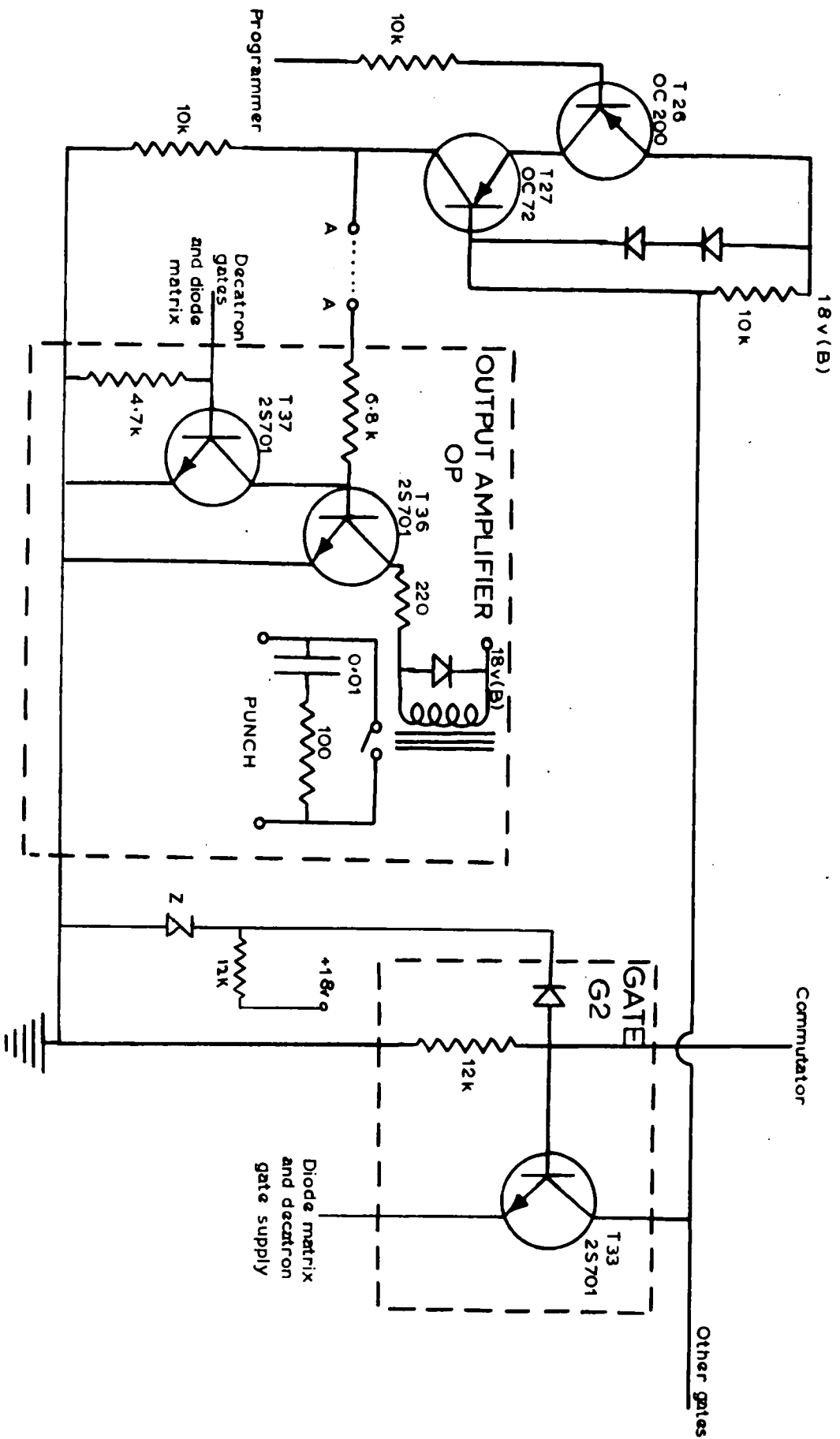
The negative step voltage on the base of T22 caused by the memory unit being switched on, is inverted by it and passed into the commutator drive transistor T28.

COMMUTATOR (FIG. 28)

The pulse from T22 is differentiated, passed into the base of the high voltage transistor T28 and the resulting differentiated sharp negative pulse drives the commutator on one position.

The positions of the discharge on this deatron determines the operation to be performed and are as follows:

- 0 - stand by position
- 1 - 'Space' is punched
- 2 - 'Hundreds' digit punched
- 3 - 'Tens' digit punched
- 4 - 'Units' digit punched
- 5 - All units reset except binary scalar unless T29 is conducting
- 6 - 'Carriage return' is punched
- 7 - 'Line feed' is punched
- 8 - Binary scalars are reset



OUTPUT AMPLIFIER AND COMMUTATOR GATE

FIGURE 29.

9 - All units reset except binary scalars.

If the discharge is from positions 1,2,3,4, 6 or 7 the current passes into gates G2 (described later) and thence to the part of the circuit where the operation is to be performed. If however the glow rests in position 5 and T29 is not conducting then the reset unit is set into operation and all decatron are reset to zero. However when the binary scaler has arrived at its present number, current flows into the base of T29 which effectively short circuits the discharge current to earth and hence no units are reset. The commutator then steps on one position at a time until, when it reaches 8, the current into the base of T30 has the property of earthing the collector potential of this transistor and hence resets the binary scalars. This can also be done manually by pushing PS6.

When the glow reaches position 9 the reset unit is activated once more and the commutator reset at the zero position.

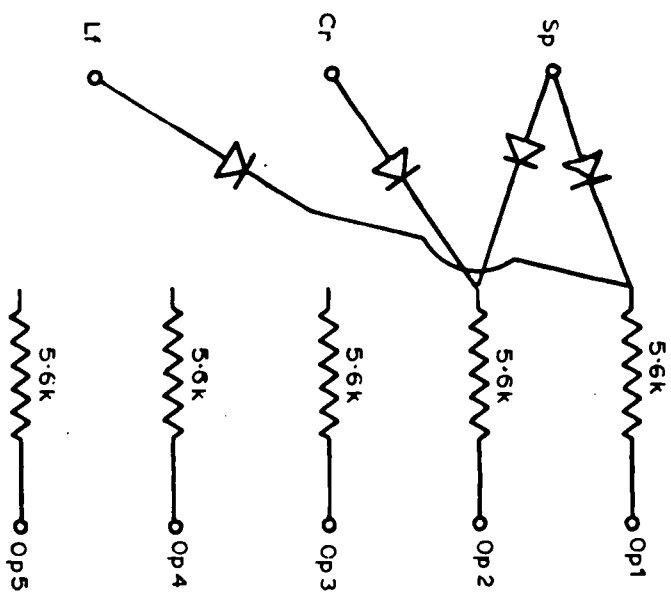
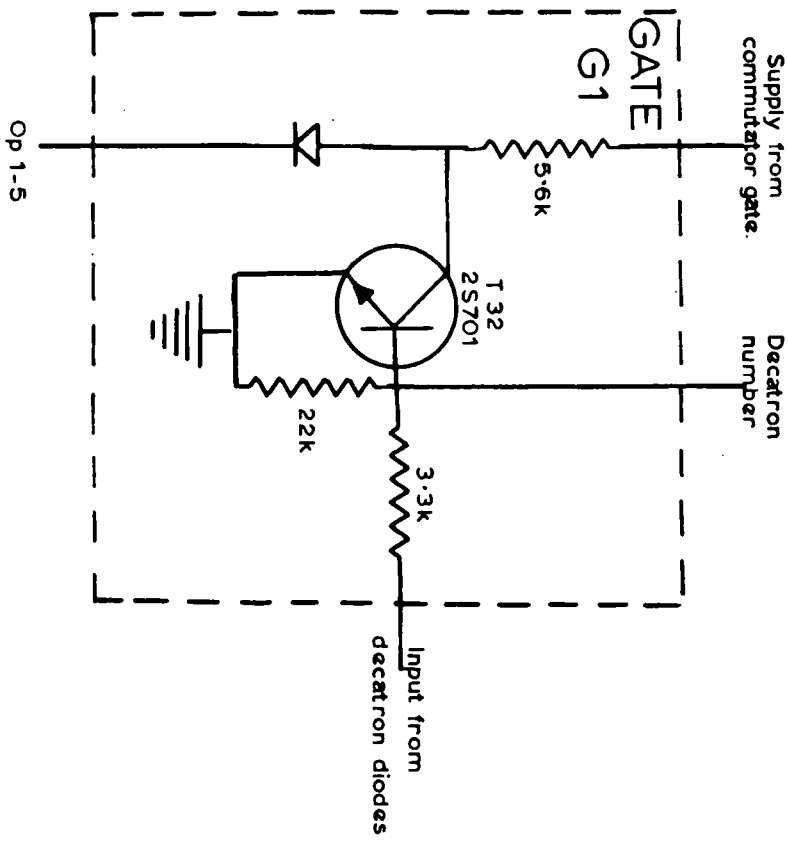
OUTPUT AMPLIFIER AND COMMUTATOR GATES (FIG. 29)

If the glow on the commutator decatron is in position 1 then current will flow into the base of T33 in the first gate (G2). This current switches on the transistor and effectively short circuits the emitter and collector. As the collector is at +18 V then this voltage is applied to the 'space' position of the diode matrix (Fig. 30) and onto the output amplifiers 1 and 2. Because of the negative logic of the circuit these positions are the ones where no holes are to be punched. The diode from the base of G2, in conjunction

with the stabilized supply from the zener diode, chops the top off the pulse from the commutator cathode. The reason for this is that the output from G2 into the diode matrix and counter gates must not be ragged and hence by squaring the commutator pulse a better shape is obtained at the emitter of T33. The incoming signal to the diode matrix is passed onto the base of T37 which conducts, and lowers the base potential on T36 switching it off. Hence that relay will not work. In the output amplifiers on which there is no signal to switch T37 on, T36 conducts and the relays will operate and punch holes. However if there was always a potential on the base of T36 (from A) the output amplifier relay would operate during the rest position and so with the aid of an 'and' circuit this power is only switched on when both the memory unit is on and a gate G2 is taking current.

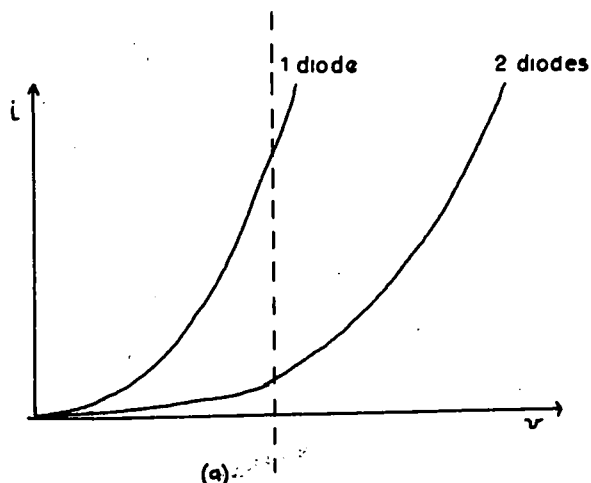
The negative step voltage from the memory unit switches on T26 and this causes the emitter of T27 to raise its potential to +18 V. Also when a gate G2 is taking current through the 10 K resistor the base potential of T27 drops and this transistor is switched on. The effect of the diodes between the base of T27 and the +18 V line is to limit the current at the base to prevent destroying the transistor. The two diodes will obviously lower the current for a particular voltage more than for a single diode. / Hence only when the 'and' circuit is on is there a current flowing into the base of T36, and the output relays will only operate at these times.

Fig. (a)



COUNTER DECATRON GATE AND DIODE MATRIX

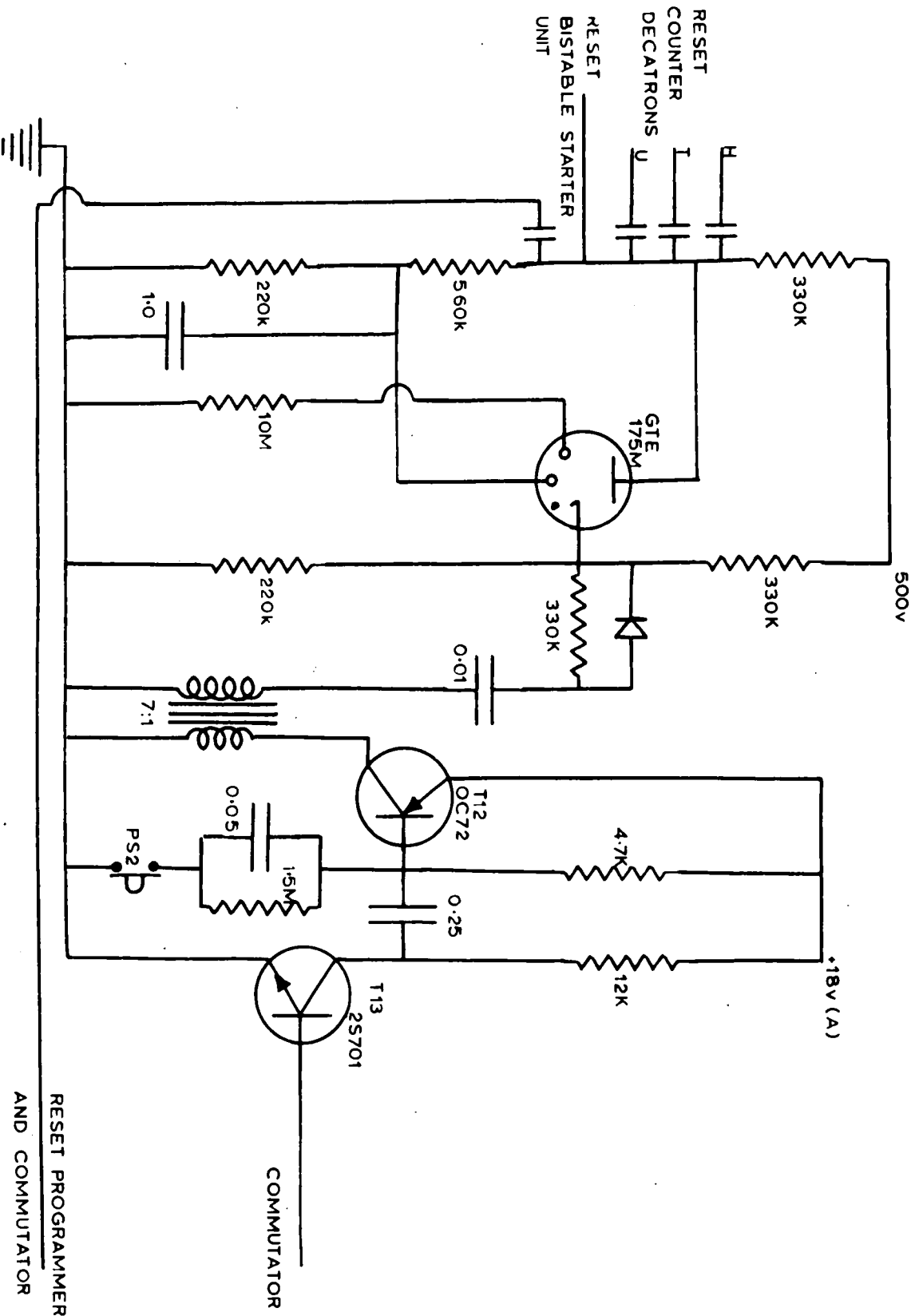
FIGURE 30.



COUNTER DECATRON GATES AND DIODE MATRIX (FIG. 30)

The second clock pulse will step the commutator to position 2 and the next gate G2 is opened. This time however the voltage is not applied to the diode matrix but to the five G1 gates of the hundreds decatron. Either one or three of these gates will have voltages applied to the base of their transistors (T52) depending on which ever of the decatron cathodes the glow is resting on. The transistor therefore conducts and the voltage from the commutator gate (G2) is fed to earth. The remaining gates (G1) are still closed and so the voltage from the commutator will pass directly to their corresponding output amplifiers and their action will be suppressed. In this case therefore holes are punched on the tape in the positions corresponding to the gates (G1) which have current flowing through their transistor bases.

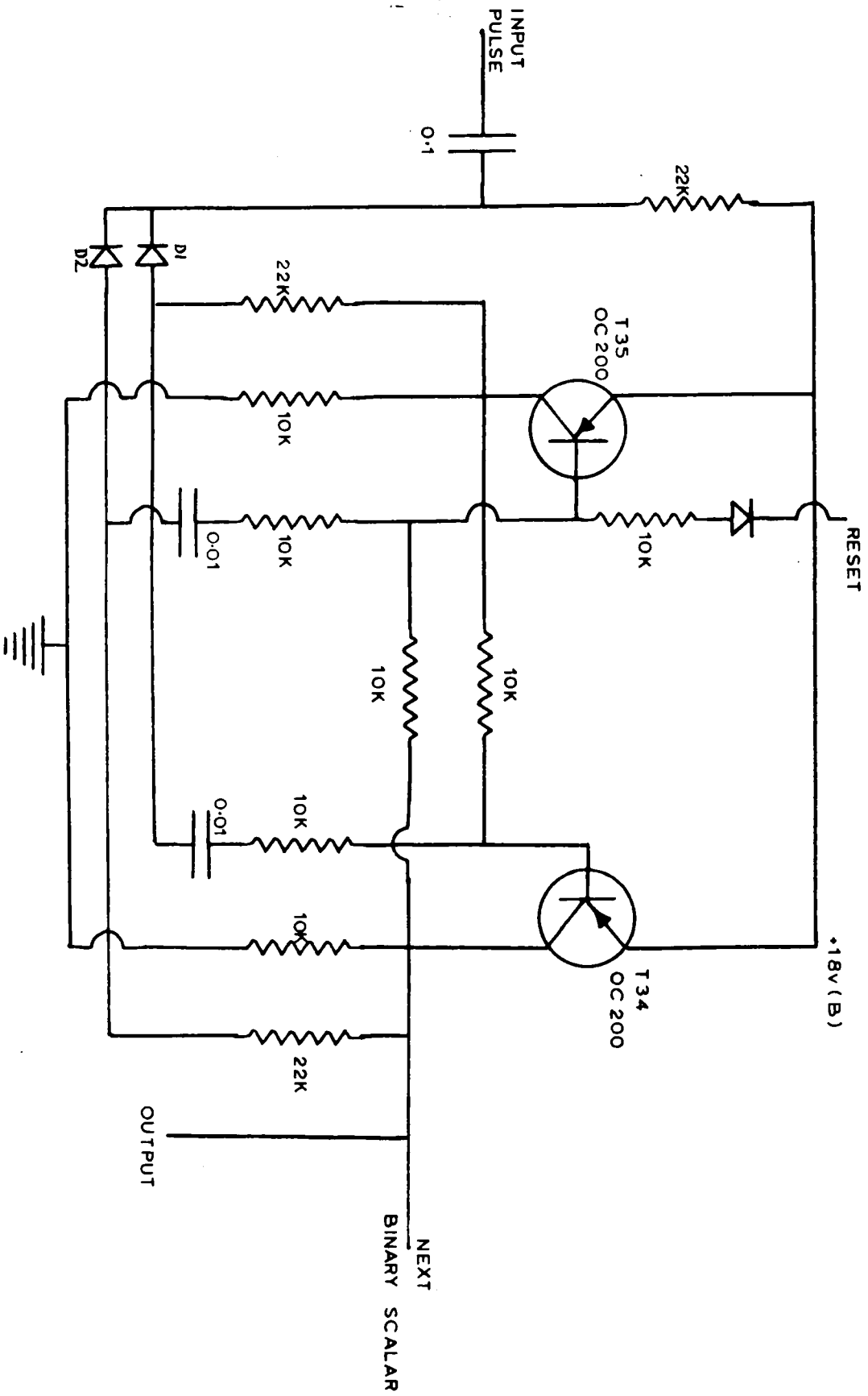
As the commutator is stepped on to positions 3 and 4 the tens and units decatron gates are activated in a similar manner, whereas when the glow is on positions 6 and 7 the current flow is once more through the diode matrix.



RESET UNIT

FIGURE 31.

RESET PROGRAMMER
AND COMMUTATOR



BINARY SCALAR

FIGURE 32.

RESET UNIT (FIG. 31)

In commutator position 9 and often position 5, current flows from the cathodes to the base of T13 which switches on a gives a negative pulse on the base of T12. This pulse can also be manually obtained by pressing PS2. The effect of this is for T12 to conduct momentarily and with the aid of a step up transformer a large negative pulse from the secondary coil is applied to the trigger of the cold cathode tetrode GTE 175 M. This causes the tube to fire drawing current through the anode resistor, and hence the anode potential drops below the running voltage of the tube, which cuts off. The large negative pulse on the anode of the tetrode is fed via condensers to reset the decatron and starter unit.

It was necessary to set the voltage of the sustainer electrode about 100 V more negative than the cathode so that its discharge does not go out when the main discharge is extinguished. The reason for this is that owing to the small number of free electrons in the tube it may be a while before ionization is sufficient for it to be restored.

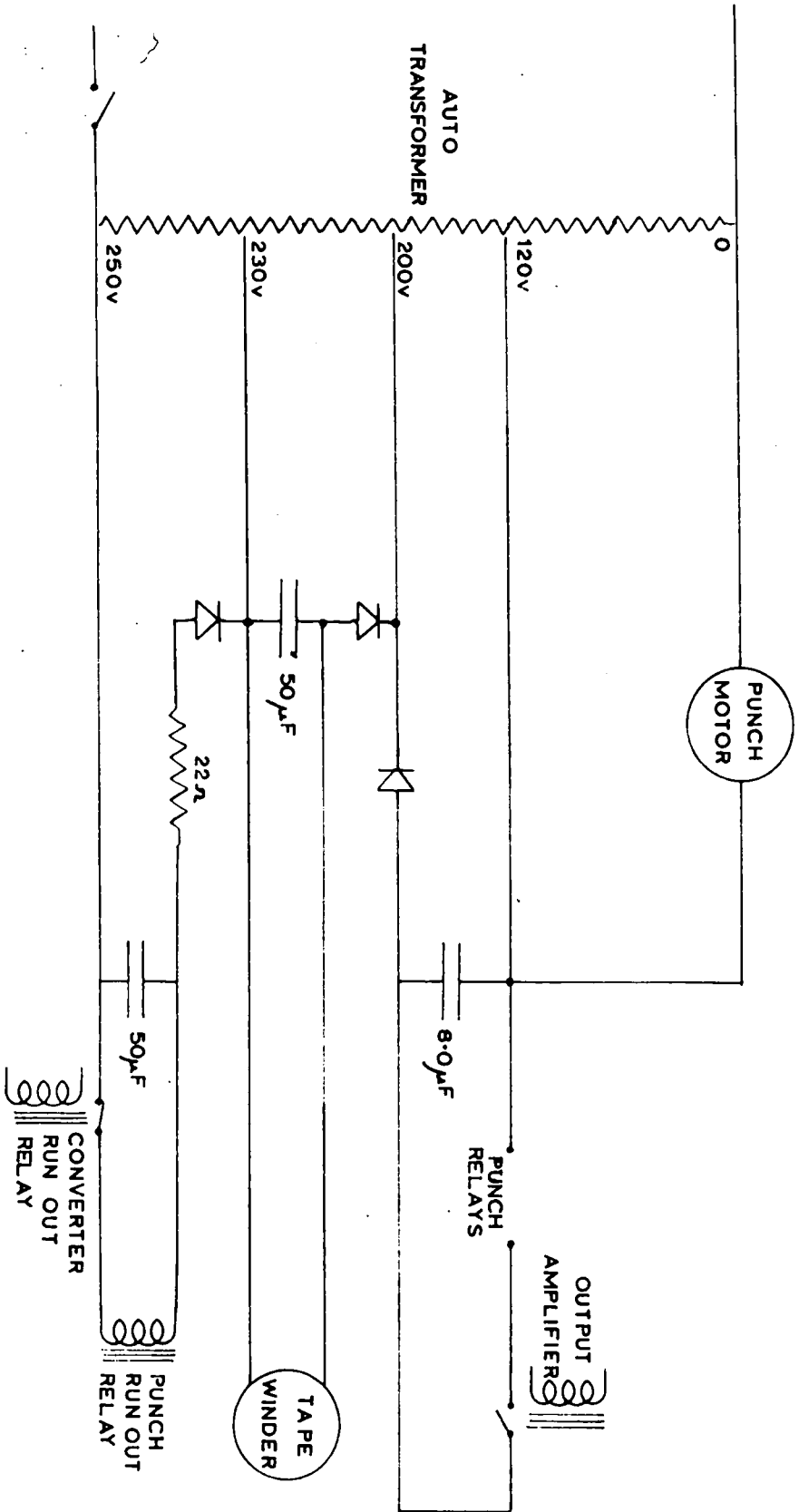
BINARY SCALER (FIG. 32)

In order for a teleprinter to print the punched data in columns, the code "carriage return line feed" has to be inserted on the tape at specified points. Fortunately the recorder is a 16 point instrument and 16 is a binary number. If therefore five scale-of-two counters are built, outputs can be obtained at the end of 1, 2, 4, 8 or 16 counts, and the output used to switch on T29. This shorts the

reset action of the number 5 cathode on the commutator which then progresses to positions 6 and 7 to punch the required code. The output of the teleprinter can therefore be set into columns of 1, 2, 4, 8 or 16 numbers.

The binary counter shown in Fig. 32 is based on the Eccles-Jordan bistable circuit. The basic requirement for such a circuit is that each of a series of unidirectional pulses applied to the circuit should cause the circuit to change from one stable state to the other. In this way the bi-stable circuit carries out one complete cycle for every two input pulses, and will give an output of one directional pulse for each cycle. A division by two is thus achieved from input to output.

Consider the state where T34 is conducting and T35 is off. The base of T34 will now be slightly negative with respect to its emitter and therefore diode D1 will be conducting. T35 is cut off and its base is at the same potential as its emitter and so D2 will not be conducting. A negative pulse applied from the starter unit through the 0.1 μ F condenser will therefore be passed by the diode which is most positively biased (D2), and this has the property of switching T35 on. The consequence of this is for the base of T34 to go positive to the potential of its emitter thereby switching it off and one cycle has been completed. The output from the collector of T34 is taken up to the next binary scalar and also to a single pole five way selector switch. This switch can then select which of

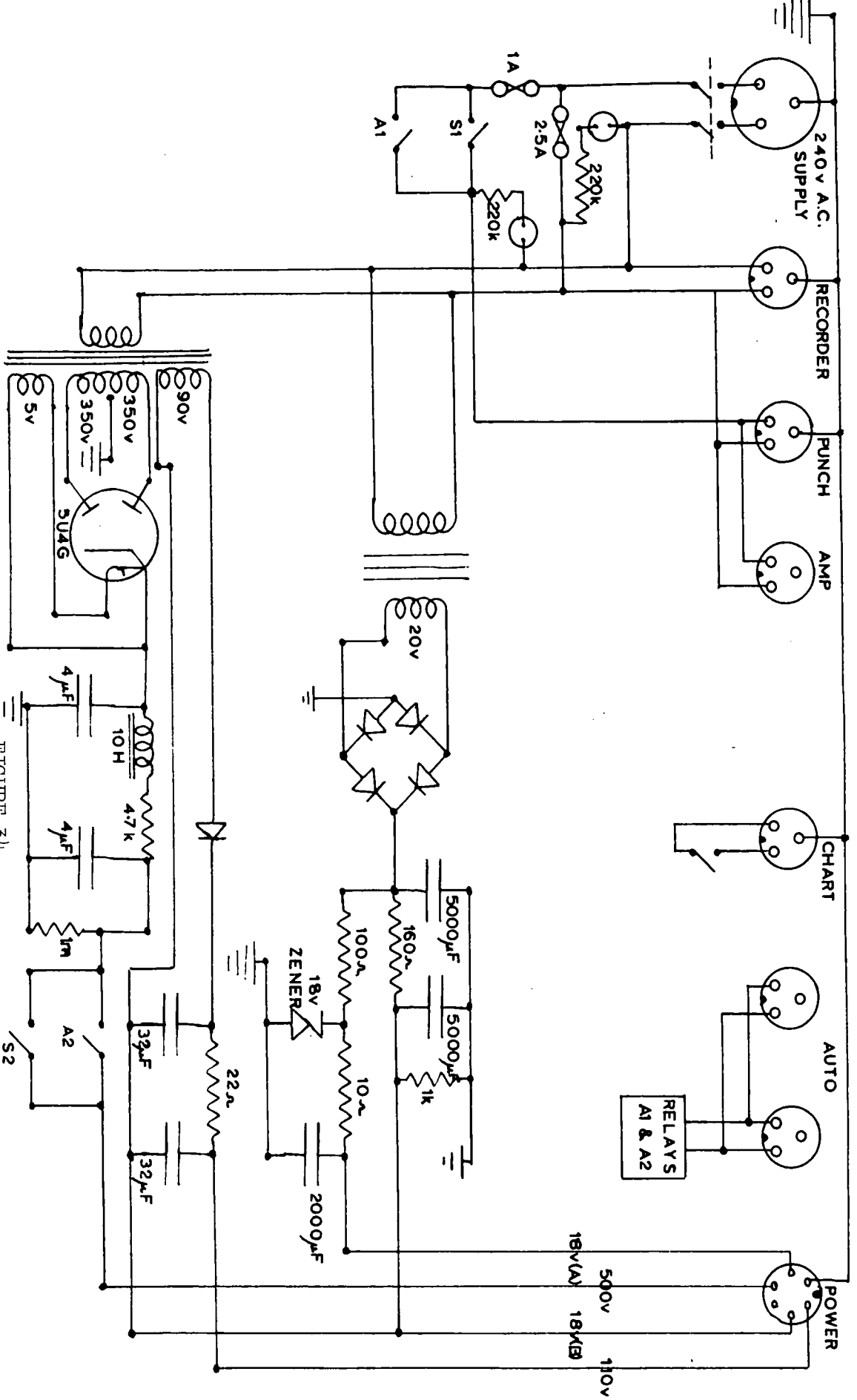


ANALOGUE TO DIGITAL CONVERTER POWER SUPPLY 'X'

FIGURE 33.

ANALOGUE TO DIGITAL CONVERTER POWER SUPPLY 'Y'

FIGURE 34.



the binary pulses it needs to pass on to the base of T29. The five scalars are reset both from the 9 position of the commutator and also from a micro-switch on the recorder which closes after channel 16 has printed. This reset action is simply the connection momentarily of the base of T35 to earth potential on all the scalars, thereby returning them all to the same state at the same time.

The tape from the punch is automatically wound onto a spool driven by a motor with a slipping drive connection. This ensures the tape is wound tightly without risk of tearing.

POWER SUPPLIES

Two power units supply the analogue-to-digital converter. Power supply 'X' (Fig. 33) is situated inside the tape punch housing and power supply 'Y' (Fig. 34) is mounted on the main rack. The former unit, employing an auto transformer, supplies 120 V A.C. to the punch motor, 80 V D.C. to the punch relays, 30 V D.C. to the tape winder and 12 V D.C. to the punch run out relay. Rectification is achieved using silicon rectifiers.

Power unit 'Y' however supplies D.C. voltages to the main analogue-to-digital converter. The 240 V A.C. input to this power pack can be switched on manually using a double pole double throw switch, and as this is done a neon bulb illuminates a red disc on the front panel. This mains voltage is also fed to the recorder amplifier and to two transformers. One transformer gives a 20 V A.C. output whereas the other transformer gives three A.C. outputs, namely 90 V, 5 V and 700 V. The 20 V, A.C., after being rectified

with a bridge rectifier, is split into two outputs, one stabilized and one not. One of these, incorporating an 18 V zener diode and a 2000 μF condenser, supplies the stabilised supply 18 V(A) to the converter, and the other using two 5000 μF smoothing condensers supplies the unstabilised 18 V(B) to the converter. This latter unstabilised supply is fed to the high current transistors and the relays, as if there had only been a single 18 V supply the constantly varying load would greatly hinder the stabilisation necessary for certain transistors.

The 5 V output from the second transformer is the heater supply to a double diode rectifying valve type no. 5U4G. To allow for full-wave rectification the centre tap of the 700 V winding is earthed and the output smoothed with two 4 μF condensers and a 10 H choke giving a 500 V D.C. source. The 90 V A.C. supply is rectified with a silicon rectifier and smoothed, but one side of the output is connected to the 18 V(B) supply giving a total of 110 V D.C. output for the decatron drive. The manual switch S1 or relay switch A1 allows 240 V A.C. to be fed into the punch power supply and therefore places this unit in the standby position; a neon bulb in this circuit illuminates a green disc on the panel. Another manual switch S2 or relay switch A2 feeds 500 V DC onto the anode of the decatron tubes. This voltage is only switched on during recording so as not to cause a glow on a position of the decatron tubes whilst they are not in use so as to lengthen their life.

It is possible to switch the relays A1 and A2 automatically along with the chart drive switch thus allowing the analogue-to-digital converter and recorder to come into operation. The socket outputs from power supply 'Y' are shown at the top of Fig. 34 and they are all placed at the rear of the unit so that they are easily accessible.

CHAPTER 6LABORATORY TESTING OF THE SPACE CHARGE COLLECTORSGENERAL

MOORE ET AL. (1961) investigated the properties of the filter medium used in these collectors by drawing air containing approximately 10^5 condensation nuclei per cm^3 through the filter, and by a photometric method of evaluation concluded that the filter removes 99% or more of these nuclei.

However, as can be seen from Table 3 the radius of large ions and condensation nuclei is a factor of 100 larger than that of small ions and, as small ions contribute a major part of the atmospheric space charge away from city air, I thought that these previous tests were insufficient to prove the reliability of the collector. If it could be shown that the space charge collector could remove a high proportion of small ions this type of apparatus would be an excellent space charge measuring device in clean air.

TABLE 3

	RADIUS $\text{cm} \times 10^{-8}$	MOBILITY cm sec^{-1} per $v \text{ cm}^{-1}$
Small ions	6	1-2
Intermediate ions	16-70	0.2-0.01
Large ions	80-500	0.008-0.0003
Fine dust, smoke, etc.	100-100,000	0.005-0.000005

The actual tests were carried out during a period of two months in a small room of dimensions 3 m x 3 m x 4 m where there was very little disturbance of the air due to human sources.

RECORDING EQUIPMENT AND CALIBRATION

During the earlier part of the tests when no accurate flow-measuring equipment was available it was difficult to measure the volume of air that the three stage centrifugal fan had sucked through the filter. A venturi tube was constructed and inserted in the rubber tubing exhaust lead from the space charge collector. Using a standard water manometer a pressure drop was observed, but in order to obtain an acceptable value for the flow it was necessary to purchase a manometer suitable for measuring the pressure difference much more accurately. However in the mean time the Northern Gas Board had agreed to our purchasing some second hand gas meters; thus the venturi tube method was abandoned.

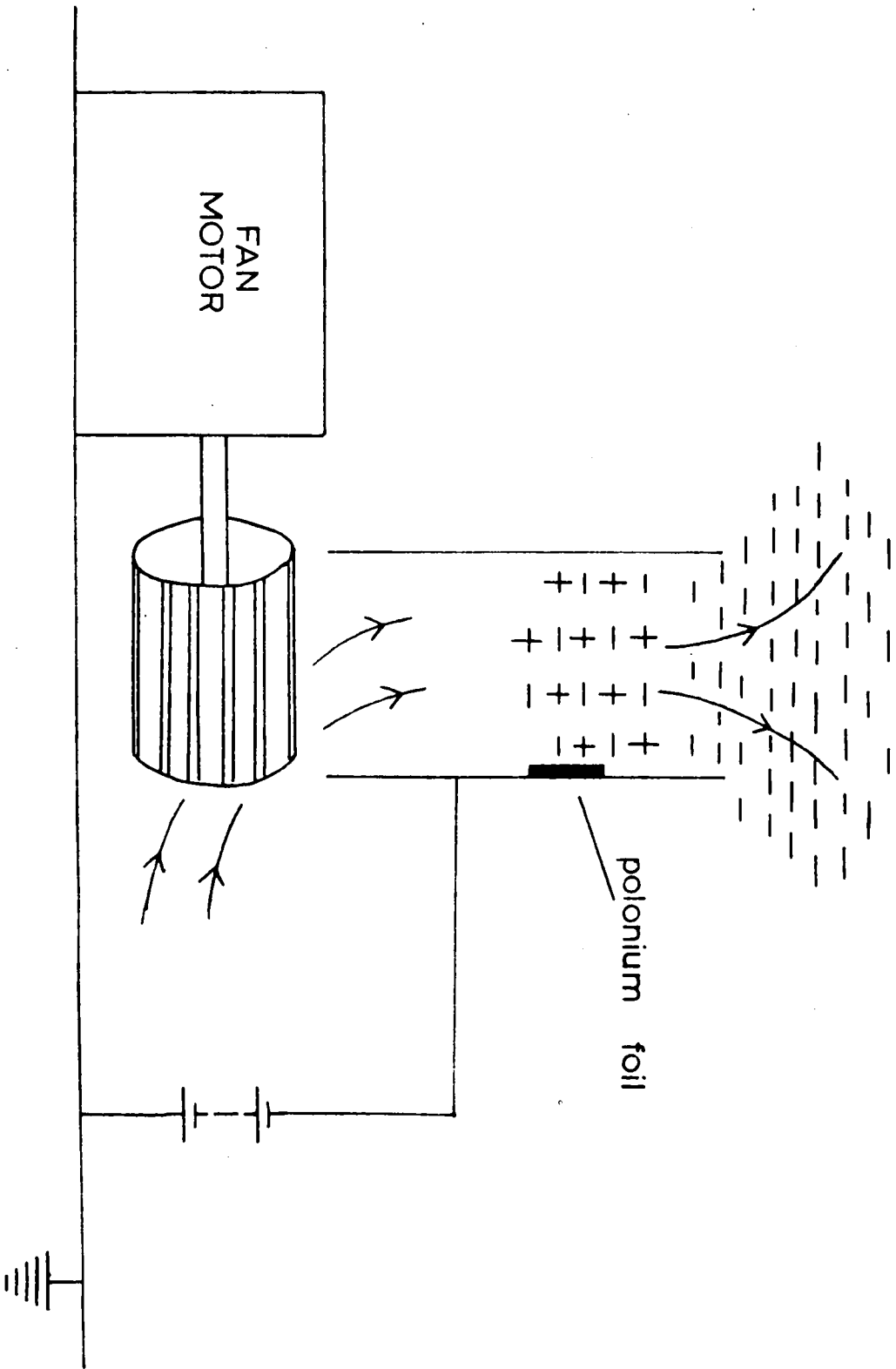
In the few weeks before the meters were due to arrive a rough calibration was carried out using a 90 cu. ft. polythene bag. This was made with a regular shape of sides 3 ft. x 3 ft. x 10 ft. with a small hole in one corner in which the extractor fan exhaust could be placed. The bag lay between cupboards so placed that its shape remained rectangular while it was being inflated, and a calibration curve drawn of voltage supply to the extractor fan against volume of air passed per sec. The resistance to flow, due to the polythene bag, would be very slight owing to the very thin polythene sheet from which it was constructed. For the later tests however the gas meters were

obtained; they had already been calibrated to 1%.

Two vibrating reed electrometers were used to measure the current flowing to earth from the space charge collectors and the outputs from the amplifiers were fed to recording apparatus in an adjacent dark room.

The recording was carried out photographically. Two Tinsley mirror galvanometers were used, each having a periodic time of 2 sec. In order to give critical damping, shunt resistors of 10 K were connected across the coils which had resistances of about 45 ohms. The sensitivity could be altered at the vibrating reed electrometer main amplifier unit which gave an output of 1 mA full scale independent of the voltage range selected.

The camera used for these recordings was made in the laboratory workshops and it was equipped to take a 100 ft roll of 240 mm width recording paper. In order to drive the camera a geared down 24 V D.C. motor was used (the supply coming from a mains rectifier unit) and this gave a paper speed of 36 inches per hour. The galvanometer lamps were focussed to give a parallel beam of light through a vertical slit. This was reflected from the plane mirrors fixed to the galvanometer suspensions onto the plastic camera lens which, being a cylindrical horizontal lens, focussed the vertical slit image to give a spot on the recording paper. In later experiments a fogging lamp was switched into operation for 50 sec in every minute to provide a time scale for record analysis purposes. This unit was operated by a microswitch and cam driven by a mains powered motor rotating once every minute.



POLONIUM ION-GENERATOR.

FIGURE 35.

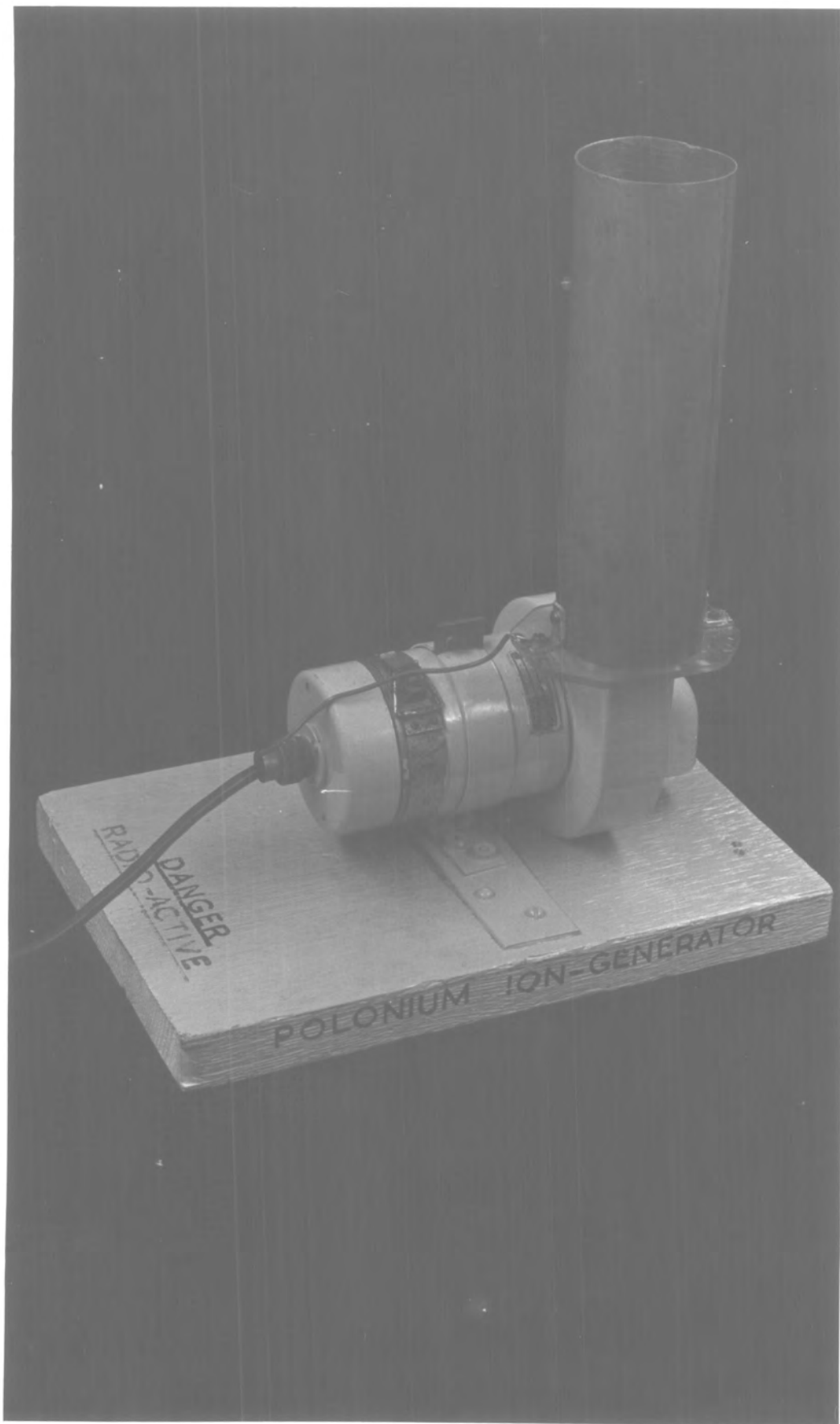


FIGURE 36.

The galvanometers were arranged to give a centre zero on the recording paper but the traces were separated slightly in order to be easily distinguishable from one another.

POLONIUM ION GENERATOR

For the purpose of the tests it was necessary to increase considerably the concentration of small ions in the air and an artificial ionizer had thus to be constructed. Usually one assumes that ions formed in the air are all of the same kind independent of the air ionizer. This assumption is, with some exceptions, correct when producing ions in pure gases under reduced pressures, but not in air at atmospheric pressure. Hot bodies and corona discharge have been found to form ions with low and high mobilities (SIKSNA 1953). Also ultra violet radiation produces a predominance of large ions (WORINDER and SIKSNA 1952). The experiments to be performed would benefit if the small ion concentration of the air far outweighed the large ion concentration and it was therefore considered advisable to build a polonium ion-generator from which only small ions would be expected.

HICKS (1956) had described such a generator for use in the biological air-conditioning of hospitals, and an instrument similar in design was constructed for the testing of the space charge collectors. A photograph and schematic diagram of the polonium ion-generator are seen in Figs. 35 and 36.

A brass tube 5 cm in diameter had a strip of Po 210 foil placed on the inside 2 cm below the top of the tube. This was insulated,

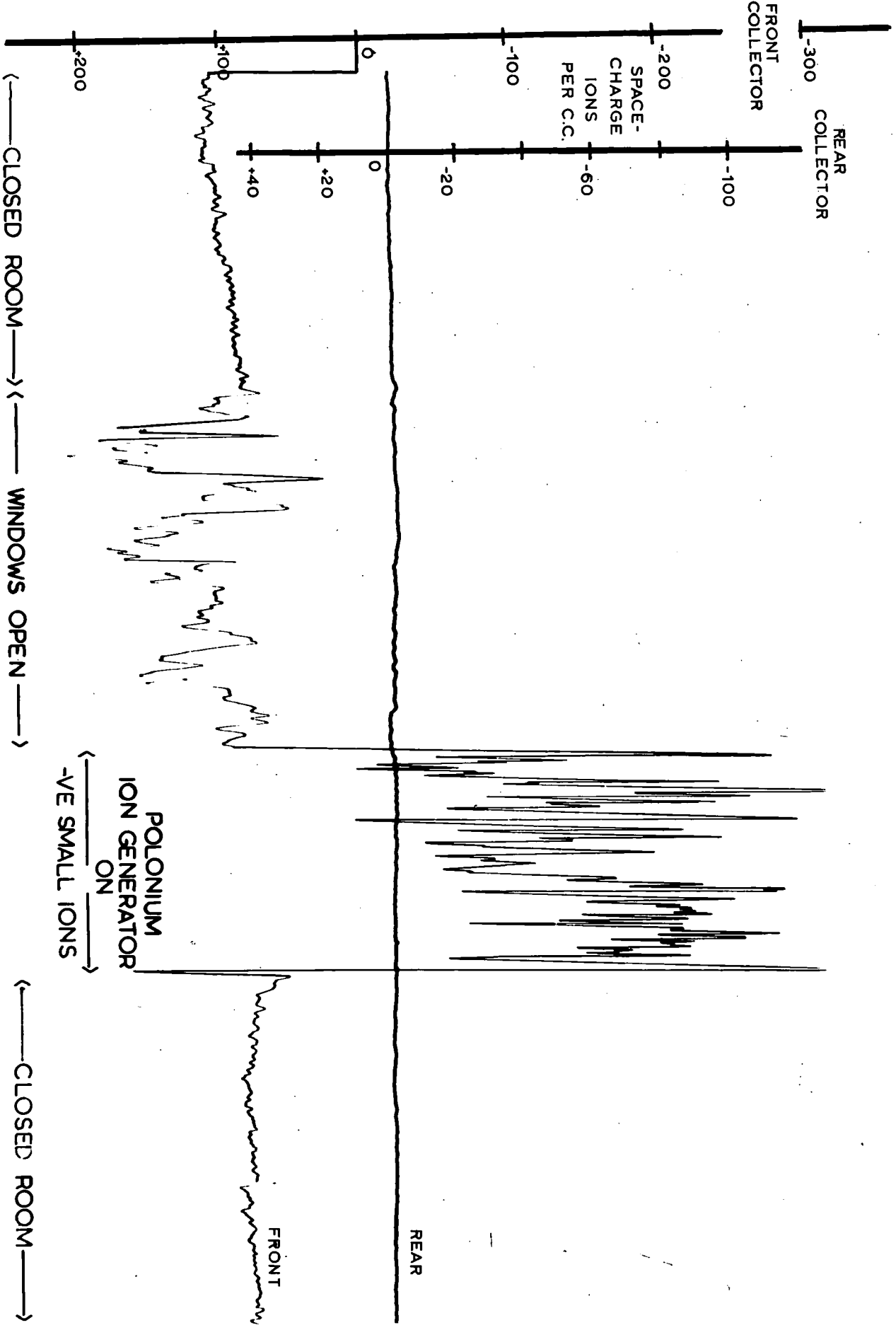


FIGURE 37.

with perspex, from a 24 V D.C. blower motor which was used to propel air through the tube and into the enclosed room where the tests were to be carried out. Negative ions were separated by connecting the negative terminal of a high tension battery to the tube and the positive terminal to earth. In the radium decay series Po 210 is the last radioactive element, giving an advantage that only α -rays are emitted without any by-products which cause large ions and therefore only small ions are produced.

THE TESTS

The space charge collectors were first placed side by side on a bench in the dust free room and the extractor unit placed outside the door to reduce ionisation caused at the carbon brushes. As the gas meters were not yet available it had to be assumed that a 'Y' junction in the extractor hose upstream from the fan would cause equal pressure drops across both filters.

The windows of the room were opened and an extractor fan switched on to aid circulation of the air. Results showed very similar traces from both collectors, but it must be appreciated that the room will contain small pockets of varying space charge giving rise to slight discrepancies between the traces.

Both collectors were now placed in tandem in order to calculate the amount of charge caught in the downstream filter, and simultaneous readings were recorded on the photographic paper. The trace shown in Fig. 37 is a photograph of a typical result where the conditions were as shown.

Prior to any set of results being taken the galvanometers were calibrated in position so as to overcome the possibility of zero change since the last record. The two traces were for different sensitivity ranges in order to amplify any effect in the downstream collector. It can be seen that less than 1% of the charge appears to escape through the first filter. Similar readings have been obtained over a wide range of flow rates and with the collectors interchanged.

These tests however did not indicate exactly how many ions were evading both filters without being recorded. The answer to this was obtained with the use of a cylindrical ion counter kindly loaned by Mr. K.A. Higazi of this Department. This was used for measuring the concentration of small ions present in the room before and after filtration.

The ion counter was first described by EBERT (1901) and it consists of a hollow cylinder with a smaller coaxial cylinder as shown schematically in Fig. (a). Screening is provided by means of an earthed aluminium box cover. Air is drawn between the two cylinders by an extractor fan and a potential difference is applied between the two.

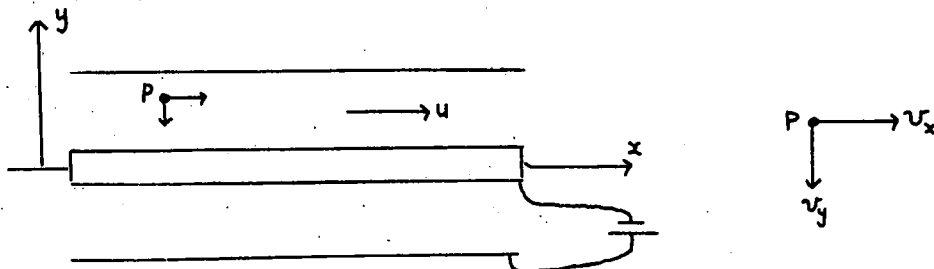


Fig. (a)

Consider an ion P of mobility K in a condenser of length L with inner and outer cylinder radii r and R respectively. Let the air flow be u and the potential difference V in such a direction as to attract the ion to the central electrode. The ion P has two perpendicular velocities

$$v_x = \frac{dx}{dt} = u$$

$$v_y = \frac{dy}{dt} = KF = -K \frac{dV}{dy}$$

where F is the intensity of the electrical field. The potential gradient at a point y from the axis is given by

$$\frac{dV}{dy} = \frac{V}{y \log_e \frac{R}{r}}$$

Therefore
$$-\frac{KV}{y \log_e \frac{R}{r}} = \frac{dy}{dt} = \frac{dy}{dx} u$$

and

$$\frac{KV}{u} dx = -\log_e \frac{R}{r} y dy$$

and in order for all ions of mobility K to be captured inside the length of the condenser

$$\frac{KV}{u} \int_0^L dx = -\log_e \frac{R}{r} \int_R^r y dy$$

$$\frac{KVL}{u} = \frac{1}{2} \log_e \frac{R}{r} (R^2 - r^2)$$

For a potential V therefore, the inside electrode of the condenser will capture ions with the mobility of

$$K > \frac{u(R^2 - r^2)}{2VL} \log_e \frac{R}{r}$$

and ions of smaller mobility will not be captured.

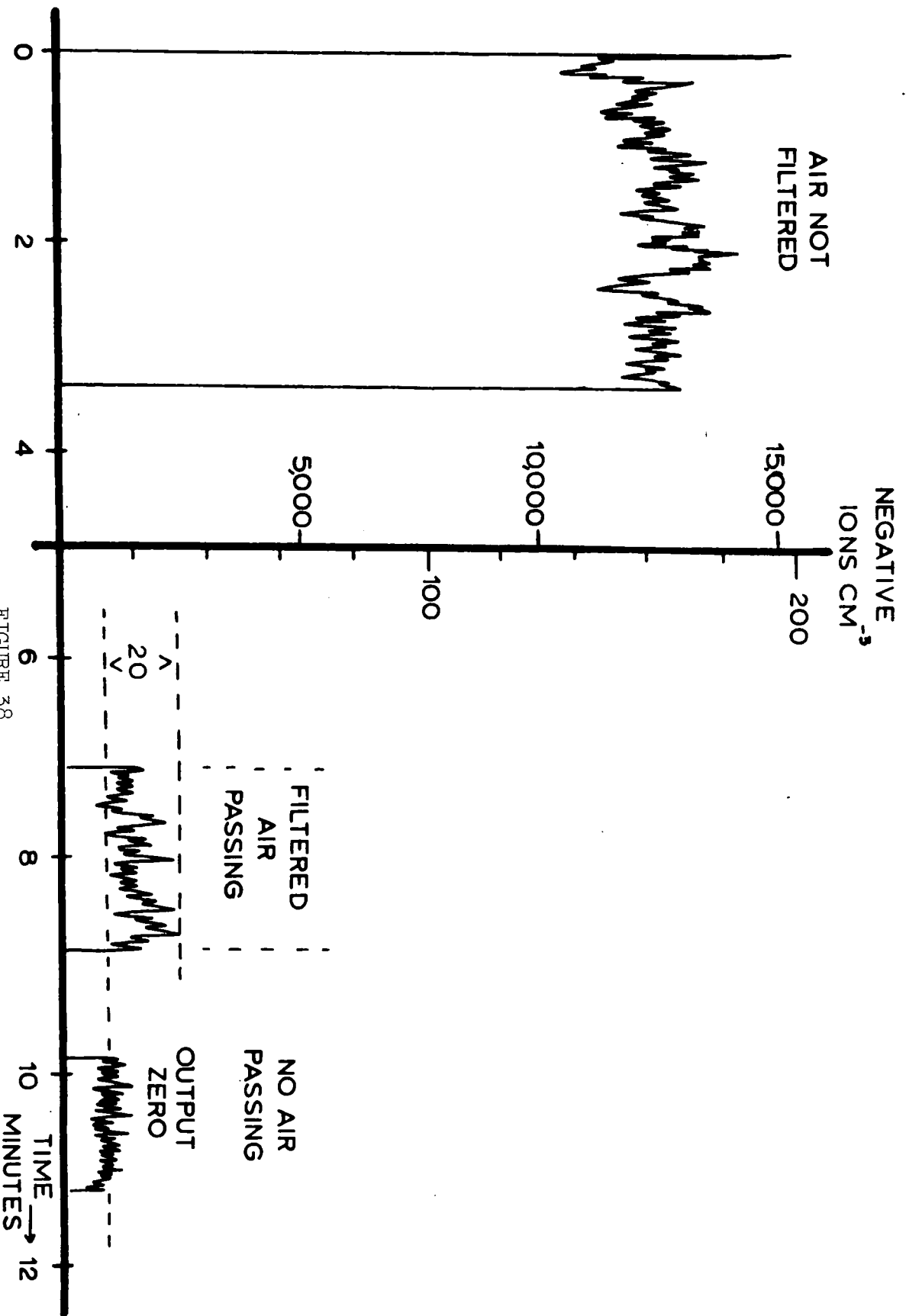


FIGURE 38.

The dimensions of the Durham ion counter were $R = 2.8$ cm
 $r = 0.6$ cm $L = 32$ cm and the potential difference V was such as
to attract all ions with mobility greater than 0.8 cm sec^{-1} per V cm^{-1}
for a 3 litres sec^{-1} air flow through the tube.

The central electrode of the ion counter was connected through a
 10^{11} ohm resistor to earth and a vibrating reed electrometer was used
to measure the potential difference across it. Gas meters were used
to measure the flow and once more the extractor fan was placed outside
the room.

The results of this experiment can be seen in Fig. 38 which has
been traced from the photographic record. Firstly the polonium ion-
generator was switched on and negative small ions were produced. A
density of $12,000$ negative small ions cm^{-3} was recorded on the ion
counter. Secondly the ion counter was attached to the exhaust side
of a space charge collector and the flow adjusted to be identical to
that in the first stage of the experiment. Photographic records were
taken of these two results but with different scale sensitivities.
The vibrating reed electrometer used for this experiment had a fluctuating
zero error on this very sensitive scale and this was also
recorded in order for corrections to be made. By measuring to the
top of the peaks recorded as air flowed, it was calculated that the
collection efficiency of the filter was better than 99.8% for small
ions with a flow of 3 litres sec^{-1} through the filter.

Some ions of lower mobility must have been recorded by the ion counter but even allowing for a 10% inaccuracy in the number collected the final results are very similar.

It can therefore be assumed that the number of intermediate and large ions escaping collection at the filter must be very much smaller than 0.2% for the flow used.



FIGURE 39.



VIEW LOOKING NE



VIEW LOOKING SW

FIGURE 40.

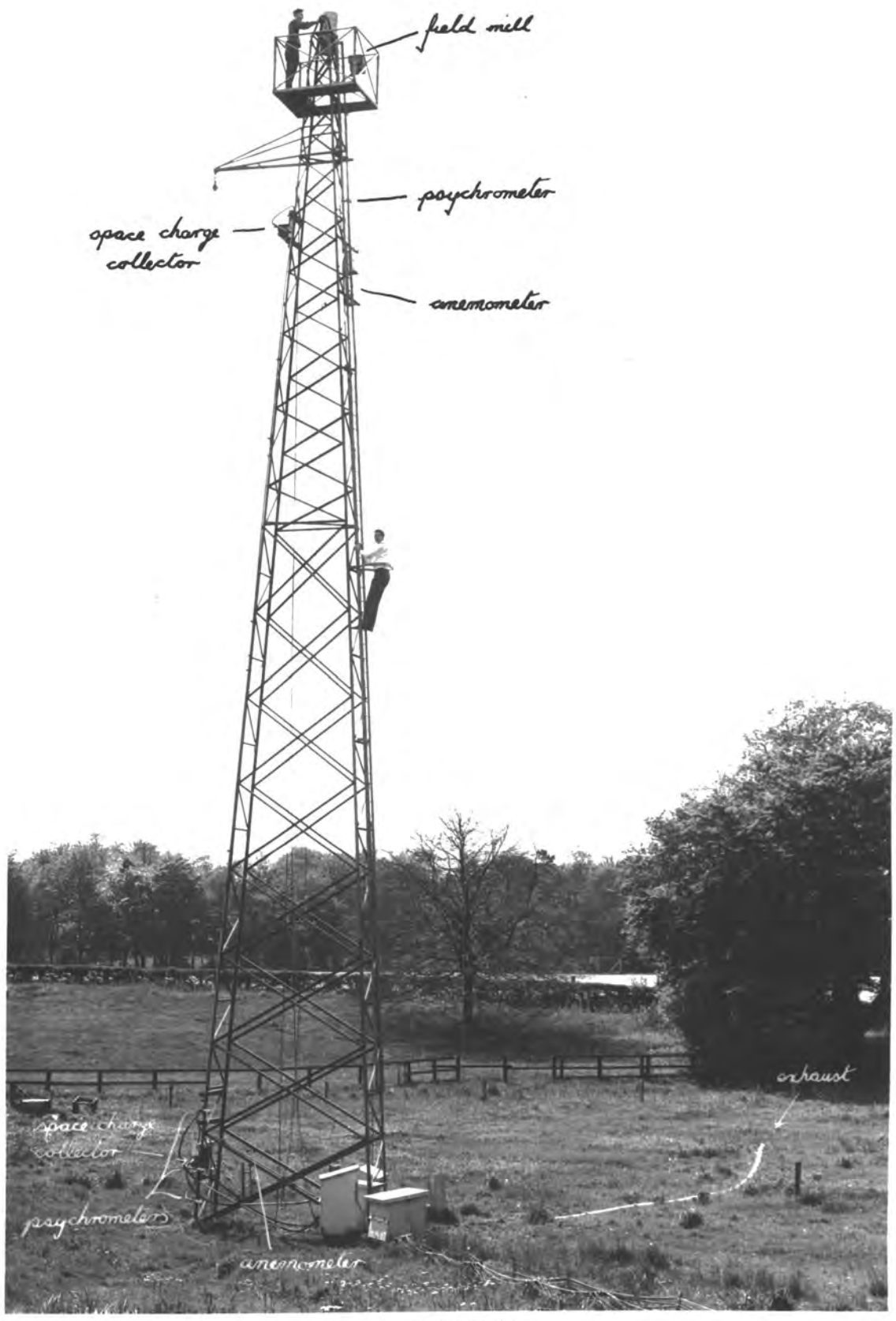


FIGURE 41.

CHAPTER 7

INSTALLATION AND OPERATION OF APPARATUS AT THE OBSERVATORY

THE SITE

Durham University Observatory stands on a hill 120 m above sea level and about 1 Km to the west of Durham City. The observatory is surrounded by agricultural land and is well away from large sources of atmospheric pollution. The site offers many advantages and a useful set of meteorological instruments are maintained there. Fig. 39 shows a photograph of the observatory and Fig. 40 gives an idea of the type of country overlooked by the building.

The 21 m lattice mast on which the instruments were placed is at the centre of a field about 80 m due west of the observatory. The mast, which can be seen in Fig. 41, was erected by the North Eastern Electricity Board in 1962 and is guyed at four points. It has a ladder rigidly bolted to one side leading up to a platform 1 m below the top, and an arm is fixed just below this platform on the southern side of the mast to carry a pulley for hoisting.

INSTALLATION OF EQUIPMENT

Because of the distance from the mast to the observatory it was necessary to install some of the electronic equipment, gas meters and junction boxes at the foot of the mast. For this reason two boxes were built. The largest of these was erected 2 m from the base of the mast and was constructed on short legs with an upper and lower compartment. The instruments in the lower compartment could be observed

by opening doors at either side whilst to gain entry to the upper deck the sloping roof had to be lifted off. The outside of the box was covered with aluminium sheet and the various connecting cables were brought through holes cut in the underside. The lower deck contained two vibrating reed electrometer indicator units along with three bulbs which were always switched on and were acting as heaters. An 18-core cable from the observatory was connected to a junction box in the upperdeck where there were also installed six 250 V A.C. sockets and a coaxial cable junction box. In another section of the upper deck a Variac transformer for varying the A.C. voltage to the extractor fan was installed along with 2 relays. These relays allowed remote control of the power to the suction fan and field mill to be performed from the observatory, as well as for automatic switching of current to the wet and dry bulb thermistors.

The second box, which was also heated, was placed between the latticework at the foot of the mast. It contained the extractor fan as well as two gas meters which monitored the flow through the space charge collectors.

Aluminium and alkathene tube of diameter 1 inch was mainly used for the suction pipes as it was very rigid and could be bolted to the mast. Inside the box however rubber tubing was used as this could be compressed with Jubilee hose clips and the flow through each instrument thereby controlled.

As the exhaust fumes from the extractor fan contained high quantities of positive space charge it was thought desirable to discharge this some distance away in order that it would not be measured by the space charge collectors. For this purpose the fumes were led, via 12 cm diameter asbestos flue-pipes, to a point some 30 m distant where the prevailing wind would carry the charge away from the mast.

Wooden cross-members were bolted onto the mast with 'j' bolts to provide easy fixing of the steel plates containing the space charge collectors and head units. However, because of the considerable weight of these units and the difficulty in assembling them together, it was decided to haul the completely assembled unit to the top of the mast with block and tackle. The most suitable position for the upper collector was probably just below the arm of the mast at a height of about 18 m, as in this position the arm would considerably reduce the enhanced potential gradient due to the mast. Also the intake of the collectors would face into the prevailing winds. This would mean that the majority of results would be obtained when the air did not first pass through the mast and hence lose ions of one sign at the surface of the mast due to the high potential gradient. In order to fix the top space charge collector in position a template was used for correct assembly of the wooden cross-members, and then the actual space charge collector unit was easily bolted on whilst still being held by the block and tackle system.

The 70 ft. cables connecting the vibrating reed electrometer head unit and main amplifier unit were well within the manufacturers'

recommended length limit of 100 ft.

The psychrometers which were fixed onto the mast with 'j' bolts at $\frac{1}{2}$ m, 1m, 2 m and 19 m faced north so that a low sun would not shine directly into the intakes. Whilst in use the water containers had frequently to be cleared of insects and refilled, and the muslin covers for the wet bulbs were replaced whenever they became dirty.

The anemometers were easily supported as their main shafts had tapered plugs at the end which were inserted into tapered sockets permanently fixed on stands. In the case of the lower anemometer a handy-angle stand was erected on the ground some 3 m from the mast and the brass ^{socket} permanently fitted at 1 m. During hours when recording was not taking place this anemometer was moved indoors. The upper anemometer was fixed at a height of 17 m protruding to the west of the mast and was held in position by handy-angle supports. Owing to the difficulty of taking this upper instrument indoors during periods of precipitation a cover could be lowered over it on 4 brass rods and a heater in the form of two 60 watt bulbs connected in series was placed in a box just below it. The lower end of the cover, which was normally $\frac{1}{2}$ m above the anemometer cups, could be lowered over the anemometer to meet the heater unit by the help of a pulley and a long wire which stretched to the foot of the mast. This upper anemometer was placed $1\frac{1}{2}$ m below the space charge collector so that it would not impede any air likely to be sucked into the collector.

The upper field mill had been built and was being used by Mr. Collin, but he kindly offered it for my use during fine weather periods. This was fastened onto the platform at a height of 21 m and was inverted. In the calibration that Mr. Collin had performed he had allowed for the high exposure factor due to the mast.

The lower field mill was placed in the surface of the earth to eliminate any effects caused by its framework, and in order to eliminate any effects due to the mast it was fixed at a distance of 30 m from its base. As dampness was likely to be a big factor in affecting the mill's performance the hole in which it was fixed was concreted and the handy-angle supports cemented firmly into the base of the hole. Heating bulbs were placed in the hole, and damp air could escape through a ventilation hole near the surface; this also aided the entry of wires. A 1 m square aluminium cover was placed over the field mill flush with the ground and a circular hole was cut in the aluminium through which the rotor of the field mill protruded very slightly. When this instrument was not in use a cover could be placed over it to prevent rain from entering the hole.

The cathode follower within the field mill case was permanently switched on so that immediately power was supplied to the motor a signal would be obtained. The heating from this valve would also help to keep the electrical components dry.

When calibration of the mill was to be performed an aluminium table with wooden legs $\frac{1}{2}$ m high could be dropped over the instrument and with the aid of a wire from the table top to the observatory different potentials could easily be applied between the table and earthed field mill rotor.

All cables from the boxes to the observatory were carried about 30 cm above the surface on stakes, so that grass and weeds did not grow over and hide them; they then passed through a channel under a path near the observatory building which they entered through a hole in the wall.

Inside the observatory a 2 KVA isolation transformer supplied power to the boxes in the field. This was a safety precaution as one side of the mains is normally very close to earth potential and therefore only the live lead needed to be accidentally touched whilst a person was on the mast for him to receive a severe shock. With the aid of the isolation transformer however both sides of the mains would have to be held to receive this electric shock.

During initial testing of the equipment the field mill output was observed to have variations superimposed on the signal once every minute, and only after extensive observations was this related to a pulse system used in an adjacent hut housing seismometers. This pulse was being fed back up the mains earth lead and onto the screening of the coaxial cable from the field mill. To overcome this difficulty and also to eliminate earth currents which were flowing in the vibrating reed electrometer outputs the earth connections were altered to be fixed to a single point on the mast.

There was also trouble with the underfloor heating system of the observatory building. As this switched on, the mains supply voltage dropped from 270 V to 220 V. This directly affected the field mill power packs as the filament voltage also dropped 20% thereby affecting the amplifier output considerably. A constant voltage transformer was therefore obtained to overcome this difficulty.

In order to rewind the data tapes for introducing into the computer, two 16 mm film winders with a 4:1 gear ratio were fixed onto a wooden base. The tape spool from the recorder was fixed on one side and the tape was rewound onto a central core protruding from a brass disc fixed to the other side. This allowed the rewound tape to be easily slid off the core and stored in boxes.

RECORDING PROCEDURE AND ANALYSIS

During recording a detailed log was kept. This gave details of the past and present weather conditions, amplifier sensitivity and psychrometer temperature ranges. In fact any observed event which might have some influence on the information being recorded was noted.

Altogether about 300 hours of recording have produced 750 ft. of record which has been analysed. This was made up of records obtained on over 75 days in the past twelve months.

The output cycle on the data tape is repeated every 32 channels and the information in every channel is represented by an integer between 0 and 100. Of these 32 numbers 16 are referred to linear relationships and an easy arithmetical sum can be performed to obtain the correct value. The remaining 16 values have to be interpolated from 10 non-linear graphs of which 2 are for wind calibrations and 8 for temperature calibrations. The computer programme has therefore to accept 32 numbers at a time, and perform operations on each number before printing the results in column form, where variations and gradients can easily be observed. The output would be of space charge, field and wind all at 2 levels, dry bulb temperature at 4 levels and absolute humidity at 4 levels. Fortunately it is just possible to fit them all on one line of the teleprinter output. In order to interpolate from the non-linear calibration curves it would be extremely difficult to feed in all the numbers on the x-axis and the corresponding values on the y-axis each correct to 1%, as this would take up too much computer time at the commencement of each run. A much better method is to find the equations of the curves, from which, on feeding in a value from the x-axis, the value of y is found to an accuracy of 1%.

The Elliott 803B computer performed the operation for finding the equations of these curves by accepting the values of x and y obtained in the calibrations, and fitting a polynomial to them using the method of orthogonal polynomials. This iteration process was described by G.E. FORSYTHE (1957). Given pairs of values

(x_j, y_j) , $j = 1, 2, \dots, m$, the programme computes a series of polynomials $P_1(x)$, $P_2(x)$, etc., where

$$P_1(x) \text{ is of the form } C_0 + C_1 x$$

$$P_2(x) \text{ is of the form } C_0 + C_1 x + C_2 x^2$$

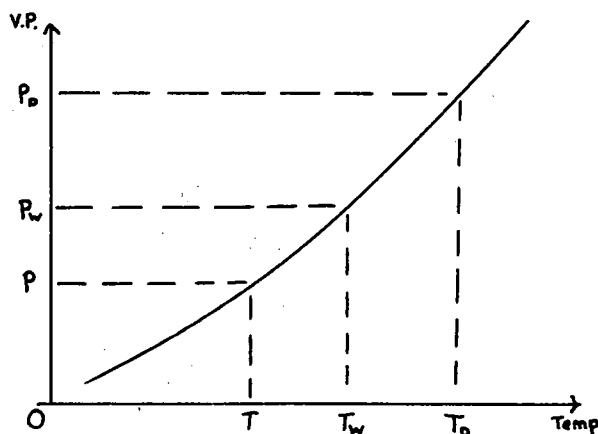
$$P_3(x) \text{ is of the form } C_0 + C_1 x + C_2 x^2 + C_3 x^3$$

and so on up to $P_{20}(x)$ if $m \geq 21$ or $P_{(m-1)}(x)$ if $m \leq 20$. Each of these polynomials $P_1(x)$ is such that if $y_{1j} = P_1(x_j)$ then the sum of the squares of the deviations $\sum_j (y_j - y_{1j})^2$ is a minimum. The data tapes are preceded by the number m and also a value δ which determines whether or not the deviation of any particular value of y_{1j} from the correct value of y_j should be punched. The criterion is that $(y_j - y_{1j})$ will be printed if and only if $|y_j - y_{1j}| > \delta \bar{y}$ where \bar{y} is the mean value $\sum_j y_j / m$. In each case δ was chosen to allow the deviation to be printed only if the error was greater than 1%. The output gives, for each polynomial in turn, the sum of the squares of the deviations, the number of points which lie both above and below the line and the maximum negative and positive deviations. Also printed, where necessary, is the important value of j for each case where the deviation is such that $\left| \frac{y_j - y_{1j}}{\bar{y}} \right| > \delta$ as well as its deviation. When this latter term is not printed the computed curve is within 1% of the calibration curve. The final print out for each polynomial is a list of the coefficients of $P_1(x)$ each preceded by its associated power of x . It is therefore immediately seen when an equation is reached satisfying the conditions required and the programme can be stopped. The polynomials computed ranged from degree 3 to degree 6 and the coefficients were quoted

correct to four figures.

It is recommended that the values of x and y be positive in the iteration process used, and therefore for the temperature curves the values of temperature were raised by 10°C whilst the recorder values ranged from 0 to 300. The 0-300 range is based on the fact that 5 temperature ranges were used in recording, each covering 10°C , and therefore -5°C on the recorder is represented by 0 and 25°C by 300. So, for example, if the range on a particular day was from 10° to 20° then 150 would be added to the number on the data tape by the computer before interpolation commenced, and then 10°C would be subtracted from the calculated value to arrive at the temperature required.

The computer will now calculate the exact values of space charge, field, wind and temperature but the values of absolute humidity still remain to be calculated. The values from tables are once more unsuitable for feeding into the computer but it is possible to obtain humidity values by considering the pressure-temperature curve for saturated water vapour.



T_D is the dry bulb temperature, T_W the wet bulb temperature and T the temperature of dew point with p_D , p_W and p their corresponding maximum saturation vapour pressures of water. Regnault's formula for psychrometers with strong aspiration rates, namely

$$p = p_W - 0.000656 H(T_D - T_W)$$

gives the value of p which is the pressure of aqueous vapour corresponding to T_W and T_D . H is the atmospheric pressure and for the purposes of this project is taken to be 1000 mb; in this formula T is measured in degrees centigrade. The value of p is directly proportional to the value of absolute humidity or vapour density of the air and it is therefore considered sufficient to calculate p instead of the absolute humidity. Once more however the equation of the curve must be found in order to obtain p_W from T_W but this can be obtained from the Clausius-Clapeyron equation. This equation is

$$\frac{d e_s}{dT} (v_2 - v_1) = \frac{L}{T}$$

where e_s is the saturated water vapour pressure, v_1 and v_2 are the specific volumes in the liquid and vapour state respectively, L is the latent heat of vaporisation and T is the temperature. But by assuming $v_2 \gg v_1$, ^{and} that the perfect gas laws hold then

$$\frac{d e_s}{e_s} = \frac{L}{R} \frac{dT}{T^2}$$

where R is the specific gas constant for water vapour. By integrating this equation, and putting in values of e_s and T from the range to be used in order to find the constant of integration, the following was

S1	S2	F2	W1	W2	T1	T2	T3	T4	VP1	VP2	VP3	VP4
90	120	70	2.9	4.5								
90	120	70	3.2	3.8	18.2	18.2	17.7	15.6				
80	110	90	2.6	3.5								
70	130	70	2.5	4.1					12.91	12.12	12.10	11.64
60	120	90	3.1	5.0								
60	120	70	3.0	4.5	18.2	18.0	17.8	15.8				
90	120	90	2.5	4.6								
80	110	90	3.4	4.6					13.10	12.24	12.22	11.13
80	150	90	2.9	4.6								
100	190	110	3.2	4.8	17.8	18.1	17.8	15.7				
240	310	130	3.1	4.3								
240	230	130	3.0	4.6					13.91	12.52	11.83	11.19
280	210	130	3.6	4.7								
240	190	110	4.1	4.6	18.2	18.2	17.9	15.8				
170	230	130	3.2	4.4								
200	240	110	3.0	3.8					12.72	11.95	11.76	11.30
210	140	110	3.4	4.5								
140	140	90	3.1	5.4	18.1	18.0	17.9	16.1				
90	110	110	3.8	5.1								
100	110	90	3.4	5.0					12.78	12.07	11.76	10.96
80	150	90	3.4	5.3								
110	220	90	3.4	5.2	\$ 18.0	17.8	15.7					
180	240	90	3.1	5.2								
270	80	70	3.6	5.5					\$ 12.24	12.03	11.08	
110	40	70	3.2	6.0								
50	30	70	3.7	5.5	17.8	17.6	17.6	15.4				
30	50	70	3.7	4.7								
10	40	70	3.0	4.7					12.01	11.30	11.41	10.93
10	80	90	2.9	4.3								
40	70	90	3.1	4.7	17.6	17.4	17.1	15.3				
50	90	110	2.8	4.8								
80	140	90	3.0	5.3					12.89	12.26	11.89	10.99
80	110	90	3.4	5.3								
60	110	70	3.4	4.6	18.0	17.7	17.6	15.6				
70	110	110	3.1	4.4								
80	110	90	3.6	4.8					12.84	12.08	11.98	11.31
80	130	110	3.2	3.8								
80	140	70	3.1	4.0	18.5	18.0	17.7	15.9				
110	110	90	2.8	3.9								
80	80	70	3.0	5.2					13.05	12.41	12.29	11.41
70	70	70	3.8	6.0								
70	60	70	4.4	6.3	18.2	18.1	18.0	15.8				
50	80	70	4.2	5.9								
70	80	70	3.6	5.3					12.72	12.01	11.50	10.47
70	40	50	3.5	6.3								
40	50	50	4.0	5.8	18.3	18.3	18.0	15.8				
20	100	90	3.6	4.6								
50	120	70	3.0	3.4					12.47	11.55	11.31	10.97
90	120	70	2.9	3.6								
110	100	70	2.8	3.5	18.8	18.6	18.1	16.4				
150	90	70	2.6	3.4								
110	90	50	2.9	2.9					12.86	12.34	12.19	11.11
60	100	50	3.1	3.5								
50	60	50	3.1	4.3	18.8	18.7	18.5	16.5				
60	0	30	3.4	4.7								
10	-10	50	4.0	5.0					12.10	11.25	11.40	10.16
-10	20	70	4.0	4.6								
0	10	50	4.2	4.5	13.5	18.2	18.1	16.0				
-10	10	30	3.9	4.5								
-10	20	50	3.4	4.4					12.28	11.95	11.42	11.01
10	50	50	2.4	4.1								
30	60	30	2.4	4.0	19.2	19.0	18.6	16.5				
40	60	50	1.9	4.5								
90	60	50	2.0	4.4					13.01	12.45	11.71	10.55
70	40	50	2.2	5.0								
50	30	30	3.0	5.4	19.2	19.0	18.9	15.9				
20	30	30	3.2	5.9								
-60	30	30	2.8	5.5					11.67	11.08	10.92	10.41
20	30	30	2.4	4.8								
30	40	30	2.5	5.0	18.7	18.7	18.5	16.0				
10	30	50	3.2	5.0								
0	30	50	3.0	4.5					11.78	10.91	11.02	10.35
0	50	50	3.0	4.5								
10	30	50	2.8	4.6	18.6	18.3	18.2	16.1				
30	70	70	2.7	5.1								
30	50	70	2.5	4.6					12.03	11.38	11.16	10.46

FIGURE 42.

obtained :

$$\log_{10} e_s = 21.648 - \frac{5423}{T}$$

where T is in °K and e_s in mb.

The computer was now able to find the value of P_w by equating the exponential of the R.H.S. of this equation and hence the vapour pressure was found. This process was repeated by the computer for all 4 wet and dry bulb temperatures in each block of 32 numbers from the data tape. The computer programme was now complete and it accepts 32 numbers at a time from the data tape, performs all the operations just described and punches the results inside 20 sec before immediately accepting another block of results.

As an example of the time saved, the results obtained from a run of only 3 hours on the computer corresponding to 8 hours recording, would take a person 1 week (7 x 24 hours) of continuous work to calculate.

Fig. 42 is a photograph of the output from the computer. The β sign signifies the rare occurrence where an error has been punched on the data tape.

CHAPTER 8

RESULTS

1. SPACE CHARGES OVER SNOW

Introduction

Space charge concentrations at two different heights, 1 m and 2 m respectively, were recorded during the winter of 1963-4. During this period there were many occasions of frosty conditions but only few occasions on which snow covered or partially covered the ground. Before discussing the results in greater detail it will be wise to consider briefly some results previously obtained of the charge in the air over snow.

It seems to be generally agreed that the blowing of snow may account for the high positive potential gradient in wintry conditions. SIMPSON (1919) found large and usually positive values of potential gradient when there was drifting snow, whilst SCRASE (1957) suggested that when ice crystals collided with one another the ice retained a negative charge and a positive charge in the form of ions was passed to the air. NORINDER and SIKSNA (1955) showed that when snow is blown, small invisible snow particles carrying several hundred electronic charges are passed to the air. Recently however MAGONO and SAKURAI (1963) found negative charge lying above positive in the first metre and positive space charge above that. During conditions of melting DINGER and GUNN (1946) reported that when a stream of air passed over melting ice the air obtained a negative charge and the ice retained a positive charge. MATTHEWS and MASON (1963) failed to

confirm this but DINGER (1964) has suggested that the presence of CO_2 in their ice would eliminate the charging effect on gas bubbles released in the melting.

Results obtained

On four separate occasions the potential gradient at the surface and the space charge density at 1 m and 2 m were recorded continuously for periods of several hours whilst snow was lying on the ground. There were also recordings on occasions when dry snow was lying on neighbouring high land and whilst there were frosty conditions without snow at Durham. Information on the state of the ground in the area surrounding Durham was obtained from the various Meteorological Office stations and consulting the records that the Durham County Water Board had obtained from their reservoir station reports. Usually under normal circumstances it was not uncommon for ^{the} space charge density to be as large as $+500 \text{ e cm}^{-3}$ but for convenience we will regard values greater than $+400 \text{ e cm}^{-3}$ as being unusual. In winter months a total of approximately 150 hours of record was obtained on 26 different days from which there were nine records where the space charge exceeded $+400 \text{ e cm}^{-3}$. On seven of these occasions it was clear and frosty and dry snow lay on the hills surrounding Durham on four of them. During the remaining months of the year another 150 hours of record did not show one occasion on a clear day in which the space charge density even approached $+400 \text{ e cm}^{-3}$.

The records obtained from the four occasions when snow lay on the ground at Durham will now be considered further. These were

- (A) 19 December 1963 1300-1900 hours
- (B) 20 December 1963 1330-1800 hours
- (C) 17 March 1964 1540-1840 hours
- (D) 20 March 1964 1000-1215 hours



and it will be seen later that period (C) is of outstanding interest. The values of humidity, wind speed and direction were obtained from the Observatory records and together with the space charge and potential gradient values the information is shown in Table 4.

During periods (A) and (B) the snow was not melting and there was a clear sky. On these two occasions the space charge and potential gradients were continuously positive and although space charge was not recorded at 2 m in period (B) the values at 1 m and 2 m in period (A) were in very close agreement with one another. During periods (C) and (D) the snow was melting rapidly and on the former occasion the potential gradient was twice measured at 1 m as well as the usual 0 m and 21 m. In the light surface winds of period (D) the potential gradient at the ground was constantly negative whilst the space charge values at 1 m and 2 m kept close together and remained negative. However during period (C) the wind speed was considerably higher and the space charge was always negative at 1 m and always positive at 2 m from the start of the record until 1800 hours; after this time, as can be seen in Fig. 45 the space charge values slowly approached one another and coincided at about 1830 hours. On the two occasions when the potential gradient records during this period were available at all three levels they showed that the value was

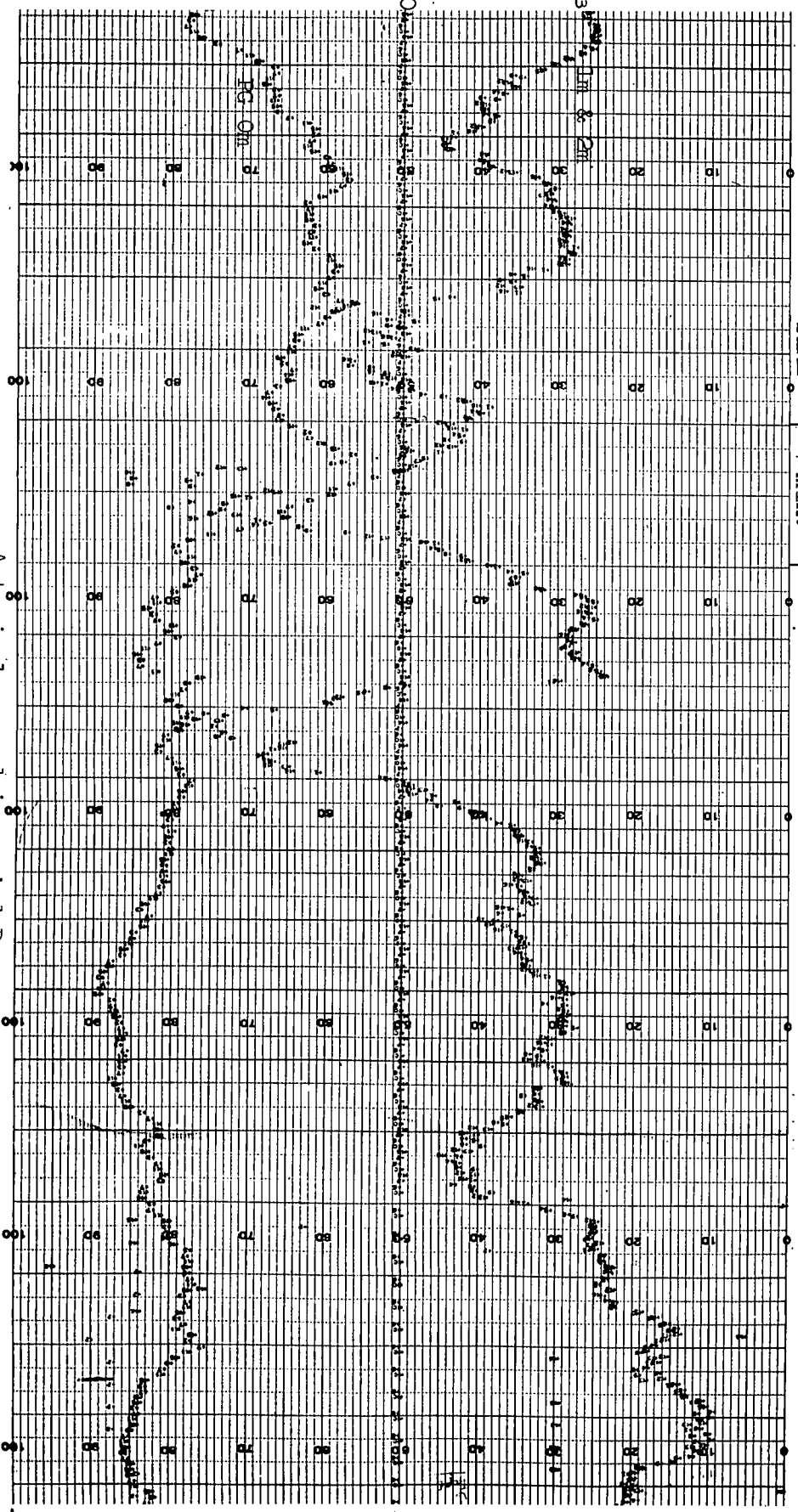
Table 4

Range of observations in periods A, B, C and D. Elementary charge $e = 1.6 \times 10^{-19}$ C.

	A	B	C	D
Period	19 Dec. 1300-1900 hrs.	20 Dec. 1330-1800 hrs.	17 Mar. 1540-1840 hrs.	20 Mar. 1000-1215 hrs.
Space charge, $e \text{ cm}^{-3}$				
at 2 m	+(100-600)	...	+(100-200)	-(100-400)
at 1 m	+(100-600)	+(100-800)	-(100-500)	-(100-400)
Potential Gradient, $V \text{ m}^{-1}$				
at 0 m	+(100 - 500)	+300	+(200-600)	-(200-800)
Wind				
Speed, m sec^{-1}	4-11	3-9	7-14	3
Direction, deg	300	285	120	180
Temp. at 1.2 m, $^{\circ}\text{F}$	30-33	30-35	35-38	37-39
Relative humidity, %				
at 1.2 m	50-53	47	50-60	90
at 8 cm	52-55	47	54-64	95
Condition of snow	Not melting	Not melting	Melting	Melting
Weather	Fine	Fine	Fine, hazy	Fine, very misty

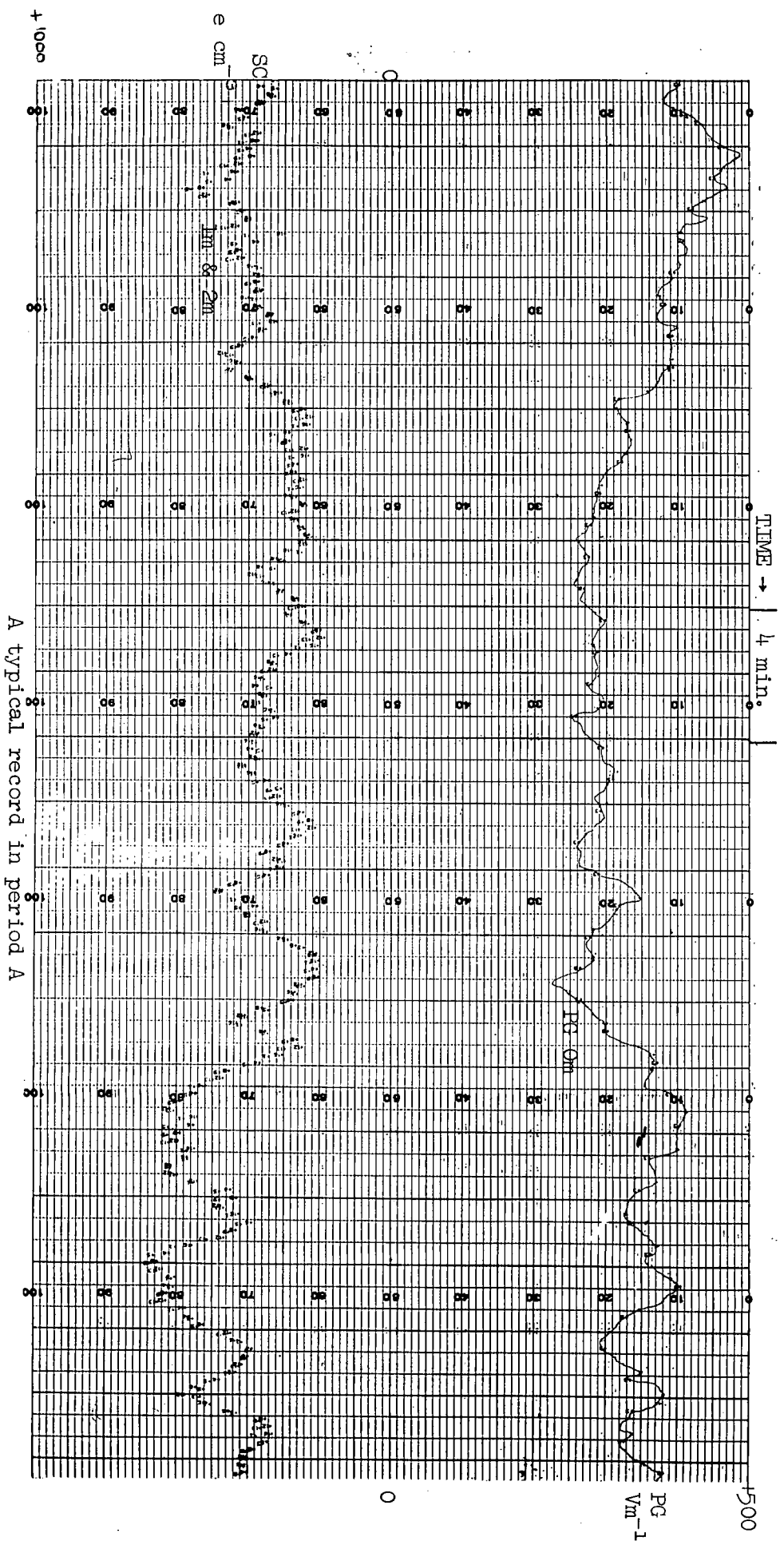
SC
CM

TIME → 4 min.



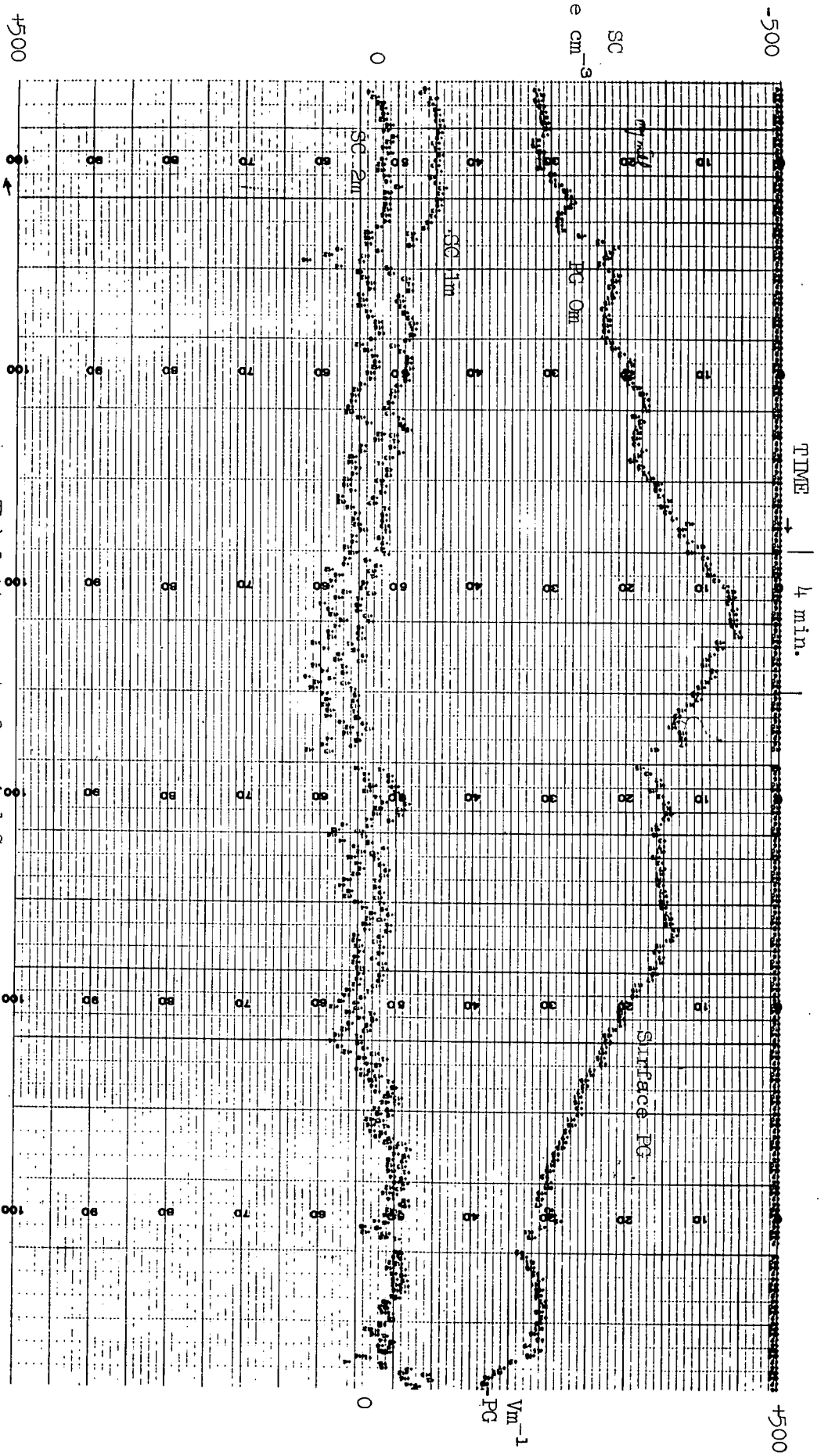
A typical record in period D
FIGURE 43.

V_m¹
PG
1000

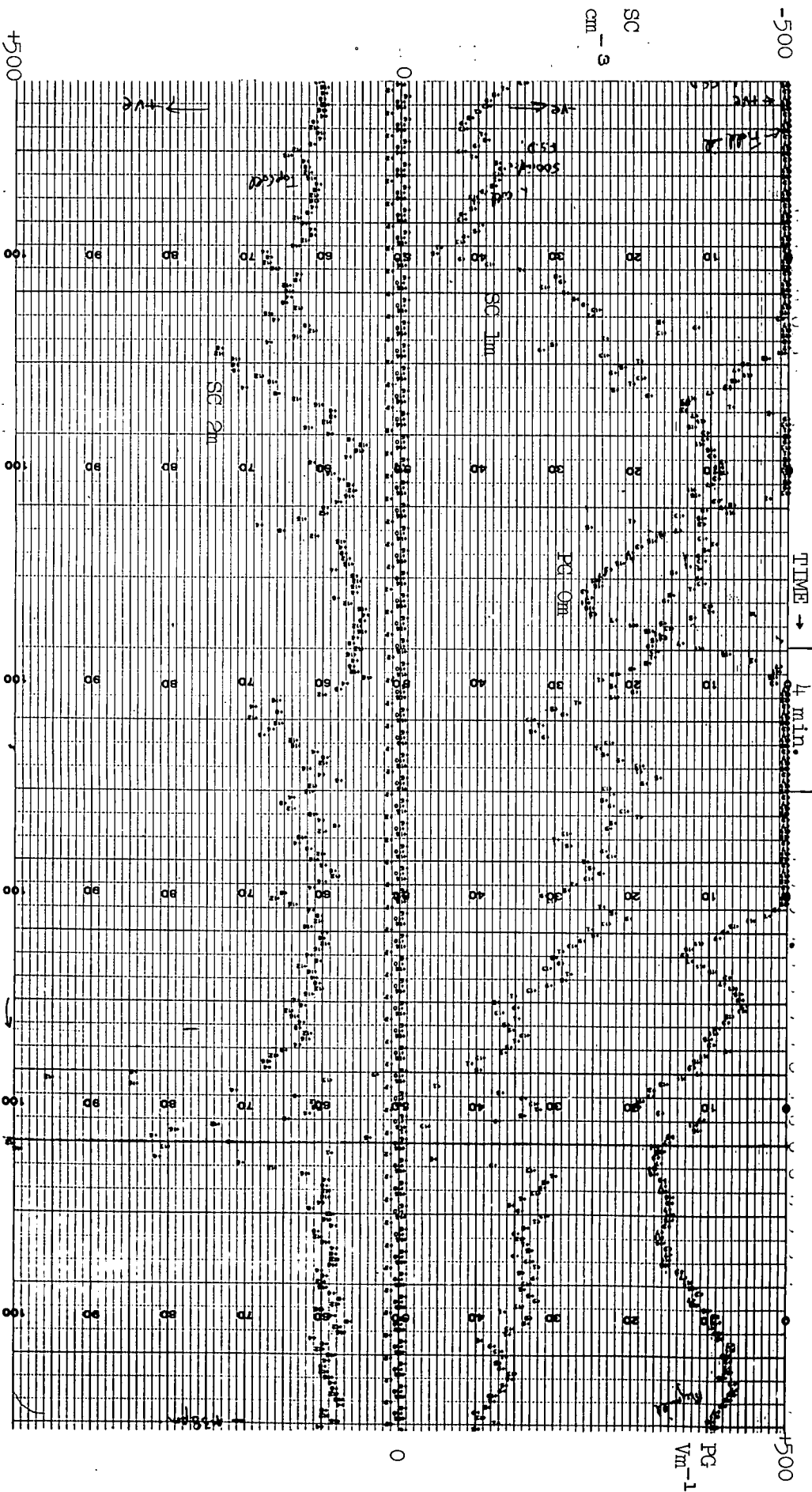


A typical record in period A

FIGURE 44.



The latter part of period C
FIGURE 45.



Earlier part of period C
 FIGURE 46.

more positive at 1 m than at the surface but less positive at 21 m than at either of these two heights.

Table 5 shows values of space charge and potential gradient on two occasions during period (C) and Figs. 43-46 show various portions of the space charge and potential gradient records in periods (A), (C) and (D).

Table 5

Space charge and potential gradient in period C

	1542 hours		1638 hours
At 21 m	+330 Vm^{-1}		+220 Vm^{-1}
2 m		+100 e cm^{-3}	
1 m	+640 Vm^{-1}	-150 e cm^{-3}	+500 Vm^{-1}
0 m			+400 Vm^{-1}

During period C the snow was very wet and certainly not blowing and the partial snow cover was rapidly disappearing. Routine observations of the state of the ground were in fact carried out at the Durham University Science Laboratories site some 1 Km distant from the observatory and whilst reference to snow was made at 1500 hours there was no such reference at 1800 hours. A new fall of snow occurred prior to period (D) but this was melting rapidly and was noted to have completely disappeared by 1500 hours. It can be seen on reference to Table 4 that period (D) was accompanied by very misty conditions and the relative humidity approached 95%. The high negative values of potential gradient

and space charge associated with misty conditions will be discussed later in this Chapter where it will be shown that they are probably caused by corona discharge at high tension cables in damp conditions, which gives an excess of negative ions to the atmosphere as suggested by CHALMERS (1952).

The wind during periods (A) and (B) was between W and NW and the reports compiled at stations on the high moorland approximately 25 Km in this direction from Durham were of fine frosty conditions with blowing snow. During period (C) the SE wind approached from the high land on the Yorkshire moors some 45 Km distant but once more the reports from this area were of dry blowing snow. All the local weather stations' reports for period (D) referred to melting snow and widespread mist or fog.

Discussion

The persistence for a period of 3 hours in period (C) of different polarities of space charge at 1 m and 2 m is the most striking feature of these observations. With a wind speed of some 10 m sec^{-1} there must have also been strong turbulent mixing and hence a separation of charge in the proximity of the space charge collectors. The fact that this space charge difference falls to zero on the disappearance of the snow leads one to wonder if the charge separation was caused by the melting process in the snow. Figs. 45 and 46 illustrate these features. The possibility that the high wind blowing over the snow would itself cause this charge separation was ruled out as in periods (A) and (B) which had wind speeds and presumably mixing comparable with those in (C),

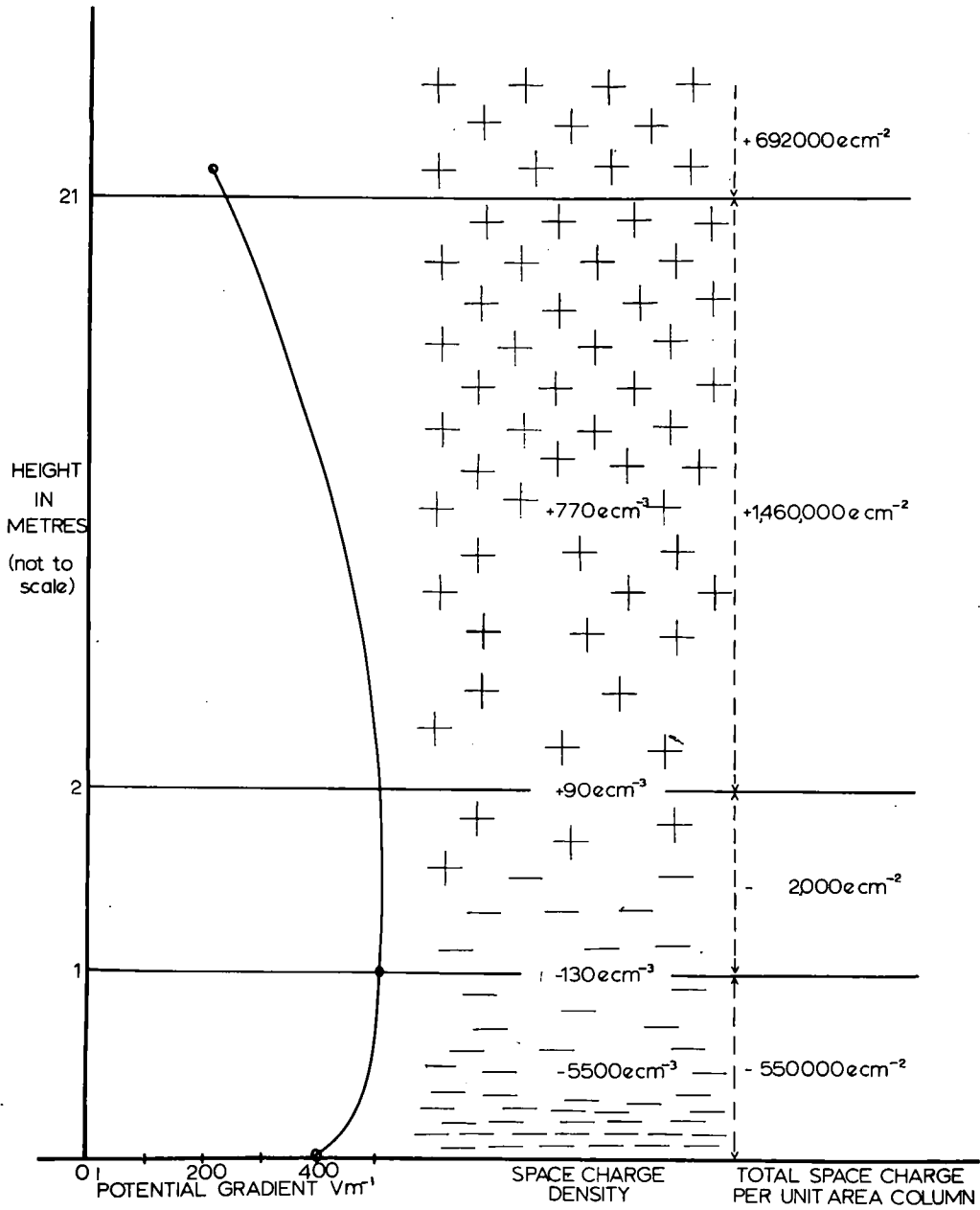


FIGURE 47.

the space charge pattern was quite different. Also in period (D) where there was melting snow but no appreciable wind the space charge pattern was again different. It seems reasonable to assume therefore that the charge separation noticed in (C) was due to the combination of the melting process and the accompanying high winds. There was perhaps the possibility that instrumental faults could cause errors in the recorded values, but the fact that a zero check had been carried out on the apparatus for some 3 hours immediately prior to the record and for a brief spell during the record appear to rule out this as a source of error. Moreover, for the 160 or so hours in which the collectors were installed at 1 m and 2 m, there was only the one occasion where the two records diverged for more than 1 min. There was therefore every reason to have confidence in the equipment, especially because the space charge results seemed to be confirmed by the potential gradient values. Fig. 47 gives an impression of the electrical state of the atmosphere at one instant in period (C). The total space charge per unit area column shown in this figure is deduced from Poisson's equation and shows the deviation from the normal fine weather value. During this period the humidity records point to an upward movement of water vapour.

There is a possibility that the field mill at 1 m which was inverted and calibrated allowing for an exposure factor would perhaps suffer an error in concentrations of high space charge, but the recorded values at this level were too small to introduce serious errors. Using Poisson's equation applied to the potential gradient

at 0 m and 1 m the space charge at 1638 hours was calculated to be -5500 e cm^{-3} , and similarly by using the 1 m and 21 m potential gradient values the space charge in this region was $+770 \text{ e cm}^{-3}$. The corresponding value almost 1 hour earlier at 1542 hours was $+860 \text{ e cm}^{-3}$. This high upper positive space charge density agrees closely with that obtained during periods (A) and (B) and can be associated with the observed blowing snow from the surrounding highland.

From Fig. 47 it appears that the negative space charge layer is situated very close to the ground especially because the calculated value of space charge from 0-1 m was -5500 e cm^{-3} and the recorded value at 1 m was only $+130 \text{ e cm}^{-3}$. Charge separation occurring at the surface would account for this reading if the positive charge remained on the melting snow, or very close to the ground, and the negative charge was blown into the air.

If a fine weather value of $+100 \text{ V m}^{-1}$ is assumed for the potential gradient, then by applying Poisson's equation to the potential gradient results, the deviations from the normal value of the space charge per unit area column are calculated to be $-550,000 \text{ e cm}^{-2}$ between 0 and 1 m, $-2,000 \text{ e cm}^{-2}$ between 1 and 2 m and $+1,460,000 \text{ e cm}^{-2}$ between 2 m and 21 m. These differences yield an excess of $+692,000 \text{ e cm}^{-2}$ above the normal for heights greater than 21 m. The negative space charge recorded at 1 m and positive at 2 m implies that there is a charge separation very close to the collectors which is detected before being dispersed, even by the winds with speeds of between 7 and 14 m sec^{-1} . These results are also consistent with the process des-

cribed by Dinger and Gunn in 1946 and Magono and Kikuchi in 1963 in which the melting snow lies on the ground and gains a positive charge whilst the negative charges are released at the surface under conditions of strong winds. This process seems to be verified by the fact that the space charge in the atmosphere reached its more usual state after the snow had disappeared from the near vicinity of the instruments. It is unlikely that this process occurs in period (D) as there is no difference in space charge densities at 1 m and 2 m. The wind however was much lighter being only about 3 m sec^{-1} .

In conclusion therefore it can be stated that the charge separation occurs when wind speeds of about 10 m sec^{-1} blow over rapidly melting snow. These results are of interest because of the fundamental role which ice and water play in the modern theories of cloud electrification.

2. SPACE CHARGES PRODUCED BY POINT DISCHARGE FROM TREES DURING A THUNDERSTORM

Introduction

Point discharge is the phenomenon which occurs in high electric fields at raised points. There is a limited region of very much enhanced field close to the point in which, if the field is large enough, there is a possibility of ionisation by collision. Depending on the sign of the potential gradient, ions of one sign will travel into the point whilst ions of the opposing sign will move away from the point to form what is known as corona space charge. If the space charge produced at the point is measured then the current through the

point can be estimated. MAUND and CHALMERS (1960) detected such space charge by measuring a difference in potential gradient at places upwind and downwind of a discharging point.

There is a possibility that a similar process could occur at natural objects such as trees and this could be a very important process in the transfer of charge between clouds and ground. In the past some measurements have been in accord with such a process whilst others have failed to show it. The results about to be discussed indicate the occurrence of point discharge at trees and a calculation of the current per tree is performed. Two methods have been employed in measuring the current through a tree. SCHONLAND (1928) cut down a small tree and supported it on insulators but, whilst it was then easy to measure the current through the tree, it soon died. MILNER and CHALMERS (1961) inserted electrodes into a tree thus short circuiting some of the current through it and their results showed evidence for point discharge currents; CHALMERS (1962) however, whilst comparing results from this tree with those from a nearby artificial point, found that at the time of a close lightning flash the currents through the point and the tree did not correspond exactly. MAUND and CHALMERS (1960) detected space charges produced from a line of trees but found no such effect from an isolated tree which was expected to give point discharge currents. However it was pointed out that this tree was in full leaf and the results indicated that a tree in leaf gives rise to less point discharge than a tree which is not in leaf.

The potential gradient between earth and cloud would be expected to increase with altitude in the presence of corona space charge but the measurements of SIMPSON and SCRASE (1937) and SIMPSON and ROBINSON (1940) failed to show this and therefore great doubt was expressed as to whether such space charge was produced at trees. In order to obtain the relation between rain currents and point discharge currents however, the presence of this space charge and also the increase of potential gradient with height are required, as pointed out by SIMPSON (1949) and CHAIMERS (1951). Measurements during thunderstorms have often showed that the potential gradient changes sign after a lightning flash and this phenomenon can be explained by the presence of corona space charge. However FRIEDER (1962) obtained results from which he deduced that there was no change of conductivity below a thunderstorm and therefore corona space charge was not produced, but CHAIMERS (1964) argues against these results.

Results

On the afternoon of Tuesday April 21st 1964 there had been very heavy rainfall but no lightning. However, after the rain had stopped a number of lightning flashes occurred between 1530 and 1550 hours G.M.T. The wind speed varied between 2.4 and 5.4 m sec⁻¹ from between directions of 135° and 175°.

During the storm the potential gradient had been recorded at 1 m and 20 m at intervals of 19.2 sec, but only after the rain had ceased, namely 1553.30 G.M.T., was space charge recorded although visual observation was carried out for 1 min. previous to this. The results

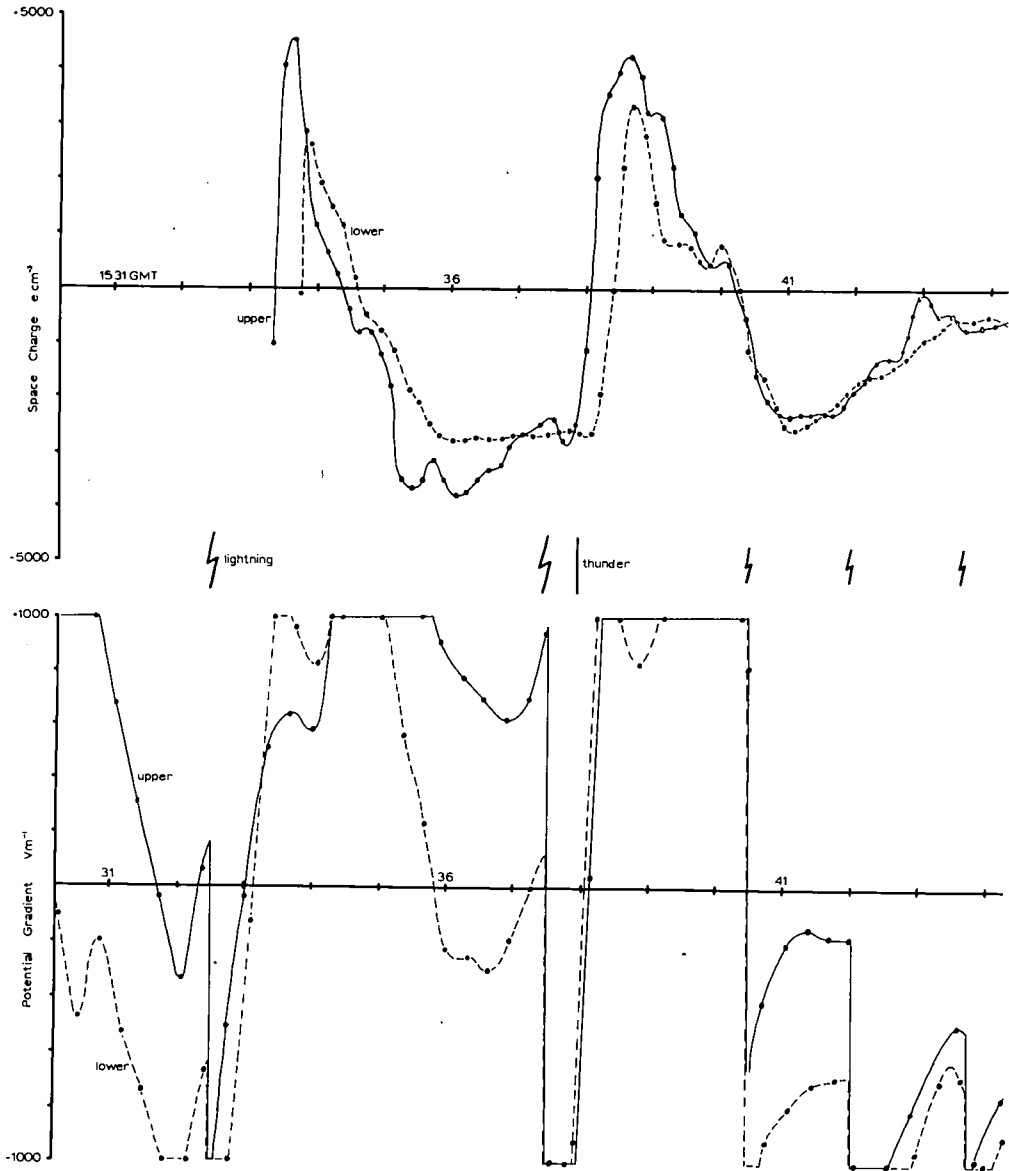


FIGURE 48.

obtained are shown in Fig. 48 where the space charge and potential gradient values are plotted separately although they were originally recorded on the same axes. In order to obtain the exact times of the lightning flashes reference was made to some continuous recordings made at the Science Laboratories site by Mr. I.E. Owolabi, and on the occasion where thunder was heard it was marked on the record at the instant of hearing. The times given are consistent among themselves but may differ by up to five minutes from G.M.T. There are more lightning flashes marked on the record but these did not give any interesting records for space charge.

Three periods seem to be worth investigating; these are

- (A) The fairly steady conditions from 1535.45 to 1537.30 hours.
- (B) The conditions after the main lightning flash at 1537.30 up to 1541.00 hours.
- (C) After the earlier lightning flash at 1532.30 up to the steady conditions at 1535.45 hours.

The recordings of the potential gradient during period (A) gives average values of $+750 \text{ Vm}^{-1}$ at the top of the mast and -160 Vm^{-1} at 1 m. Also during this time, the average space charge density at the upper collector was -3120 e cm^{-3} whilst the lower collector registered -2670 e cm^{-3} . The lightning flash at 1537.30 caused the potential gradients to decrease quickly and the time constant for their recovery was approximately 25 sec. For a few seconds after this flash the space charge at the two levels remained constant but then it went rapidly positive with the greatest rate of change for the upper collector occurring 41 sec after the flash. The values reached

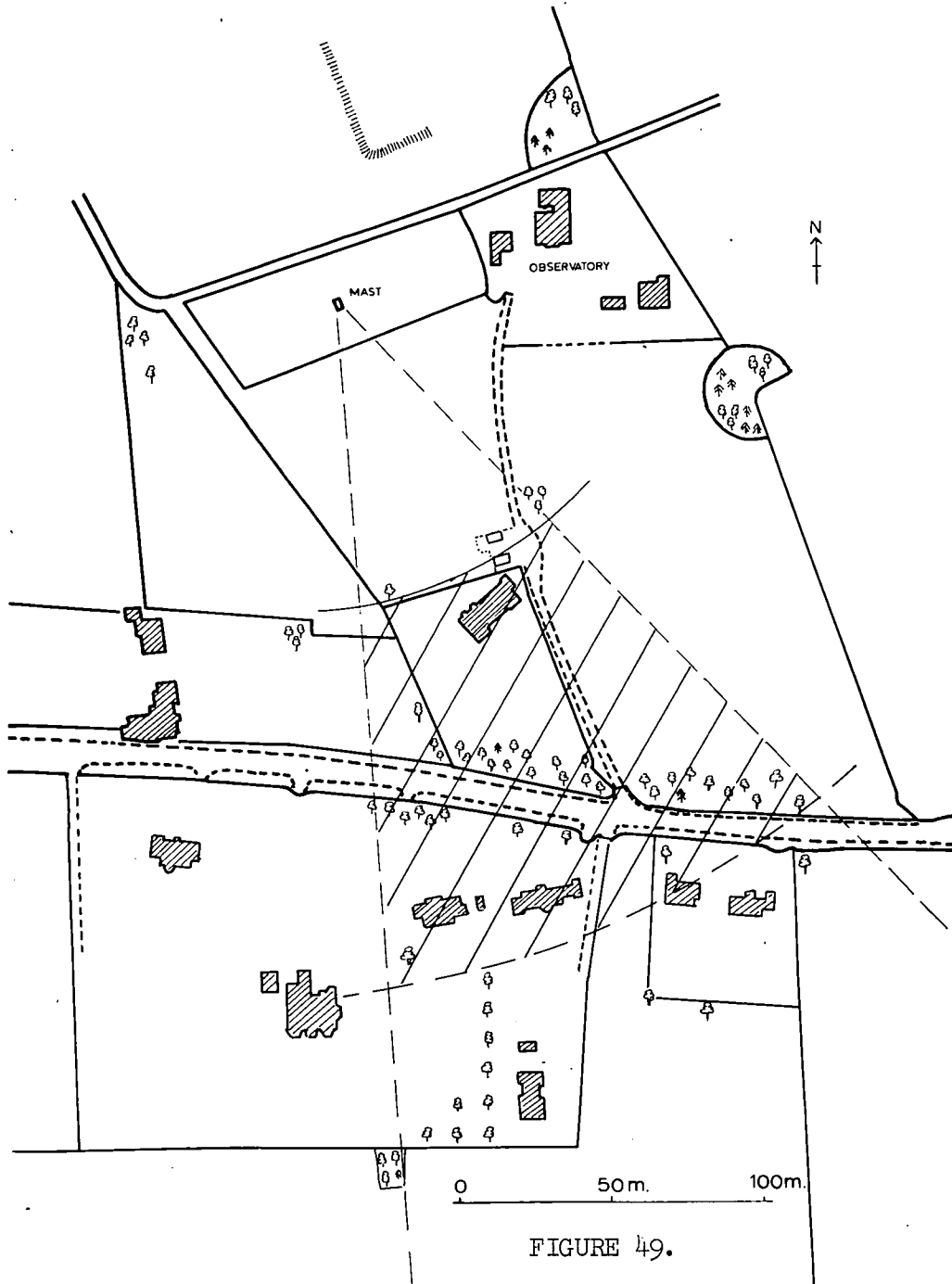


FIGURE 49.

maxima of 4200 e cm^{-3} at the top and 3400 e cm^{-3} at the foot of the mast, and a period of about 3 min. elapsed before they returned to their original negative values. As can be seen from Fig. 48 a similar state of affairs occurred after the flash at 1532.30 in period (C) and visual observations showed negative space charge of about -4000 e cm^{-3} prior to the flash.

Discussion

The results point to the possibility of point discharge somewhere to the windward of the mast producing the positive space charge recorded. The position of the point discharge area can be calculated by measuring the time from the lightning flash to the instant where the greatest rate of increase of space charge occurred in the upper collector, and by knowing the wind speed the distance can be estimated. The wind speed at the top of the mast varied between 2.4 and 5.4 m sec^{-1} and in 41 secs this corresponds to distances of between 98 and 221 m. A map of the area is shown in Fig. 49 and the shaded area shows the region in which this corona space charge appears to have been formed. By studying this shaded portion it seems most likely that this space charge originated at the line of trees bordering the road and the house to the north. The houses to the south were completely dominated by the adjacent trees and can therefore be neglected. It is interesting to note that the trees were at this time in bud but not yet in leaf. In order to obtain the average distance between trees a tape measure was obtained and a more accurate map drawn before estimating the average linear separation to be about 3.4 m between each tree.

During period (A) there is a potential gradient difference between the two field mills of 920 Vm^{-1} and there is an average space charge density of -2900 e cm^{-3} . Using Poisson's equation this space charge density corresponds to a 1050 Vm^{-1} difference between the two field mills, and whilst this is only 14% more than the observed value there could be three factors tending to cause the error. In the first place there is possibly a non-uniformity of space charge throughout the height of the mast, whilst another error would be caused by corona space charge produced at the mast itself which, when travelling with the wind, would affect the upper mill more than the lower one. Finally an error could arise in the calibration of the mills due to the exposure factors, as these factors were determined in ordinary fields and not under conditions of excessive space charge. In these latter conditions the space charge will have a similar effect on both mills and therefore using the calibrated exposure factors the lower mill will record a greater value than it should whereas the upper mill will record a lower reading. During period (A) the space charge is reasonably constant at -2900 e cm^{-3} and it is therefore possible to calculate approximately the average current per tree provided the height of the space charge layer is known. It is difficult to estimate such a height however and therefore it is more realistic to measure values of current per tree which must then be multiplied by a height factor. As the wind was blowing at an average speed of 3.9 m sec^{-1} the total current per metre length perpendicular to the wind direction can be estimated to be

0.036 μA reaching the height of the mast. This however could be the value up to a point several times the height of the mast thereby giving a much greater current. The tree separation of 3.4 m therefore gives a current value of 0.12 μA per tree, to be multiplied by this unknown factor due to the height of the space charge.

It is possible to estimate the corona space charge after the lightning flash per metre length of trees in the horizontal layer between the ground and the top of the mast by calculating the area under the peak in the space charge curves of Fig. 48. The total charge per metre length of trees was calculated to be 7.65 μC and by assuming that the potential gradient remained negative for 25 sec the average current per tree was about 1.0 μA which again had to be multiplied by the uncertain spread factor. These values are of the order to be expected because the immediate current after a field change would be greater than the steady current, due to the fact that the space charge would not have had time to build up and oppose the local field at the point.

The negative change of potential gradient when the lightning occurred gives an impression, at first sight, that the cloud is of negative polarity (positive charge at the bottom) which is not the most common type of cloud. However this change could be caused by a flash within a cloud of positive polarity if the flash was further away than the reversal distance which is usually about 7-10 Km. The fact that, as the sky cleared, the potential gradient was negative suggested that the cloud was of negative polarity but this information is not

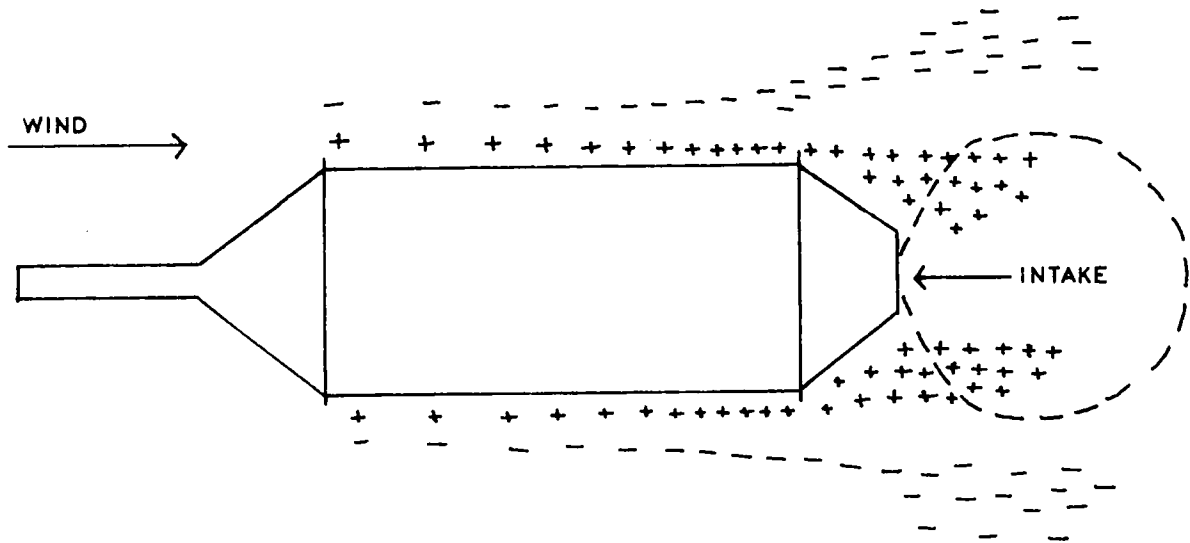
important. Referring again to the peaks in the space charge record of Fig. 48 it is of interest to notice the delay in arrival of the corona space charge to the bottom collector. This shows that the wind speed is lower closer to the surface than at the top of the mast. Also turbulence has distributed the corona space charge reasonably uniformly in such a short distance as the charge collected by the lower instrument was only 25% below that collected by the upper instrument.

These results indicate that corona space charge is formed during a thunderstorm at trees which are in bud and the amounts are similar to those liberated by artificial points. Hence the estimates of the total point discharge currents below clouds seem to be accurate and this process must be important in the transfer of charge between clouds and earth.

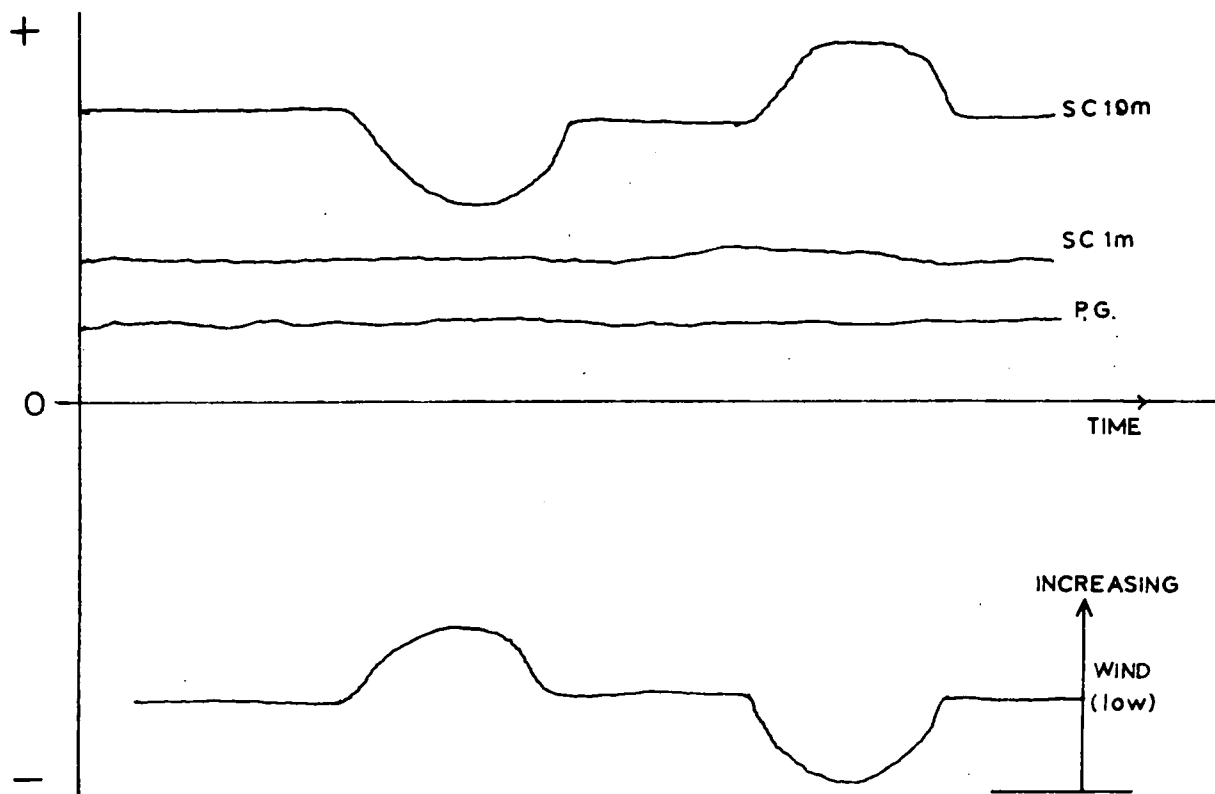
3. AN ELECTRODE EFFECT DUE TO THE MAST AND SPACE CHARGE COLLECTOR

Introduction

When the two space charge collectors were situated at 1 m and 2 m respectively there were very few occasions on which the two records were ^{not} practically identical. However, when the upper collector was installed at 19 m there was often a recorded difference of space charge between the two levels. As more records were obtained it became evident that the upper collector reading was inversely correlated to the upper wind speed and when there was a strong gust of wind the 1 m and 19 m records converged. It then seemed that an electrode effect existed towards the top of the mast.



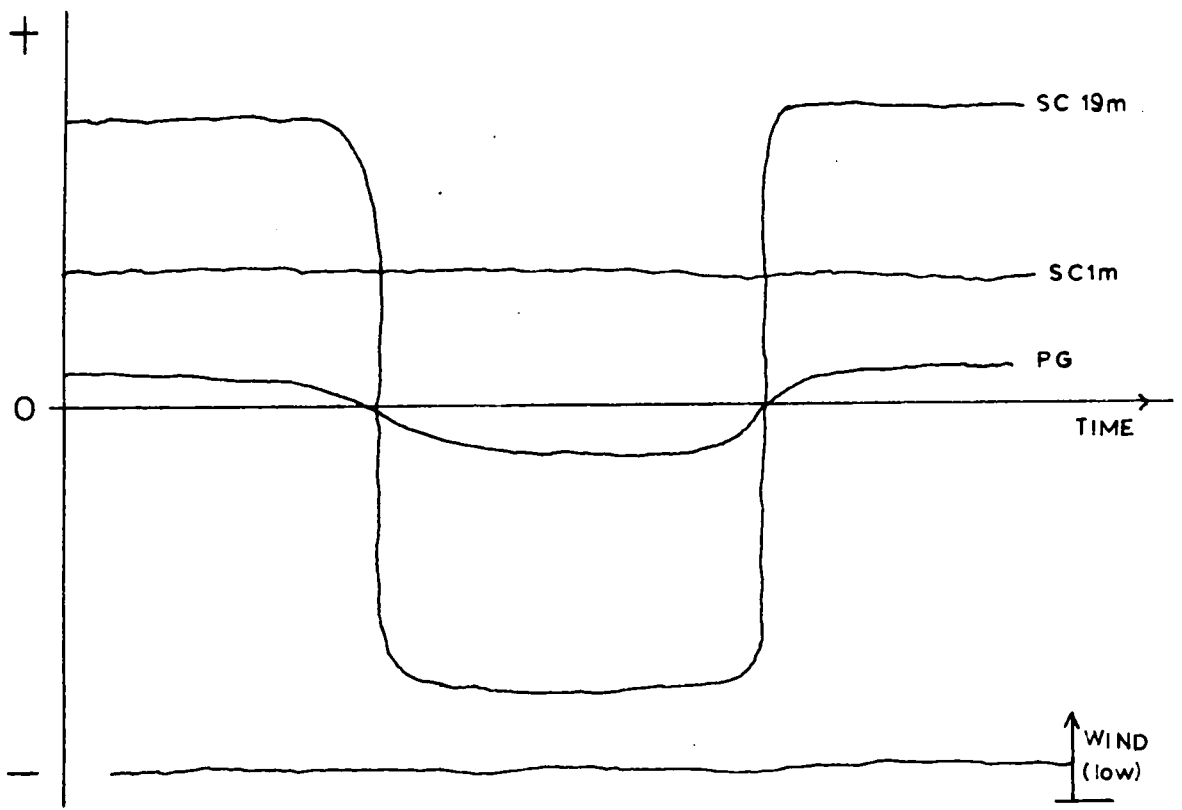
(a)



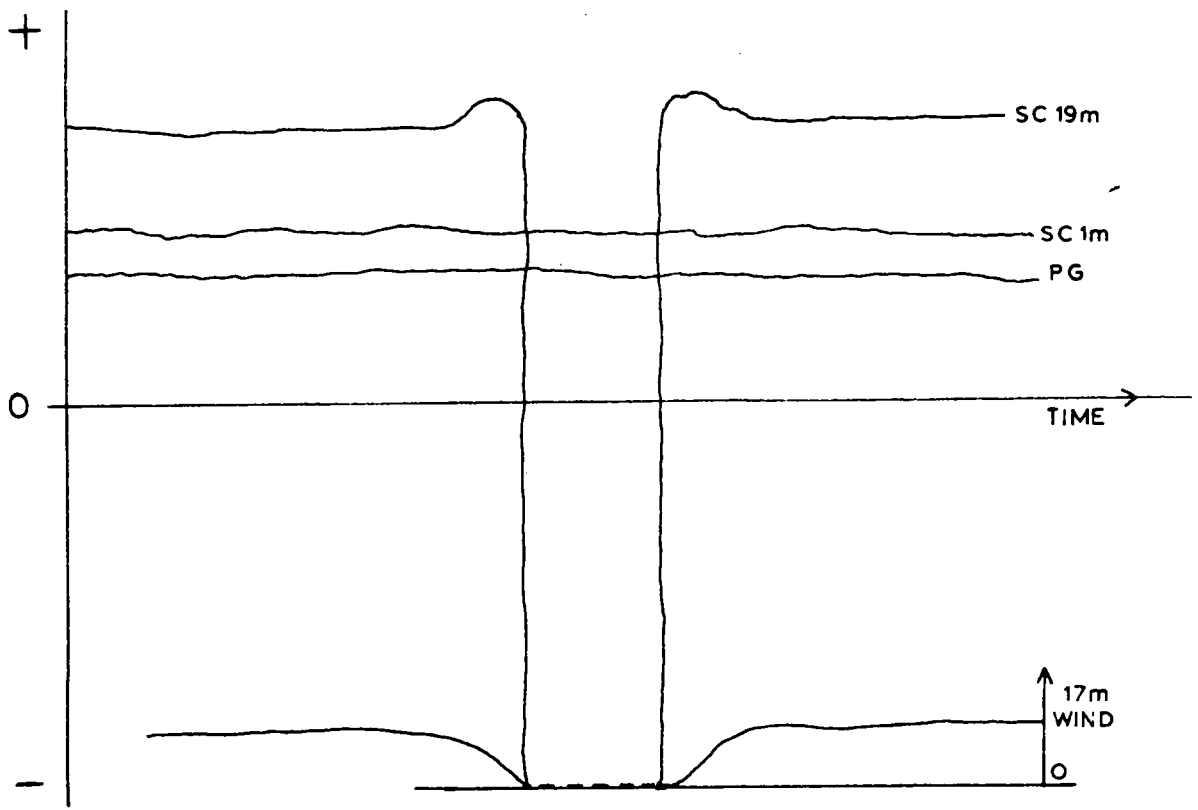
(b)

Fig 50.

There are two different effects likely to be produced which would depend on the wind speed, wind direction, potential gradient and small ion concentration. For the purposes of explaining these effects consider that the space charge density is constant and positive and is being measured at 1 m and 19 m, potential gradient is being measured at the surface and wind at the top of the mast. KIRKMAN (1956) measured the potential gradient perpendicular to the mast structure on a 33 m mast at a point 10 m below the top. He found that this value was 125 times greater than that at the surface of the earth at a point well clear of the mast. It is reasonable to assume therefore that the potential gradient is enhanced about 100 times near the 19 m collector and whereas at the foot of the mast it will be reduced. It is also not unreasonable to assume that the small ion concentration is about 500 cm^{-3} for each sign, and to neglect the effect of large ions owing to their very low mobility. In the vicinity of the 19 m collector the small ion speed is likely to be comparable to the horizontal wind speed and thus in the air lying close to the collector there will be a very much enhanced positive space charge. If the wind blows from the rear of the collector some of this positive charge will be carried by the wind and drawn into the intake of the collector as shown in Fig. 50(a). The instrument will thus record a higher positive value of charge density than the value expected at that level if the mast had not been there. If the horizontal wind speed was increased this electrode effect would be reduced, and as the wind speed falls so the electrode effect will increase. This effect is illustrated



(a)



(b)

Fig 51.

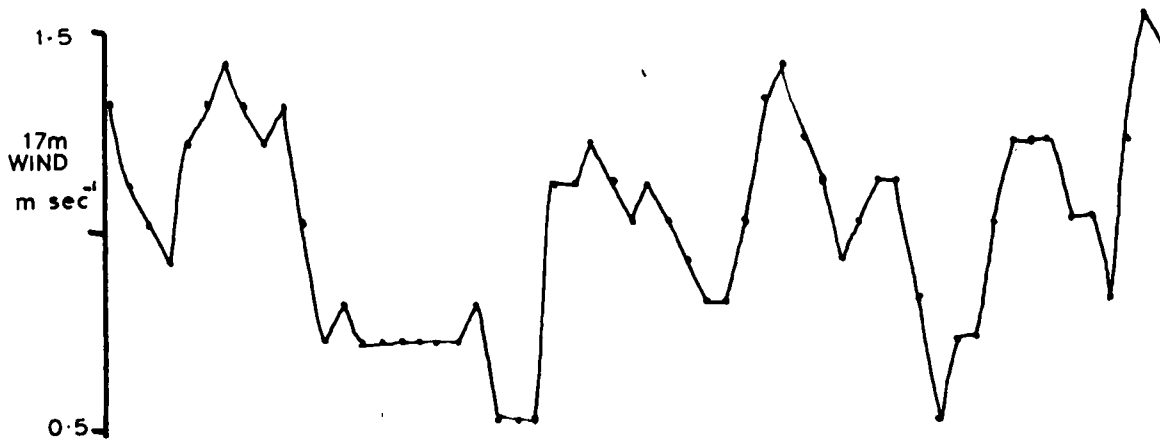
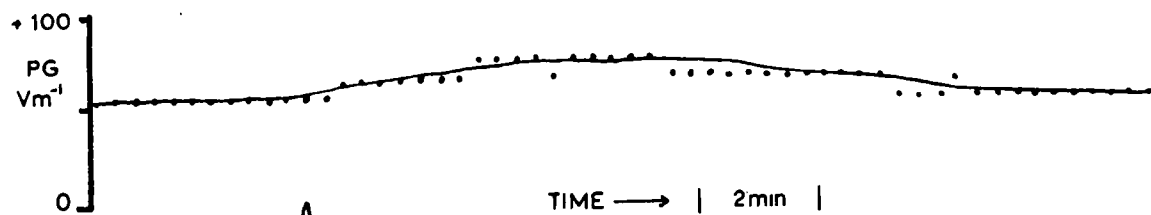
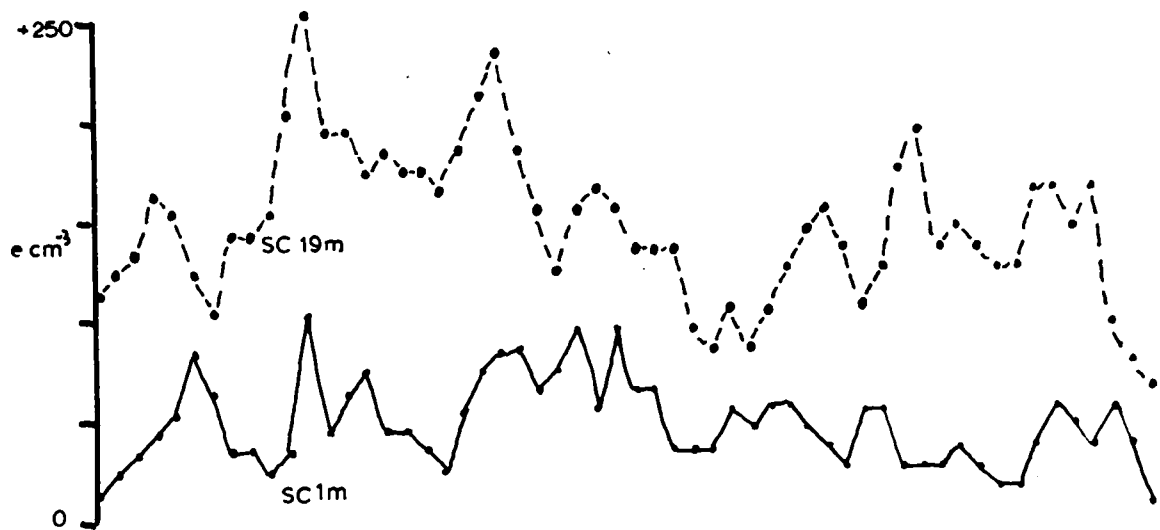
in Fig. 50(b). The 19 m charge density is greater than that at 1 m due to the electrode effect but as the low wind speed increases or decreases so the upper charge responds inversely.

Another point to consider is when the potential gradient at the ground changes sign as in Fig. 51(a). If the surface potential gradient changes by 30 V cm^{-1} in 1 min and changes sign, it corresponds to a change from $+0.5 \text{ Vm}^{-1}$ to -0.5 Vm^{-1} in 2 sec, or from $+50 \text{ Vm}^{-1}$ to -50 Vm^{-1} in 2 sec at the 19 m level on the mast. Thus if the wind speed is approximately 0.5 m sec^{-1} a small mass of air will take 2 sec to pass the space charge collector. During this time the potential gradient will change from $+50 \text{ Vm}^{-1}$ to -50 Vm^{-1} and the speed of attraction to the collector of the positive small ions in this cubic centimetre will change from $+0.5 \text{ cm sec}^{-1}$ to -0.5 cm sec^{-1} . In a 0.5 cm layer of air very close to the mast therefore, the space charge density could change from $+500 \text{ e cm}^{-3}$ to -500 e cm^{-3} within two seconds and the recorded output would be as in Fig. 51 (a).

These two illustrations just described show one aspect of the electrode effect on the mast but another entirely different result is likely which can be explained as follows. Consider that the wind speed is very low and is blowing through the mast structure before arriving obliquely behind the intake of the space charge collector. An electrode effect similar to that described will therefore be in operation. However, assume that the surface potential gradient is $+100 \text{ Vm}^{-1}$ and hence the small ion speed at 19 m will be 1 m sec^{-1} . If the advection is low enough there is a possibility that all the

positive small ions that blow through the mesh of the mast, which is approximately 1 m at this level, will be filtered to the structure, and hence the normal electrode effect would not occur owing to there being very few or no positive small ions left in this pocket of air. Referring to Fig. 51(b) therefore, in the first case the electrode effect causes an increase of positive space charge in the 19 m collector with a further increase as the wind speed drops. A point will be reached when very few or no small positive ions remain in the air at this level as they will have been filtered out, and hence there will be a rapid change of sign of space charge. The downward movement of positive small ions will be affected by the enhanced field at the top of the mast and these will therefore not reach the level of the recorder.

With these effects just described an increase of potential gradient would presumably have an effect similar to a decrease in advection and vice versa, whereas if the wind was from such a direction as to blow directly into the intake of the collector the effect would be reduced or eliminated. The electrode effect due to the mast and collector can therefore cause an excess of space charge at the 19 m level within the range of the small ion concentration of approximately ± 500 ions cm^{-3} . There will be no noticeable difference in the potential gradient caused by such an electrode effect and it can thus be distinguished from other effects.



27 MAY 1964

FIG. 52

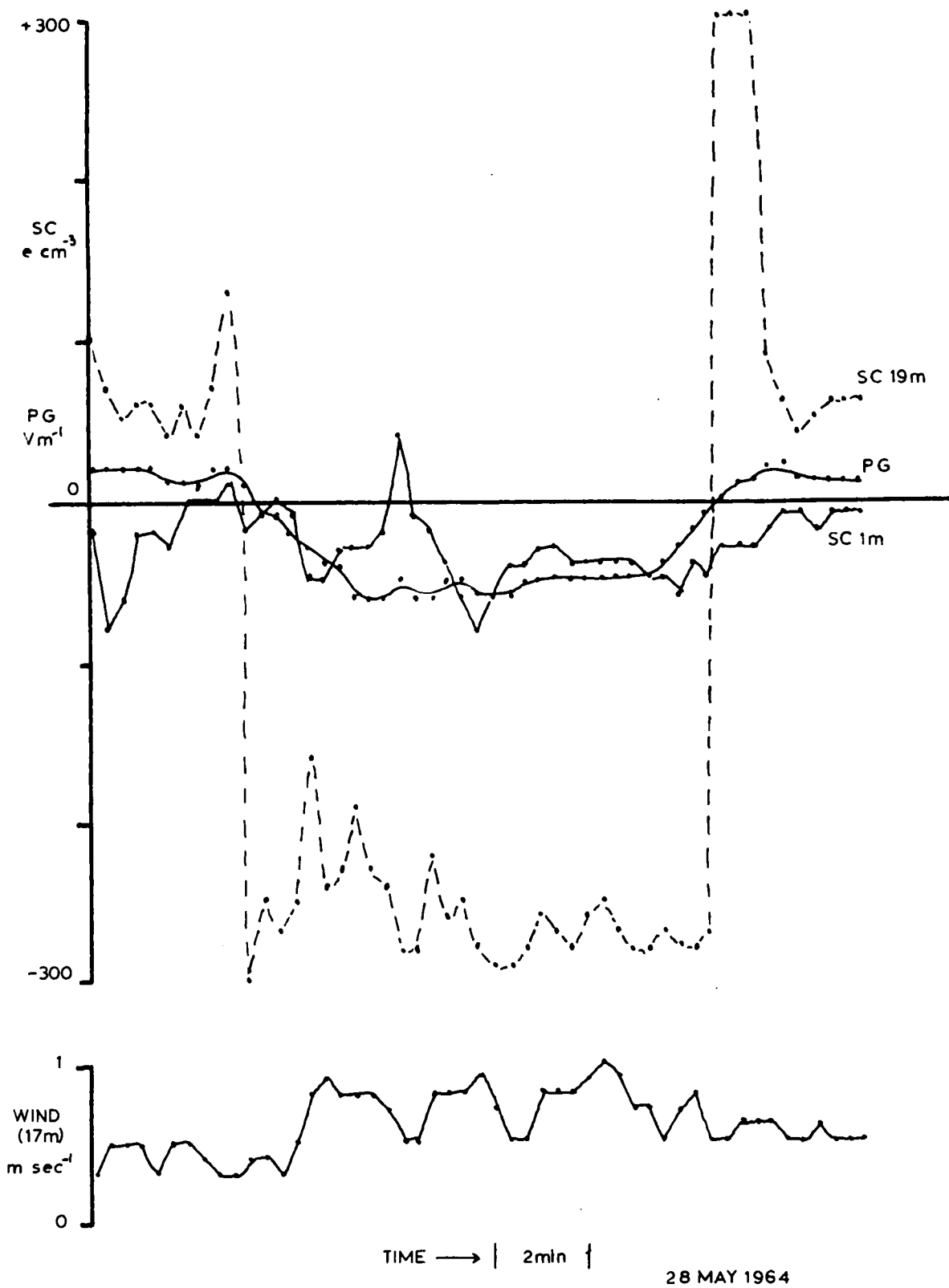


FIG. 53.

Results

There have been many occasions where the effect shown in Fig. 50(b) has been observed. A copy of such a record can be seen in Fig. 52 where the wind speed measured is at 18 m, the potential gradient at the ground and space charge at 1 m and 19 m. It will be noticed that the 19 m space charge density approaches the 1 m reading when the wind increases. Also plotted on the same record is the difference in space charge densities between the 2 levels which shows the inverse correlation with wind speed. The wind direction on this occasion was from the rear to the front of the collector. It can also be seen that there is no inverse correlation between wind and space charge at the 1 m level; this is presumably because the small ion speed at the 1 m collector will be of the order of $1/400$ that at the 19 m collector.

The effect illustrated in Fig. 51(a) was noted to occur on ten occasions. On these days the wind speed was once more low and from a direction to the rear of the collector, and the potential gradient was fluctuating from positive to negative. One such record is shown in Fig. 53 where the space charge concentration changes suddenly by over 400 ions cm^{-3} to a value that prevails for some ten minutes whilst the lower space charge reading follows a more stable path. The values quoted for the calculations performed earlier whilst referring to Fig. 51(a) are similar to those in this example and will therefore not be repeated. It could be argued that the arrival of a cloud of negative ions at the upper level causes the sudden changes on all ten

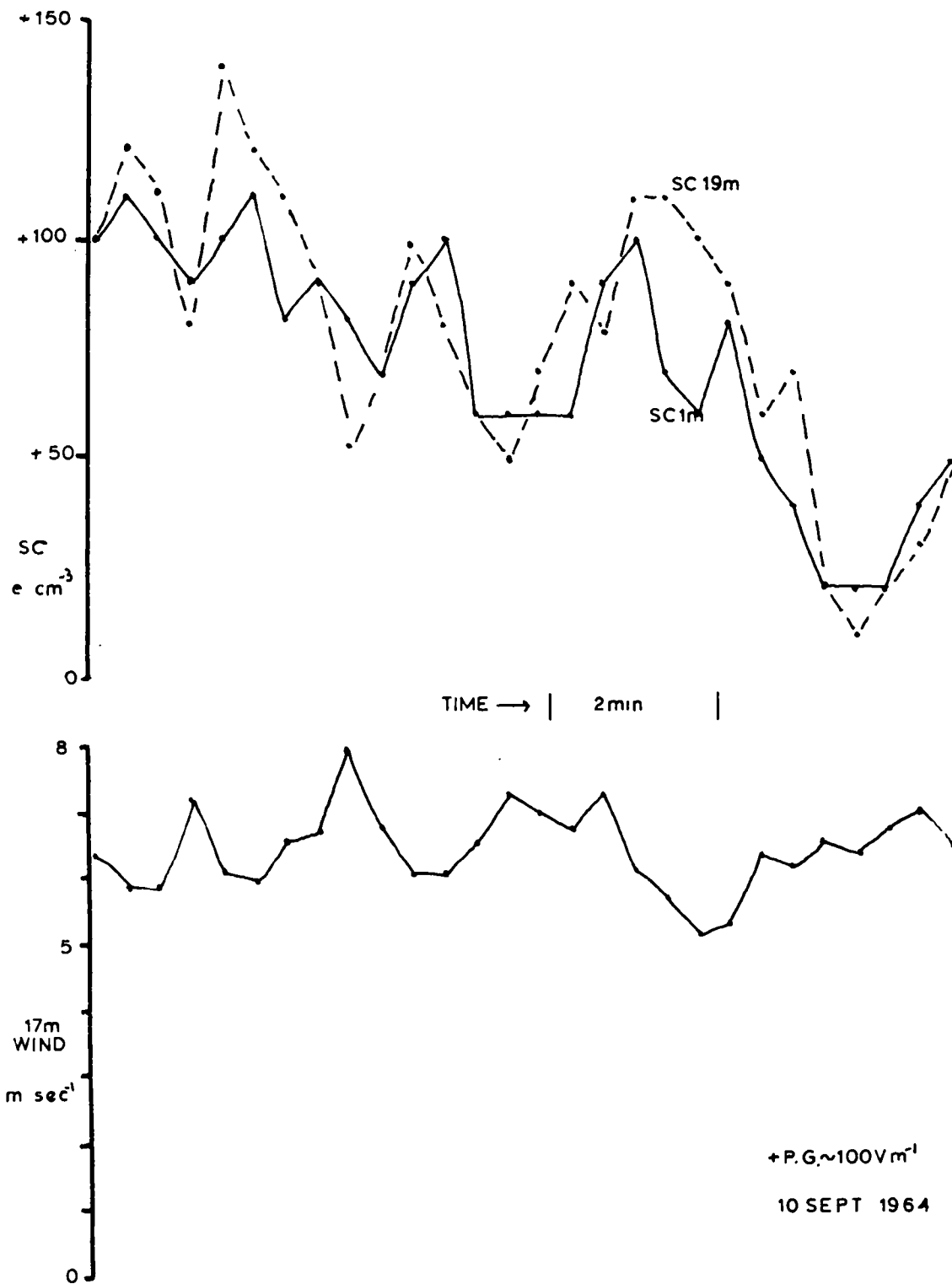


FIG. 54

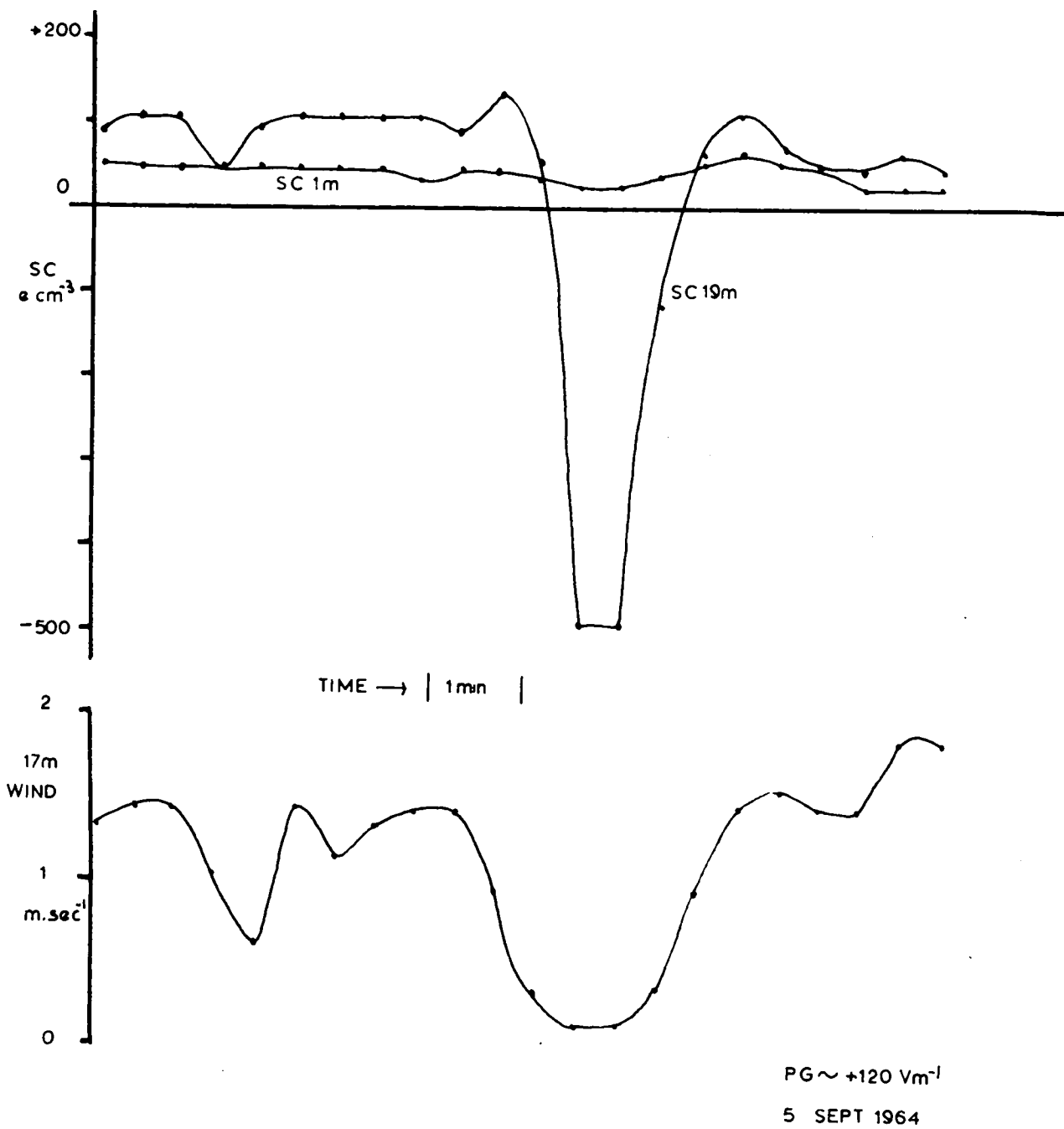
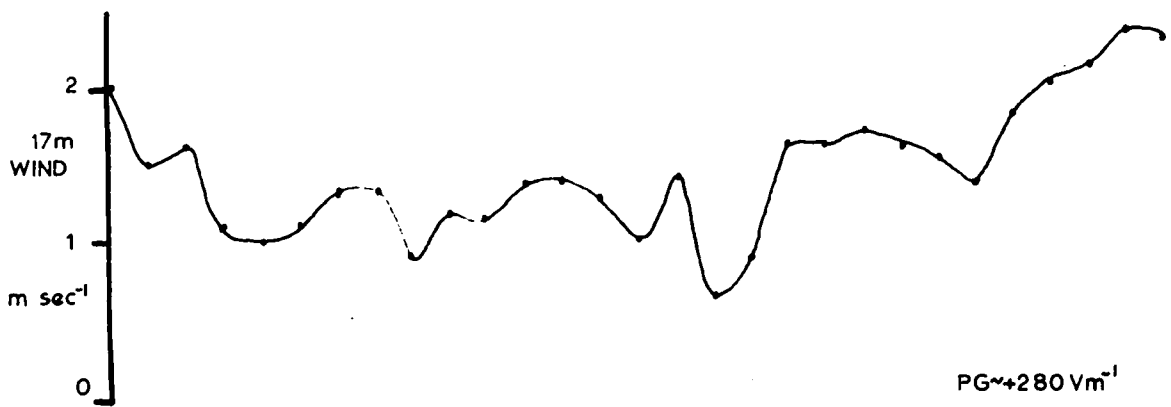
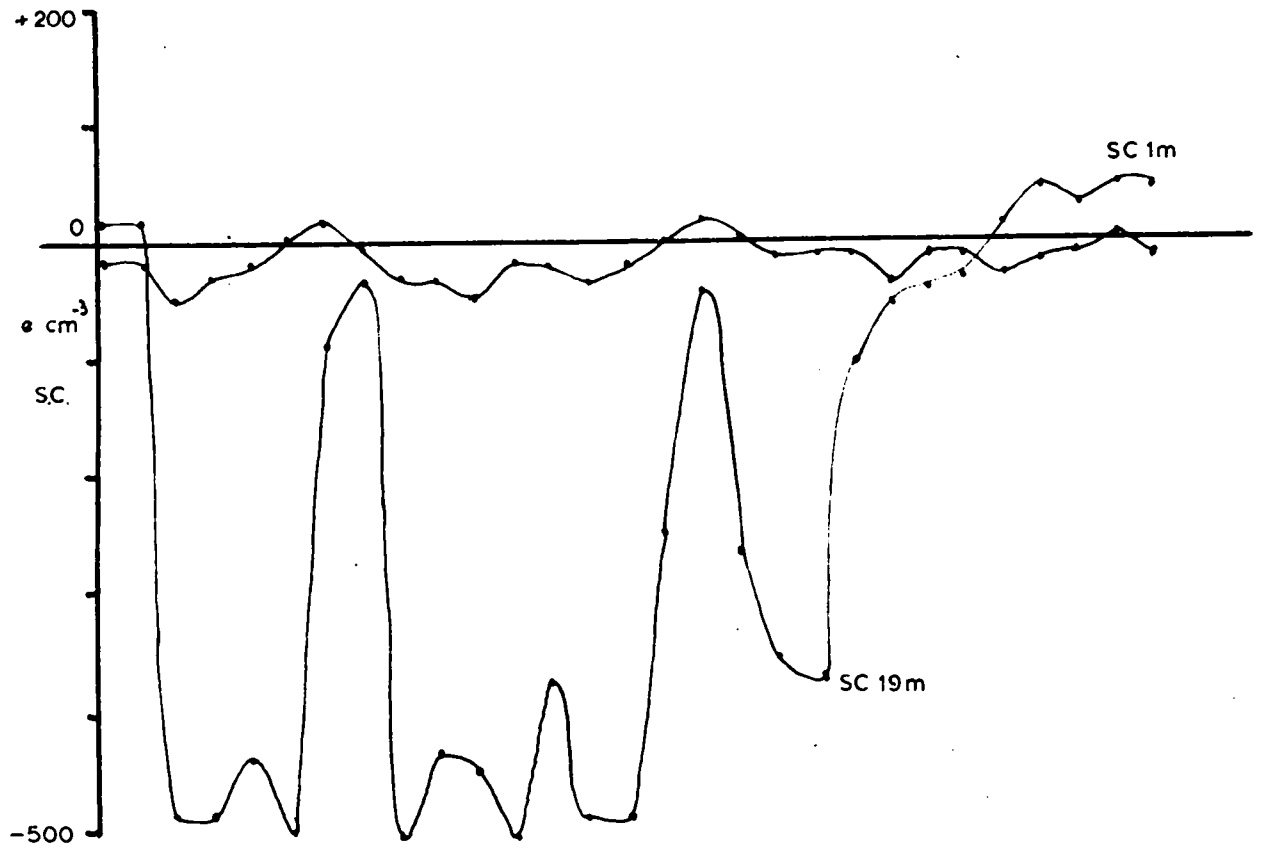


FIG. 55

occasions but does not extend to the 1 m level. However, by applying Poisson's equation to the 400 ions cm^{-3} change in ion concentration and the 30 Vm^{-1} change in potential gradient, the ~~thickness of the~~ layer of space charge causing the changes would be only 5 m thick. The likelihood that this is the cause of the sudden change in space charge concentration at 19 m, persisting for several minutes, therefore seems unreasonable.

Fig. 54 is a typical record on a day where there was a strong wind blowing directly into the intake of the collectors and it is seen that the electrode effect does not appear to exist on these occasions.

There were four periods when the effects referred to in Fig. 51(b) were noticed under low wind conditions. In each of these cases the upper wind speed dropped to a value lower than 0.1 m sec^{-1} and with a positive potential gradient the upper space charge readings became erratic, making frequent excursions to values of between -200 and -500 e cm^{-3} . The more usual state of affairs returned when the wind speed increased. Of the four occasions referred to, one of which is illustrated in Fig. 55, two occurred on the same day separated by a period of one hour and the other two occasions were on different days. It was at first thought that it was by chance that the drop in wind occurred at the same time as the violent space charge movements to negative values. However another record was obtained which lasted for over 40 min showing similar effects and in which the wind speeds were higher and from the direction of the mast to collector; but the



$PG \sim +280 \text{ Vm}^{-1}$

22 JULY 1964

FIG. 56

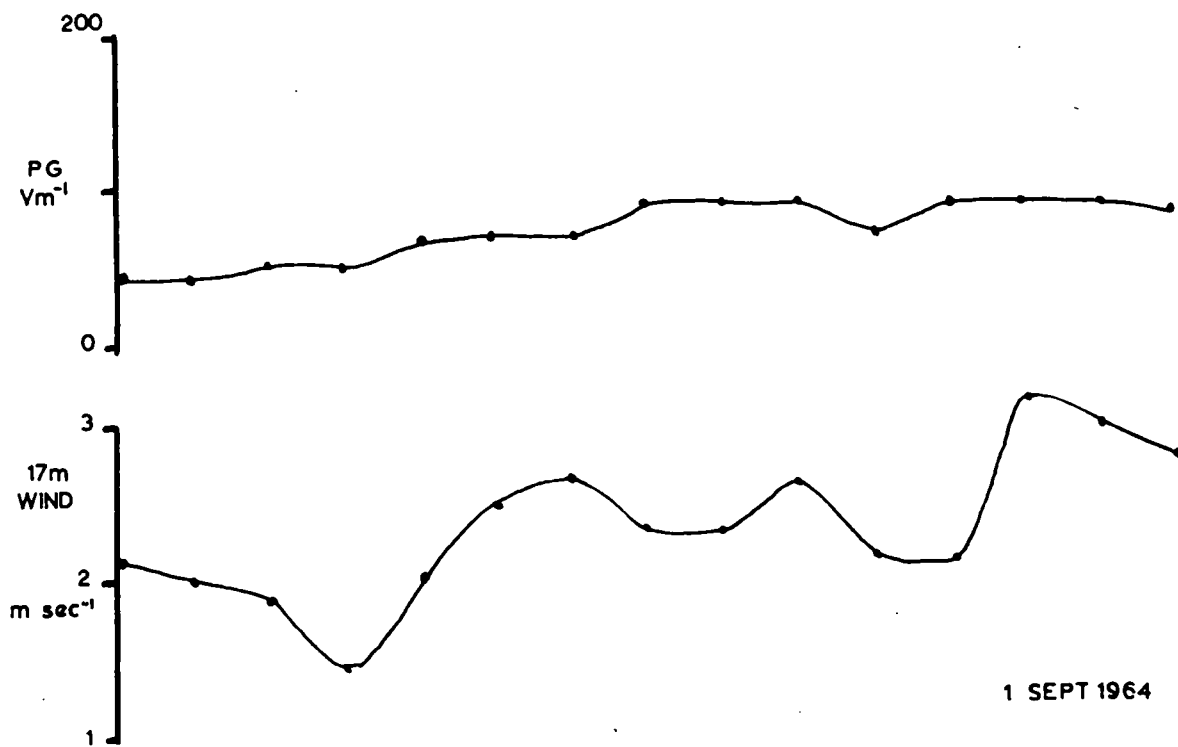
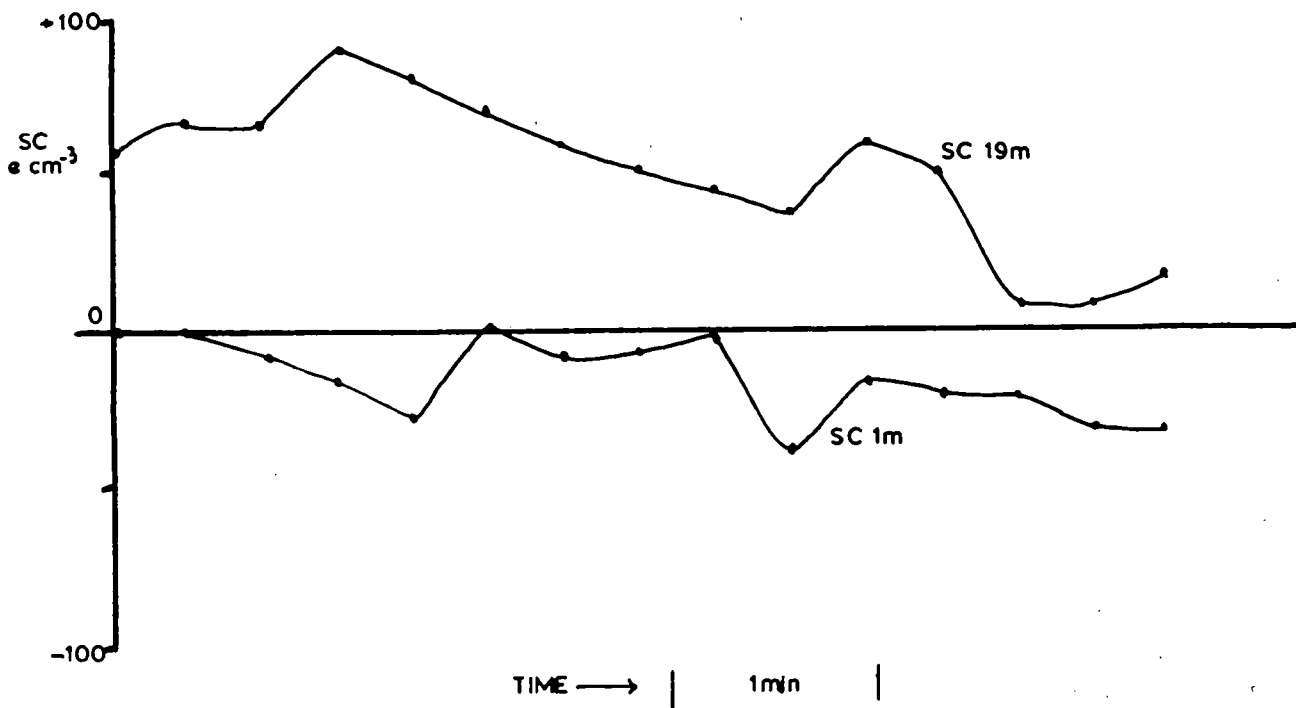


FIG.57

potential gradient in this case was over $+300 \text{ Vm}^{-1}$. During the whole of this period the top space charge record was very erratic and had frequent excursions to values of -500 e cm^{-3} whilst the lower reading did not appear to be affected. This record is shown in Fig. 56 and calculations show that the ion speed of 3 m sec^{-1} at the 19 m level is high enough to filter out nearly all the positive small ions with the wind speed as observed.

Occasionally records have been obtained showing negative space charge at 1 m and positive at 19 m with positive potential gradient as seen in Fig. 57. There is a possibility that the radio-activity in the surface of the earth, and in the air in close proximity to it, is giving rise to the negative excess. In considering the electrode effect due to the mast however these assumptions become dubious. If there had been a negative space charge concentration throughout the height of the mast due to some other cause, then with a positive potential gradient the upper collector could quite easily record a positive value of space charge, whereas the lower collector records the negative value.

Discussion

There are therefore two electrode effects which can be observed by the 19 m space charge collector in this very much enhanced field. Firstly if the potential gradient is positive and the wind is slight and blows through the mast or from the rear of the collector, then the positive ions migrating to earth are sucked into the collector as was seen in Fig. 50(a). Secondly, if this advection is extremely low

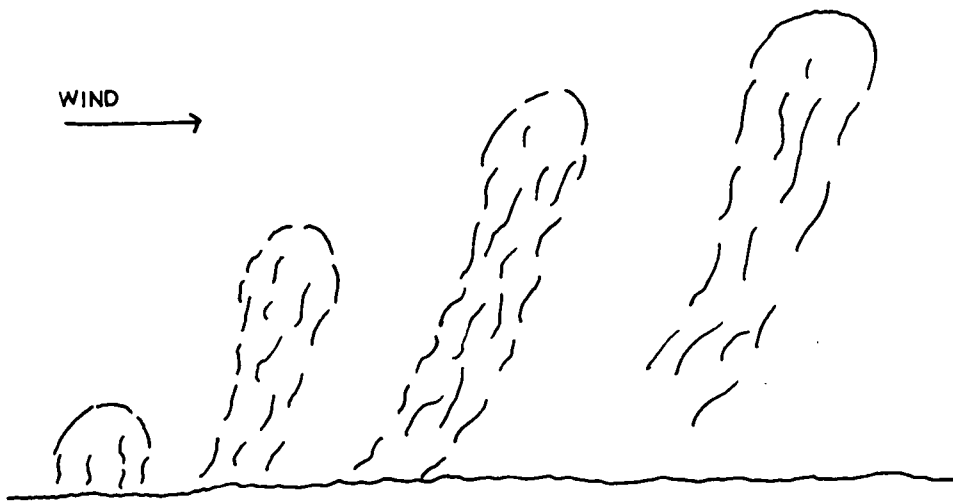
or non existent in normal fields, or slightly higher in high fields, the positive ions will all be filtered from the air leaving a negative excess to be sucked into the space charge collector. It may at first seem that an allowance could be made in order to correct for this effect in the upper collector, but the size of the electrode effect will be dependent on the potential gradient, wind speed, wind direction and small ion content in the air at that time. It appears therefore that results obtained with the upper collector under low wind conditions must be treated with caution. However, by observing the wind speed and lower space charge concentration it is possible to estimate the approximate record expected had the electrode effect not existed.

The fact that the upper collector is below the arm of the mast will tend to reduce this electrode effect to a value below what it would have been if the arm were not there. However, it appears that the potential gradient in this region and particularly around the nose cone is still far greater than at the bottom collector. It can therefore be expected that the space charge concentration recorded at 19 m can differ from what might be expected in the absence of the mast, by an amount equivalent to the small ion concentration of approximately $4500 \text{ ions cm}^{-3}$.

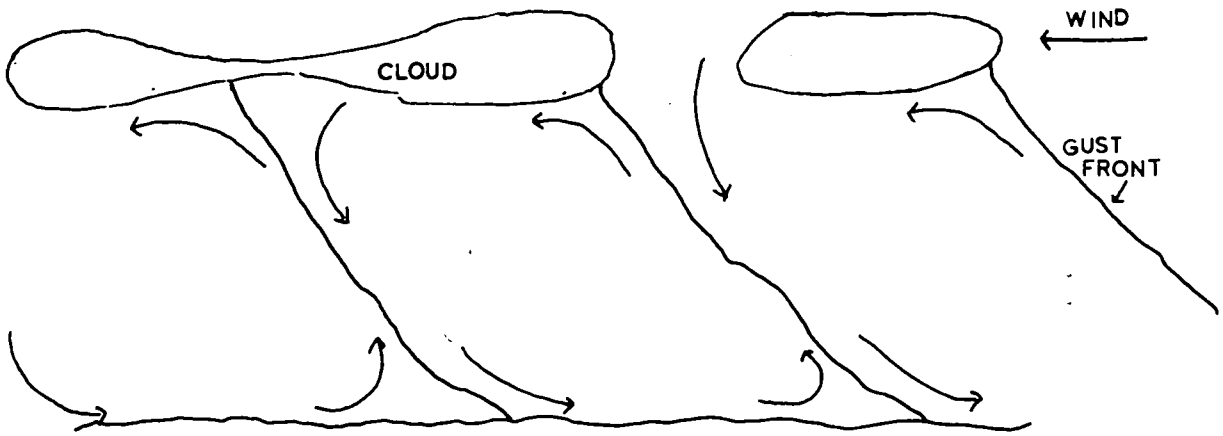
4. CONVECTION CELL MEASUREMENTS

Introduction

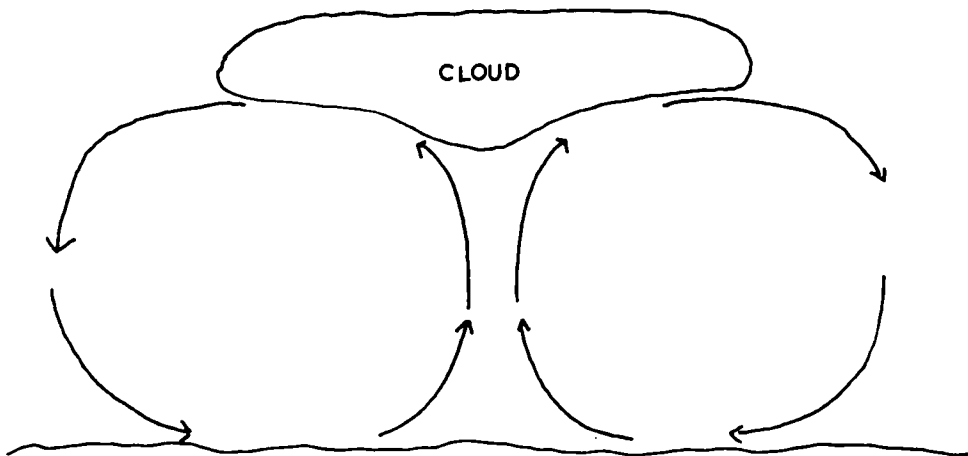
A number of results obtained during the summer of 1964 suggested that convection cells drifting under cumulus clouds were responsible for some sort of charge transport. The results referred to were found



(a)



(b)



(c)

FIG. 58

only under cumulus conditions and their effect became more pronounced as the heat of the day increased. Firstly however it is wise to introduce briefly three possible convection cell structures which have been suggested. The most recent picture of convective motion is that of SCORER and LUDLAM (1953). Here a bubble of warm air breaks away from the surface and rises up along a curved path to about the inversion level as shown in Fig. 58(a). A wake is formed under the bubble in which warm air rises and this wake blows along the surface of the earth. There are some doubts as to whether this wake drags along the surface for very long but there must be some upward movement of air from the ground early in the life of the bubble. Aircraft observations have detected these bubbles and there have been suggestions that they are between 0.1 and 2.5 Km in diameter.

Earlier theories were suggested by DURST (1932) and BÉNARD (1901). Durst's idea of convective motion is that the cellular patterns, which move with the wind, are separated by gust fronts. Fig. 58(b) shows such a pattern in which the circulation shown is that when the mean wind speed has been removed. Inside the cell the rising air having recently lost momentum by contact with the ground is slow-moving. The sinking air will bring down the higher momentum, lower humidity, turbulence and direction of the wind from a higher layer. Thus, as a gust front passes an observer the temperature will suddenly fall, the humidity will fall, there will be a sudden rise in wind velocity and a decrease in the small scale turbulence. After the gust front passes the wind speed will gradually decrease as the friction with

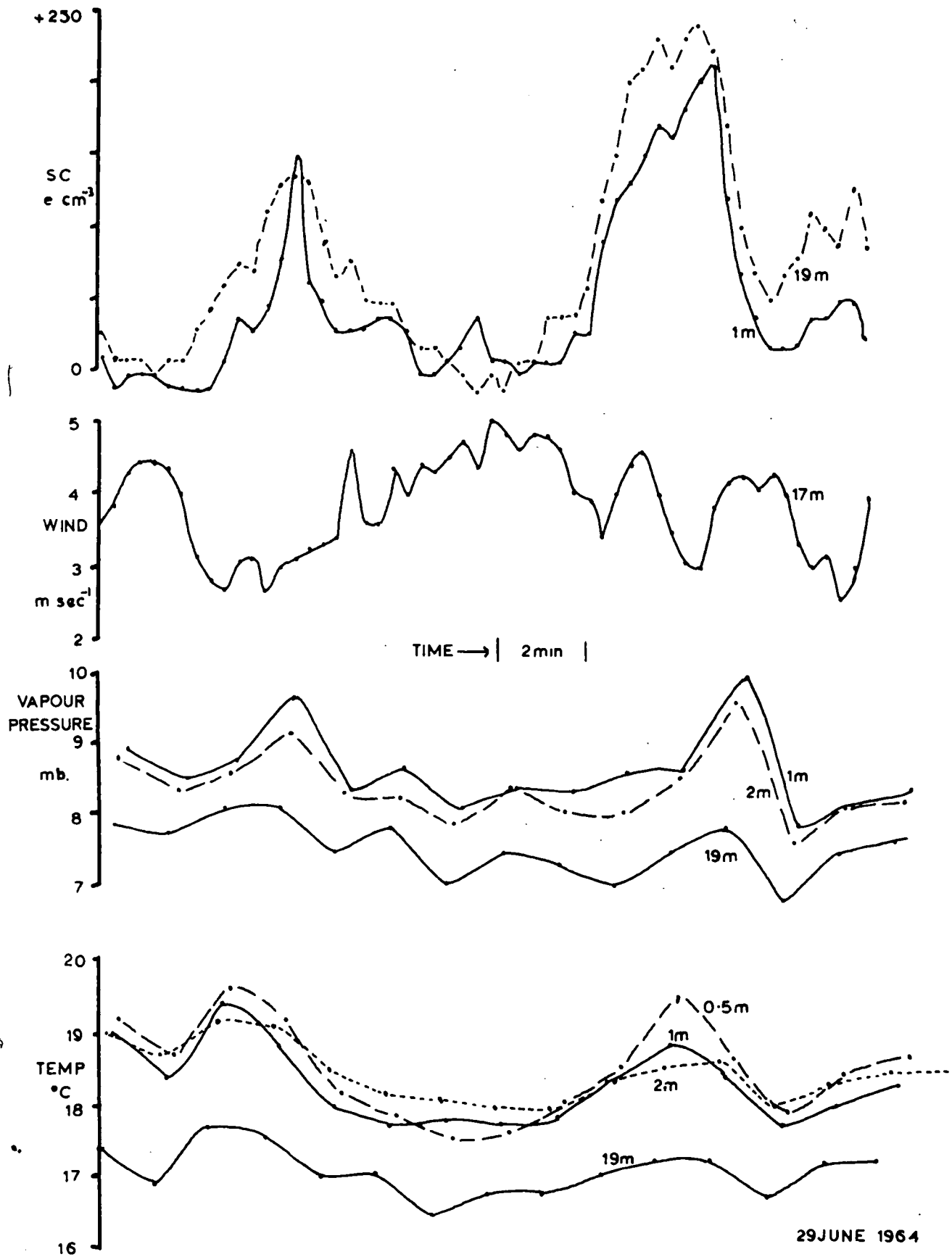


FIG.59

the ground surface retards the air flow, the temperature will slowly rise due to the heating up by contact with the surface and the humidity will rise if the ground surface is damp. The structure of the Bénard cell is shown in Fig. 58(c) where there is an upward motion at the centre, diverging motion at the top, and descending motion in the outer regions. When this cell passes an observer the changes in wind, temperature and humidity will be less severe than in the Durst cell. Both the Durst and Bénard cells are expected to be 1-3 Km in diameter.

Results

During the summer of 1964 results were obtained on 8 separate days when convection cells would be expected owing to the presence of convection cumulus clouds. The results can be seen in Table 6 where the numbers of large cells observed are listed along with the average diameters of the cells calculated from the mean period and upper wind speed.

On analysing the records a striking feature is that an increase of temperature occurred at the same time as an increase of space charge and humidity, and a decrease in horizontal wind speed. One part of such a record is illustrated in Fig. 59 where the different variables have been separated vertically.

Discussion.

The most important clue as to the origin of these patterns is that they co-exist with cumulus clouds and are therefore probably related to some form of cell structure. The average diameter of the 34

observed cells is 2100 m and they have an approximate period of 9 min. In Fig. 59 the rise in temperature recorded in the first 2 m of the

Date	No. of large cells	Mean Period min	Average wind at 17 m m sec ⁻¹	Average diameter m
26/6/64	8	9	4.0	2200
29/6/64	7	11	3.6	2300
2/7/64	3	9	5.8	3100
6/7/64	4	8.5	4.0	2000
13/7/64	4	11.5	3.3	2300
10/7/64	3	6	5.8	2100
20/7/64	3	9	3.0	1620
31/8/64	2	6	3.0	1080
Average		9.0 min	4.0 m sec ⁻¹	2100 m

TABLE 6

DETAILS OF CONVECTION CELLS

atmosphere could be expected when the wind decreased but this would not be expected at 20 m unless there was a pocket of warm air passing the mast or an upward motion of air. On observing the vapour pressure record however, as there is also a rise in this variable at all four levels, it appears that there could be an upward movement of air bringing with it the moist conditions from the first few centimetres above the ground. Referring again to Fig. 59 it can be seen that there is usually a temperature inversion somewhere in the lowest few metres until the peak in the variables occurs. This again points to an upward movement

of air from the surface to 20 m occurring only at these peaks. In all 34 recorded peaks this temperature lapse was recorded and it was not uncommon for the immediate conditions before or after to contain an inversion. The evidence of the temperature and humidity variables therefore points to an upward movement of air.

The space charge density at both levels often rises by some 150 e cm^{-3} within this upward motion and it appears that it can be caused by two effects. In the first case if an electrode effect exists at the ground then the high positive space charge lying close to the ground would be drawn up into the air. This is a reasonable assumption because the humidity rises and signifies that the air has probably been brought from very close to the surface.

The second effect causing the increase in positive space charge could be due to the speed of the small ions and upward wind velocity. In the potential gradient recorded their speed will lie between 1.5 and 3 cm sec^{-1} with no upward air motion, but if there is an updraught at this lower level, of similar speed, there will be a region of increased positive space charge. The reason for this increase is that the two opposite vertical forces acting on the positive ions would be approximately equal and thus give rise to the positive enhancement. The negative ions will move upwards at a velocity equivalent to the sum of their speed and the vertical wind speed. The constant production of small ions will replenish the layer when those present are neutralised or converted to large ions and carried by the wind.

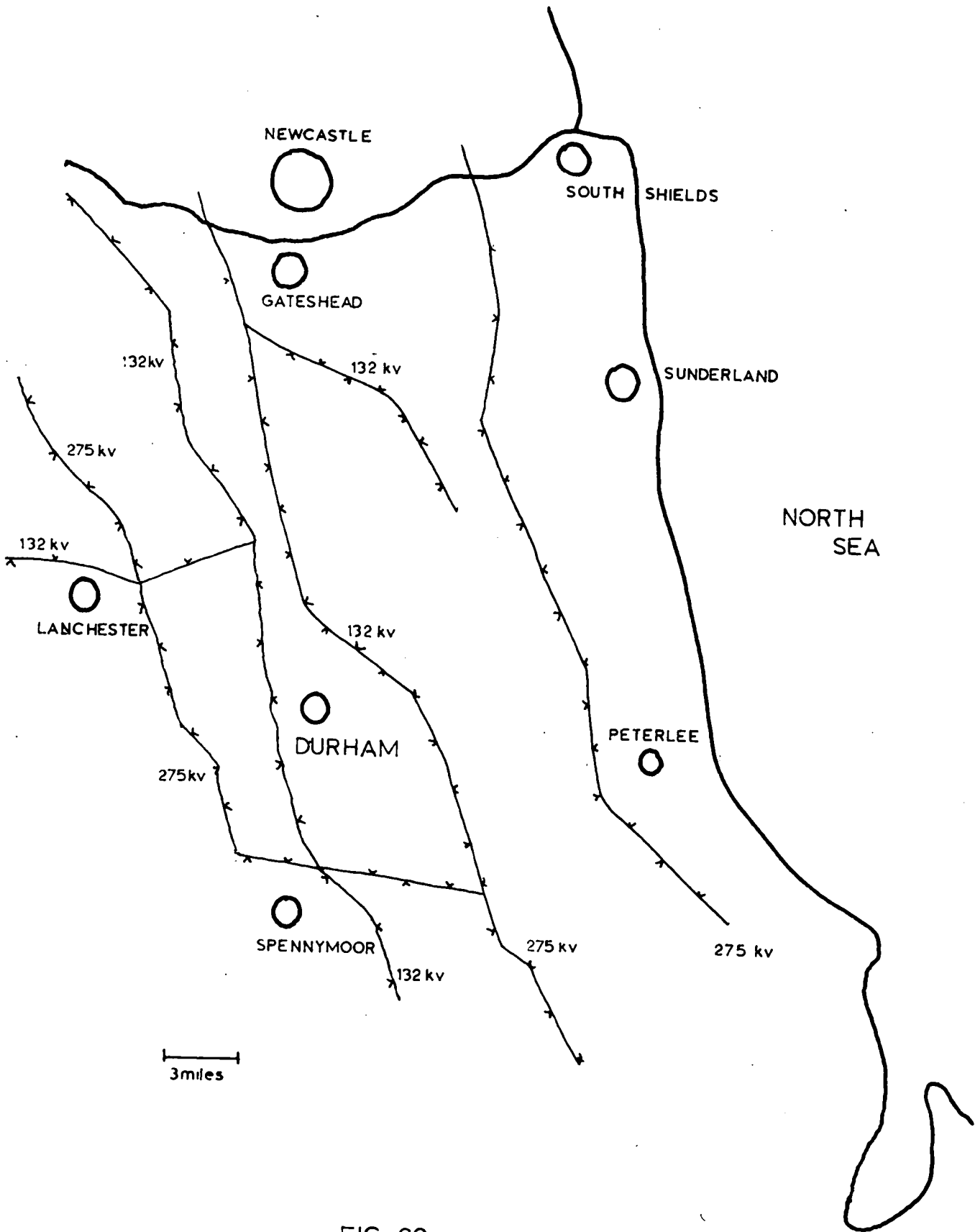


FIG. 60

Throughout the whole region of upward motion of air there will therefore be an increase of positive space charge caused by either or both of these two effects. However, in the latter effect one would expect the value at 1 m to be greater than at 19 m owing to the increasing vertical component of wind with height which will carry ions of both signs upwards. The records show that the upper collector is reading more than the lower collector but this could be a consequence of the mast electrode effect. It will be difficult to determine the actual type of cell structure unless continuous records are obtained at more land stations close to the mast.

5. NEGATIVE SPACE CHARGES

As was mentioned on page 23, Chalmers (1952) found conclusive evidence that negative space charge is formed at high tension cables during periods of mist or fog. Durham is completely surrounded by overhead H.T. cables as can be seen in Fig. 60 and it can therefore be expected that in misty or humid conditions there will be a predominance of negative space charge.

There were 15 occasions when records were obtained of persistent negative space charge and potential gradient during daytime conditions. On eleven of these days there was mist or fog locally thus confirming the H.T. cable effect. The remaining four days all had high negative space charges and potential gradients but the sky was cloudless and visibility excellent. During these four days there was one occasion when the wind blew from the NW whilst on the other three it was easterly. There is a possibility that wood fires or a local industrial

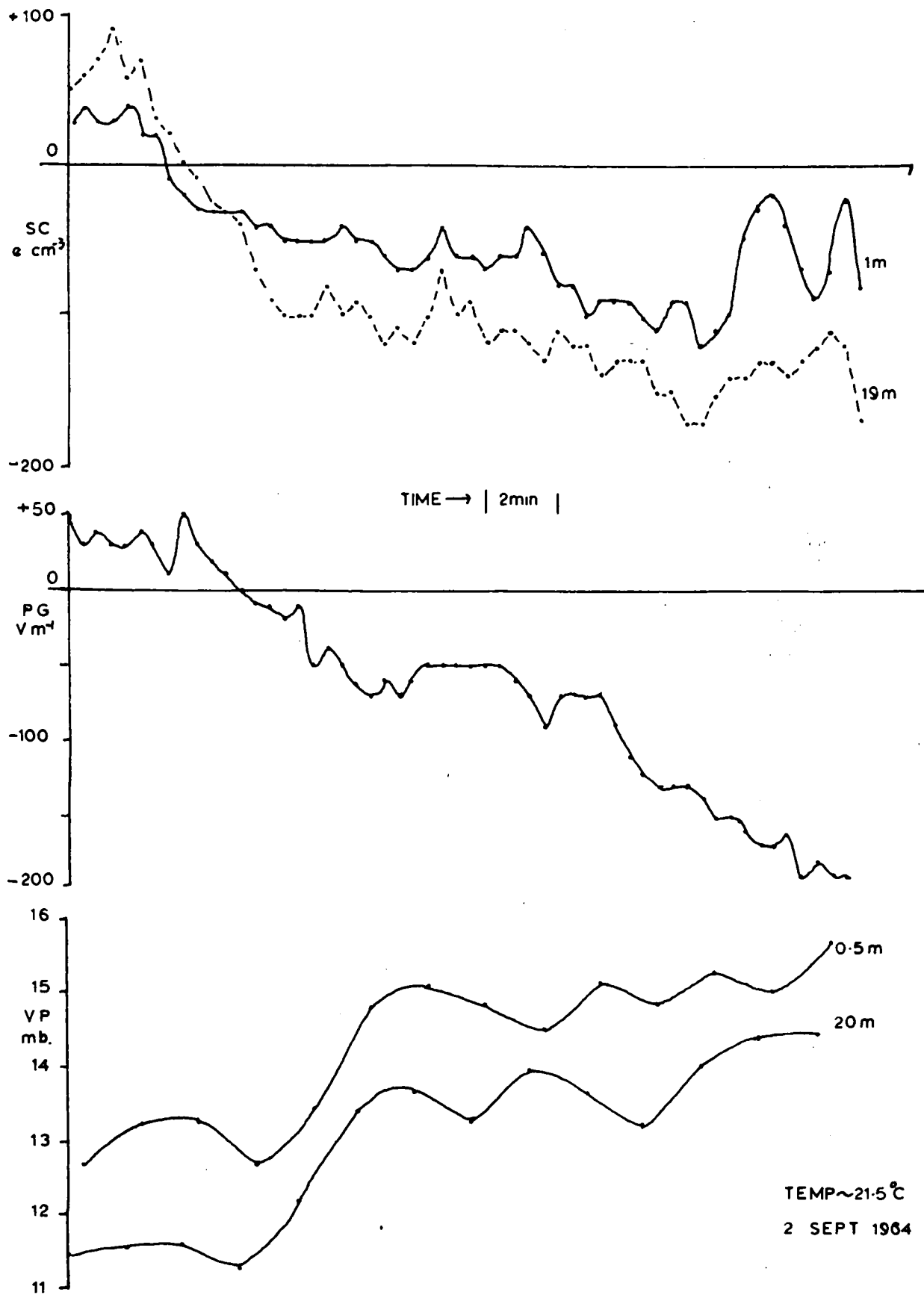
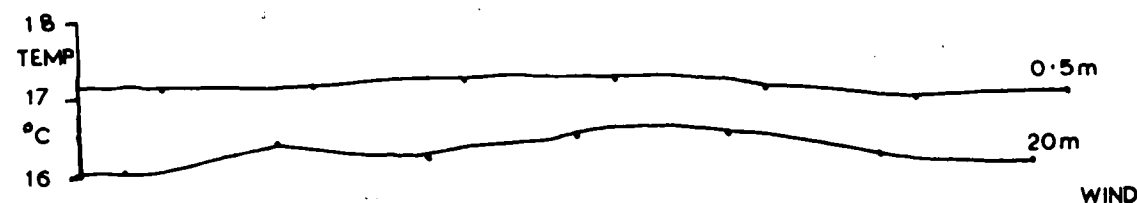
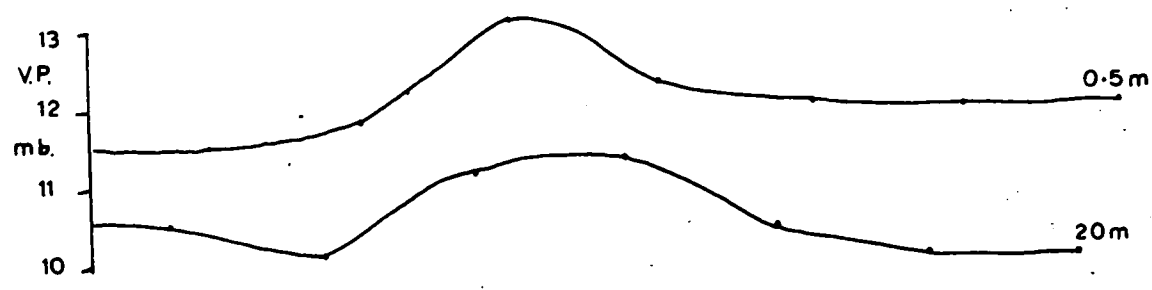
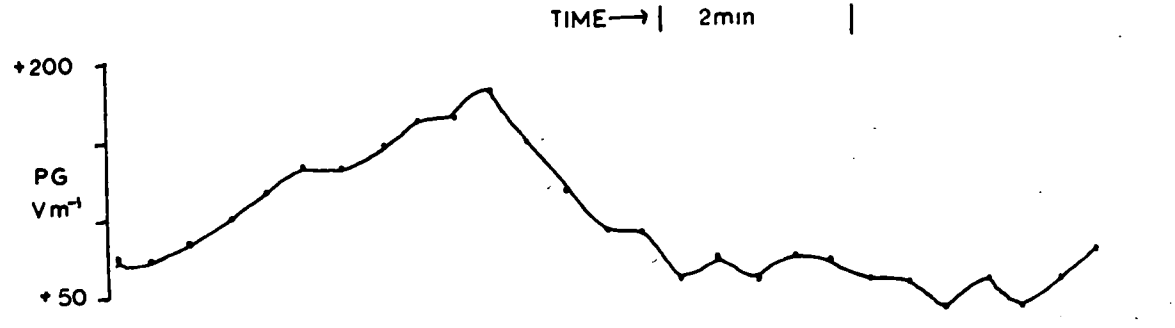
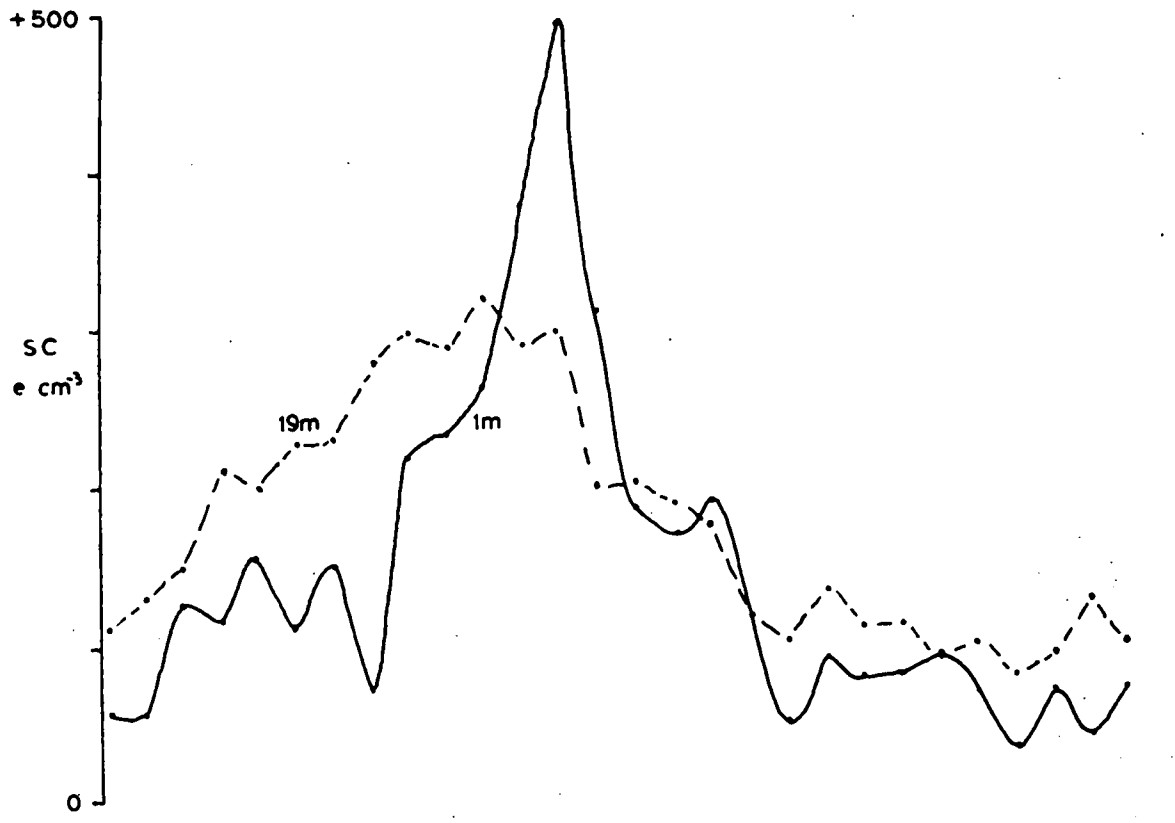


FIG. 61

source to the NW caused the negative space charge in the first case, but a more interesting explanation was available for the three occasions when there was an easterly wind. On these three days the space charge and potential gradient had been consistently positive for some few hours but on each occasion at about mid-afternoon the signs of these variables rapidly changed. Fig. 61 illustrates this point but it will be noticed that the vapour pressure increases considerably at the same time. However, it was found that about 40 min. earlier a mist had descended on the coast to the east and hence around the ²⁷⁵~~400~~ KV cables in this region. The wind speed was such as to cause the increase of humidity in Durham 40 min. later. In order to explain the negative space charge, however, we must assume that it was formed at the H.T. cables on the coast, and as the negatively charged mist blew inland it evaporated but the charge remained. This would give rise to the observed effect of vapour pressure increase with space charge and potential gradient going negative, even though the visibility remained good.

Recordings were also taken on eight clear but humid summer nights when it was noticed that the space charge and potential gradient readings were consistently slightly negative. This could be explained by dew forming on the insulators of the H.T. cables in the night air so that negative ions would be formed in the same way as during misty conditions.



WIND 3m sec⁻¹
25 JUNE 1964

FIG. 62

6. SPACE CHARGE PULSES CAUSED BY STEAM-ENGINES

There have been many occasions when the potential gradient and space charge records have shown positive pulses which last for approximately 4 min. and at times occur approximately once in 45 min. These have occurred in turbulent air when there has been no noticeable change in wind speed and temperature, but the humidity has risen sharply for the same period of time as the charge concentration. An example of such a pulse is shown in Fig. 62. The observed charge concentrations could not exist for long in a turbulent atmosphere as the dispersion process will be quite rapid. This indicates that the positive charge has occurred fairly locally.

MÜHLEISEN (1953) and CHALMERS (1952) both reported potential gradient increases of over 200 Vm^{-1} near to steam locomotives and as there is a main line railway running north and south only $\frac{3}{4}$ Km from the Observatory, this seemed a possible reason for the charge pulses. It was very difficult to associate a particular pulse with a particular train, and as passenger trains on this line are now all pulled by diesel locomotives it was doubtful if such a rise of humidity would be associated with this type of train. However, steam-engined goods trains pass at least three times per hour and a greater humidity rise would be expected in this case.

Other points of interest which tend to confirm the above suggestions are, a) that such rapid pulses were not noticed on days when the wind did not approach from the railway lines, b) the potential gradient pulses occurred slightly before the upper space charge

collector pulses, which signifies that the cloud of space charge is moving faster at the upper level, and c) whilst exact timetables of goods trains were not available there were certain periods during the day reserved for them and these could be associated with the observed pulses.

CHAPTER 9CONCLUSIONSAND SUGGESTIONS FOR FURTHER WORK

The space charge collector medium proved to have excellent filtration properties, as it abstracted over 99.8% of the small ions from the air at certain flow rates, and it was therefore ideal for this purpose. It was unfortunate however that the material could not be used during periods of precipitation. The only fault seems to be the possibility of ions being filtered to the mast structure before being sucked into the intake but it would be advantageous if it could constantly face into the wind.

The analogue-to-digital converter proved to be of invaluable help. The design is such that any faults can quite easily be traced; also, owing to it being constructed with solid state devices, and the only mechanical parts other than the punch being microswitches, faults should be very limited. It will be of great help to anyone who wishes to use the recorder in the future where an accuracy of 1% is adequate. Without its assistance it would have taken months to analyse the results to the same extent. Whilst it can be argued that it took three months to build the converter, this time was better spent learning the art of circuit development instead of performing countless hours of calculations.

Of the results obtained probably the most important when considering any further work is that of the electrode effect on the mast. It was found that there were two different forms of this effect caused

by the enhanced potential gradient towards the top of the mast. One was caused by the enrichment of ions near the surface of the collector, as described on page 115, being blown by the wind into the volume of air being sucked into it. This effect becomes more pronounced with a lower wind speed. The other effect is caused when air first blows through the mast structure before reaching the collector. There is a possibility that if the advection is low enough and the potential gradient high enough then the small ions of sign similar to the potential gradient will be attracted to, and neutralised at, the mast structure, thereby leaving an excess of ions of the other sign. It is difficult therefore to estimate the space charge density at the top of the mast if the air is not blowing directly into the collector and the error can be considerable and either positive or negative. It may be concluded therefore that space charge concentrations measured near the top of such a mast must be treated with considerable caution.

Another most important result was that a separation of charge seemed to occur at the surface of rapidly melting snow. This separation may be explained if we assume that a negative charge was given to the air and a positive charge remained on the snow during conditions of high wind speeds. On the other hand if there was dry snow in the vicinity of the collectors or on neighbouring high land and there was a strong wind, then a high positive charge was measured in the air, presumably carried by small particles of snow.

It was also found without much doubt that at the time of a nearby lightning flash corona space charge was produced at trees

which were in bud.

Calculations showed that the current through trees in this period were similar to those found by other observers to be liberated by artificial points. Hence it appears that previous estimates of the total point discharge currents below clouds seem to be accurate and this process must play an important role in the transfer of charge between cloud and ground.

Interesting results were obtained during periods when convection cells were apparently active. At the time of temperature and humidity peaks the space charge density rose. This occurred at the arrival of that part of the cell in which air was moving up from the surface. The increase in space charge was probably due to an electrode effect close to the surface, from whence the space charge was drawn by the upward movement of air. This additional space charge and water vapour occurring at the same time seems to verify that both these effects come from very close to the surface. Another reason for this increase in charge concentration would be if the upward movement of air was of similar speed to the downward movement of small ions due to their mobility, hence creating a relatively stable space charge layer.

Negative space charge was found to be predominant during misty conditions and overnight in humid conditions. This appears to originate at the overhead H.T. cables surrounding Durham. An interesting effect was observed when mist was covering the cables some 9 miles to the east of Durham. The easterly wind carried a high negative concentration of charge into Durham which was enjoying summer conditions of clear sky and excellent visibility.

The final outstanding observations of space charges was when pulses of high charge concentration arrived, presumably from railway engines travelling on a line $\frac{3}{4}$ Km from the mast.

It appears that it will be unprofitable to carry out much more recording of space charges towards the top of the mast, but it will be interesting to measure the concentration closer to the earth as well as the vertical component of wind. This would help to ascertain whether an electrode effect close to the earth is causing the space charge increases noted under convection cumulus conditions. By measuring these quantities at two more land stations it may become possible to detect the structure of the convection cell.

It would also be worth studying further the cause of the night-time negative space charge to see if this does originate at the H.T. cables. Whilst it has been proved without much doubt that insulation breakdown at these overhead lines causes negative space charges during mist, no such evidence has come to hand that the night-time effect is similarly caused.

ACKNOWLEDGMENTS

The author is greatly indebted to Dr. W.C.A. Hutchinson and Dr. J.A. Chalmers for their continual interest, encouragement and discussion during this research project.

Thanks are also due to Professor G.D. Rochester for the facilities granted and to the Physics Department workshop staff, in particular Mr. D. Jobling, for their assistance.

The writer is indebted to Dr. L. Molyneux of Newcastle University, for his valuable help and advice in the designing of the analogue-to-digital converter and to Mr. H.L. Collin during its construction. Thanks are also due to my fellow research students for their continual help and advice and in particular, once more, to Mr. H.L. Collin.

Gratitude is expressed to the Department of Scientific and Industrial Research for a Research Studentship which made this work possible and to Durham University for a Senior Demonstratorship which makes it possible to continue this research.

Thanks are also expressed to Mr. S. Coroniti for making possible my visit to the Third International Conference on Atmospheric and Space Electricity at Montreux in 1963, and finally to Mrs. G. Brooke for her speed in the preparation of the typescript.

REFERENCES

- ADKINS, C.J. 1959 Quart. J. R. Met. Soc., 85, p. 237.
- AITKEN, J. 1880 Trans. R. Soc. Edinb. 30, Collected
Scientific papers 1923 pp. 34-64.
- BÉNARD, H. 1901 Ann. Phys. Chem., Paris, 23.
- BRASEFIELD, C.J. 1959 J. Geophys. Res., 64, pp. 141-148.
1959b Science, 129, p. 1610.
- BROWN, J.G. 1930 Terr. Magn. Atmos. Elect., 35, pp. 1-15.
- CHALMERS, J.A. 1946 Quart. J.R. Met. Soc., 72, pp. 199-205.
1951 Quart. J.R. Met. Soc., 77, pp. 249-259.
1952 J. Atmosph. Terr. Phys., 2, pp. 155-159.
1957 Atmospheric Electricity, Pergamon Press,
p. 56.
1962 J. Atmosph. Terr. Phys., 24, pp. 1059-
1063.
1964 J. Geophys. Res., 69, pp. 357-359 and
p. 362.
- CHAUVEAU, B. 1902 "Recherches sur l'électricité
atmosphérique", Mem. II, p. 103.
- COULOMB, C.A. 1785 Mém. Acad. Sci., Paris, p. 616.
- CROZIER, W.D. 1963 J. Geophys. Res., 68, pp. 3451-3458.
- DAUNDERER, A. 1907 Phys. Z. 8, pp. 281-286.
- DINGER, J.E. 1964 Quart. J.R. Met. Soc., 90, p. 208.
- DINGER, J.E. and GUNN, R. 1946 Terr. Magn. Atmos. Elect., 21, pp.
477-494.

- DURST, C. S. 1932 Met. Off. Geophys. Mem., 54, pp. 57-63.
- EARNshaw 1956 Elect. Engin., 28, p. 26.
- EBERT, H. 1901 Phys. Z. 2, pp. 662-666.
- ELSTER, J. and GEITEL, H. 1899 Phys. Z. 1, pp. 245-249.
- FORSYTHE, G. E. 1957 J. Soc. Indus. Appl. Maths., 5, p. 74.
- FREIER, G. 1962 J. Geophys. Res., 67, pp. 4683-4692.
- HESS, V. F. 1911 S. B. Akad. Wiss., Wien., 120,
pp. 1575-1584.
- 1928 "The Electrical Cond. of the Atmosph."
Constable & Co. Ltd.
- HICKS, W. W. 1956 J. Frankl. Inst., 261, p. 209.
- HOGG, A. R. 1939 Proc. Phys. Soc., Lond., 51, pp.
1014-1027.
- KÄHLER, K. 1927 Met. Z. 44, pp. 1-5.
- KELVIN Lord 1859 Proc. Lit. Phil. Soc., Mnchr. Papers
on Electrostatics and Magnetism,
pp. 200-203.
- 1862 Proc. Lit. Phil. Soc. Mnchr. Papers
on Electrostatics and Magnetism,
pp. 230-235.
- KIRMAN, T. D. 1954 "The measurement of atmospheric space
charge", ARL (Teddington), Unpub.
report.
- KIRKMAN, J. R. 1956 Ph.D. Thesis, Durham Univ.
- KRAAKEVIK, J. H. 1958 Rec. Adv., pp. 75-78.

- LANGEVIN, P. 1905 C.R. Acad. Sci., Paris, 140,
pp. 232-234.
- LAW, J. 1963 Quart. J.R. Met. Soc., 89, pp. 107-121.
- LEMONNIER, L.G. 1752 Mém. Acad. Sci., 2, p. 233.
- LINSS, F. 1887 Met. Z., 60, pp. 340-351.
- MACHE, H. 1903 Phys. Z. 4, pp. 587-588.
- MAGONO, C. and SAKURAI, K. 1963 J. Met. Soc. Japan, 41, pp. 211-217.
- MATTEUCCI, C. 1850 ANN. Chem. Phys., Lpz., 28, p. 385.
- MATTHEWS, J.B. and 1963 Quart. J.R. Met. Soc., 89, p. 376.
MASON, B.J.
- MAUND J.E. and CHALMERS, 1960 Quart. J.R. Met. Soc., 86, pp. 85-90.
J.A.
- MILNER, J.W. and 1961 Quart. J.R. Met. Soc., 87, pp. 592-596.
CHALMERS, J.A.
- MOORE, C.B., VONNEGUT, B. 1961 J. Geophys. Res., 66, p. 3219.
and MALLAHAN, F.J.
- MÜHLEISEN, R. 1956 J. Atmosph. Terr. Phys., 8, pp. 146-
157.
1959⁸ "Recent Advances in Atmospheric Elec."
Perg. Press., pp. 213-222.
1961 J. Atmosph. Terr. Phys., 20,
pp. 79-80.
- MÜHLEISEN, R. and HOLL, W. 1952 Geofis. pur. appl. 22, pp. 3-8.
- NORINDER, H. 1921 Geogr. Ann., Stockholm, 1, pp. 1-96.
- NORINDER, H. & SIKSNA, R. 1952 Ark. Fys., 6, p. 130.

- NORINDER, H. & SIKSNA, R. 1955 Ark. Geofys., 2, pp. 343-369.
- OBOLENSKY, W.N. 1925 Ann. Phys., Lpz., II, pp. 644-666.
- PASQUILL, F. 1949 Quart. J.R. Met. Soc., 75, pp. 239-248.
- PLUVINAGE, P. and STAHL, P. 1953 Ann. Geophys. 9 pp. 76-85.
- POLLOCK, J.A. 1915 Phil. Mag., 29, pp. 636-646.
- SAGALYN, R.C. and 1956 Quart. J.R. Met. Soc., 82, pp. 428-445.
- FAUCHER, G.A.
- SCHONLAND, B.F.J. 1928 Proc. Roy. Soc. A, 118, pp. 252-262.
- SCORER, R.S. and 1953 Quart. J.R. Met. Soc., 79, p. 94.
- LUDLAM, F.H.
- SCRASE, F.J. 1935 Geophys. Mem., Lond., 67.
- 1937 Proc. Roy. Soc. A, 161, pp. 309-352.
- SIKSNA, R. 1953 Ark. Fär. Fysik. 6, Nr 28, p. 280.
- SIMPSON, G.C. 1949 Geophys. Mem., Lond., 84, pp. 1-51.
- SIMPSON, G.C. and 1940 Proc. Roy. Soc. A. 177, pp. 281-329.
- ROBINSON, G.D.
- SIMPSON, G.C. and 1937 Proc. Roy. Soc. A. 161, pp. 309-352.
- SCRASE, F.J.
- SMIDDY, M. 1958 Ph.D. Thesis, Durham Univ.
- SMIDDY, M. and 1960 Quart. J.R. Met. Soc., 86, pp. 79-84.
- CHALMERS, J.A.
- VONNEGUT, B. and 1958 Final report to Geophys. Res. Dir.,
Contract AF 19(604), 1920. Research
Centre, Bedford, Mass.
- MOORE, C.B.

- VONNEGUT, B., MOORE, C.B., 1962 J. Geophys. Res., 67, pp. 3909-
 SEMONIN, R.G., 3927.
 BULLOCK, J.W.,
 STAGGS, D.W. and
 BRADLEY, W.E.
- WILEMAN, P.J.L. 1962 Ph.D. Thesis, Durham Univ.
 WILSON, C.T.R. 1900 Proc. Camb. Phil. Soc., 11, p. 32.
 WORMELL, T.W. 1953 Quart. J.R. Met. Soc., 79, pp. 3-50.
 WRIGHT, H.L. 1936 Proc. Phys. Soc., Lond., 48, pp.
 675-689.

